UNDERSTANDING THE PRESENT AND PAST CLIMATE-FIRE-VEGETATION DYNAMICS OF SOUTHERN SOUTH AMERICA (40 – 45° S)

by

Ayodele Gilbert Ogunkoya

A dissertation submitted in partial fulfillment
of the requirements for the degree

of

Doctor of Philosophy

in

Ecology and Environmental Sciences

MONTANA STATE UNIVERSITY
Bozeman, Montana

January 2020

DEDICATION

I dedicate the dissertation to God and my Late mother, Adebimpe Silifat Ogunkoya (nee Quadri). I love you, sweet mother, but God loves you most. Continue to rest in the bosom of the Lord till the day we meet and part no more.

ACKNOWLEDGEMENTS

I want to express my sincere gratitude and appreciation to my advisor and committee co-chair, Dr. Benjamin Poulter, for his guidance, advice, and thoughtful critique throughout all stages of this project. His support, understanding, and encouragement proved to be invaluable. I want to extend special thanks to Dr. David Roberts, Dr. Cathy Whitlock, Dr. Jed Kaplan, and Dr. Laura Burkle for their valuable and constructive suggestions and for serving as members of my committee. I am forever grateful to my wife Atinuke Ogunkoya and my beautiful daughters, Omolola and Oluwateniola Ogunkoya. I love you guys so much and pray that God will continue to bless you. I am grateful to my family, my father Babatunde Ogunkoya, and my siblings, Omolola, Damilola, and Tolulope Ogunkoya. Finally, I would like to thank my in-laws, who provided me with moral and spiritual support throughout my studies.

TABLE OF CONTENTS

TABLE OF CONTENTS CONTINUED

LIST OF TABLES

Table Page

LIST OF FIGURES

Figure Page

LIST OF FIGURES CONTINUED

Figure Page

LIST OF FIGURES CONTINUED

Figure Page

ABSTRACT

The forest-steppe boundary that runs north-to-south along the eastern Andes is particularly dynamic over millennial time scales. Yet the relative role of long-term climate change and fire is poorly understood. In this study, I analyze the potential in using a process-based model in predicting species distribution, and the role fire and climate played in shaping the vegetation and treeline dynamics of Northern Patagonia (lat. 40 – 45 ° S). Paleoecological data, e.g., pollen, has been extensively used to study the relationship between climate and vegetation but has a low spatial resolution to distinguished between climate-fire-vegetation dynamics. Process-based model thus offers a transparent and robust method of incorporating a varying degree of complexity to understand fire behavior and fire-vegetation dynamics. Recently, LPJ-GUESS was parameterized to simulate major regional plant functional type (PFTs) and tree species distributions in this region. The model is able to predict regional species distribution across spatial scales by coupling establishment, growth, and mortality processes. Predicting spatial and temporal scale species distribution cannot be achieved without having the right climate and soil data, the climate data used was downscaled from 50 km to 1 km resolution using Worldclim climate data (~ 1 km) as the reference data. LPJ-GUESS model produced regional species distribution with fair to very good agreement with observation. The optimization of bioclimatic parameters and drought tolerance that is related to root depth, adaptability of plant to seasonal drought, and movement of nutrients consistently improved the accuracy of regional prediction of the species range. The model predicted that the vegetation distribution of present-day is mainly determined by climate and CO_2 rather than fire., while forest productivity responds strongly to elevated CO_2. However, based on the employed statistical methods of Canonical Correspondence Analysis (CCA) and Random Forest machine learning, combined with simulation results using paleoclimate. Results show that an increase in winter temperature drives the postglacial species distribution while changes in precipitation control radial growth and seedling establishment in the upper and lower treeline. These findings emphasize the importance of combining paleoecological methods with modeling to disentangle coarse-scale climate drivers from local influences.

CHAPTER 1

INTRODUCTION TO DISSERTATION

The Earth system is warming at a very rapid rate, and a recent report from the IPCC (2018), has shown that this trend is projected to accelerate future ecosystem change. The effect of rising temperature, atmospheric CO_2 concentration, and other greenhouses gasses, as well as nitrogen deposition, will likely cause land-use changes, modified disturbance regimes, and introduce new species assemblages (Steffen et al. 2011), and these changes will affect the terrestrial ecosystem services that they provide such as carbon storage, water supply and quality, food production (Dale et al. 2001). The immediate causes of climate change have been strictly suggested to be human-driven and are responsible for most of the warming since the industrial revolution (IPCC 2013). The impact of potential future climate change (e.g., the effect of rising temperature) on the biosphere has been evaluated by various climate models (Flato et al. 2013), but they were based on projected climate changes. In order to understand how the Earth system might respond to projected anthropogenic climate change, it is vital to understand how it has responded to climate changes in the geological past. By investigating postglacial vegetation and climate history, long-term records of past change can be compared with present day and future projections of ecological change to determine the range of ecosystems response that may be possible (Blois et al. 2013).

For this reason, a robust prediction of past and present effects of climate change requires comparison and evaluation of simulated and reconstructed vegetation patterns to estimate and infer how the biosphere will react to changes in the physical climate system (Kaplan 2003).

Objectives

This dissertation centers around the use of the Lund-Potsdam Jena Dynamic Global Vegetation Model (LPJ-GUESS DGVM) (Smith et al. 2001). Here, LPJ-GUESS is used first to simulate the modern vegetation distribution of northern Patagonia, and the results are tested by simulating postglacial vegetation. In view of this context, the objectives of this dissertation are to (1) use a Dynamic Global Vegetation Model (DGVM) to evaluate the individual and interactive effects of climate, CO_2, and fire on present-day northern Patagonia forest cover; (2) investigate potential climate drivers on past changes in the forest cover and treeline dynamics along the eastern Andes of northern Patagonia.

To address these objectives, I focused on parametrizing LPJ-GUESS DGVM with seven Patagonian tree species, two types of C_3 grasses based on elevation, and two plant functional types. This attention to individual plant species rather than exclusively plant functional types (PFTs) allows for a better assessment of variation in regional plant behavior because individual plant species have particular traits that enhance their competitive ability in a community. The local species parameterization was done in collaboration with experts from Laboratorio Ecotono, INIBIOMA CONUCET-Universidad Nacional del Comahue, Bariloche, Rio Negro, Argentina. An agriculture land masking system was implemented into LPJ-GUESS to ensure that fire does not occur in the masked coordinates when a fire is switched 'on' in the model. This approach acts as a fire suppression technique in our study area. In order to simulate postglacial forest cover, I used the output from GENMOM (Genesis Modular Ocean Model), a coupled atmosphere-ocean climate model (AGCM) (reference) and applied it to modern climate research unit (CRU) climate data. The AGCM data was provided by Dr. Steve Hostetler, College of Earth, Ocean, and Atmospheric Sciences, Oregon State

University. The location of treeline position was based on the method I developed with Jed Kaplan. I worked closely with paleoecologists collaborators (Cathy Whitlock, William Nanavati, and Virginia Iglesias) to interpret postglacial vegetation history of Patagonia and compare simulated output with pollen and charcoal reconstruction.

The northern Patagonia region (latitude, longitude) of southern South America represents a new region to explore environmental drivers (e.g., climate, fire) because of the influence of Southern Westerlies and ENSO related variability. The north-south alignments of the Andes and the resulting moisture gradient makes this a particularly good system to address the study questions.

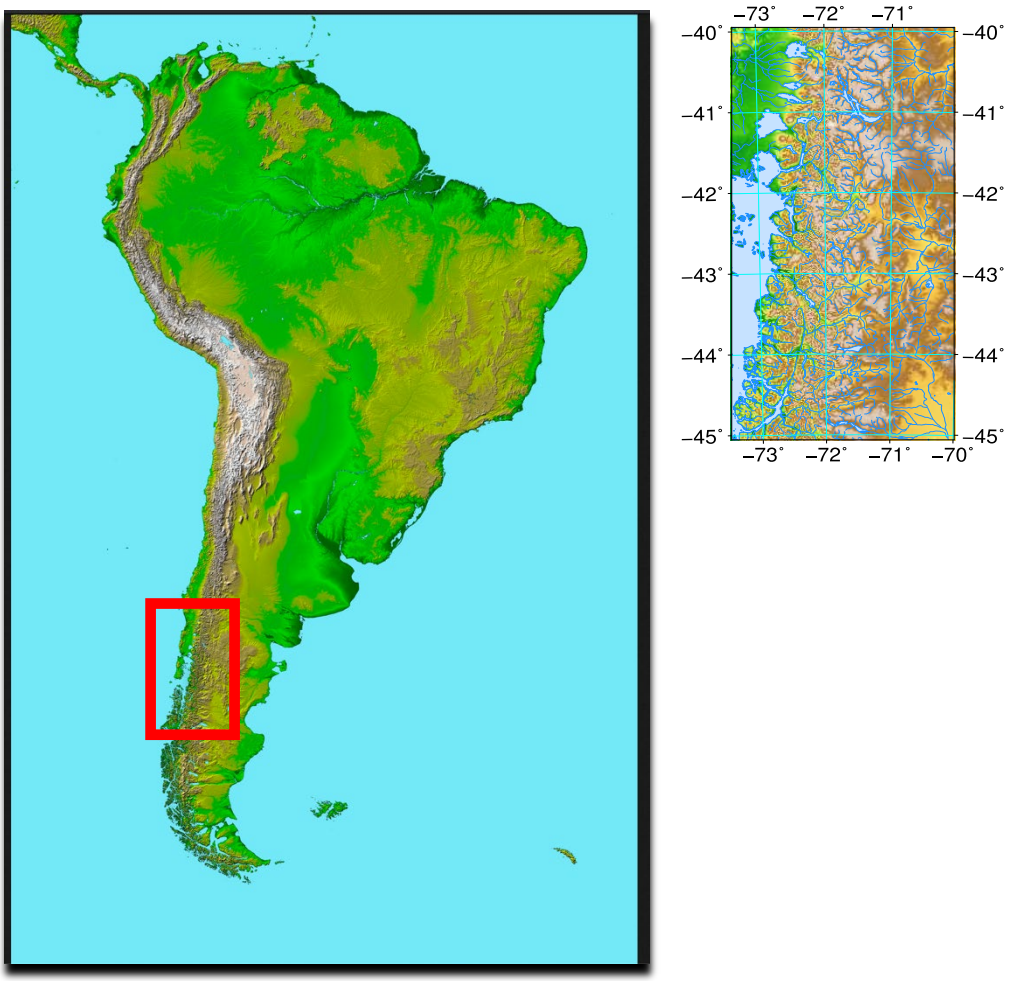

Figure 1.1: Topography map of South America showing the location of the study area (red square). Data source for South America map: Wikimedia

Overview of Dissertation

In my dissertation, I examine the effect of climate, fire, and CO_2 in controlling present-day and past biogeography and biomass productivity of the northern Patagonia forest. Whereas an empirical analysis alone cannot explain the interactions between climate, fire, and CO_2 interaction on forest productivity. A process-based model can assist in explaining these interactions because different drivers of forest productivity can be changed one variable at a time. This work uses the Lund-Potsdam-Jena global Ecosystem Simulator (LPJ-GUESS) DGVM to explore the effect of environmental drivers (e.g., climate) on a much broader and larger scale.

In Chapter 2, I used LPJ-GUESS DGVM (Smith et al. 2001) to explore the ways in which fire, CO_2 concentration and climate act separately and in combination to influence forest cover. I tested a series of experimental setup simulations to evaluate the effects of running combinations of pre-industrial and dynamic CO_2 with pre-industrial (1901- 1930) and historical meteorology climate data (1901 – 2016) respectively in northern Patagonia (lat. 40º – 45ºS). The modeling provides insights on the variability in species composition across this biomass-rich vegetation type and vegetation response to climate drivers under contemporary conditions. This is a groundbreaking attempt to model the modern vegetation of the study area using local tree species within a DGVM framework. The idea to parameterized LPJ-GUESS DGVM with local tree species was conceived in the January 2016 at a workshop in Bariloche, Argentina, where I, Benjamin Poulter, Jed Kaplan, and experts at the Laboratorio Ecotono, INIBIOMA CONUCET-Universidad Nacional del Comahue worked together to make it a reality. However, in a situation where there is no literature available to parameterize the local tree species characteristics, such as minimum and maximum temperatures for

photosynthesis, we used European values (for both local tree species and PFTs) because of the close physical climate system (temperate region). Although not a perfect parameterization of the landscape, it provided an excellent representation of the vegetation. One of the challenges was modeling the sharp gradient between the forest and the steppe. Due to the abrupt nature of the ecotone, I had to constrain the forest to grow more to the west. The similarity between the simulated biomass and observed biomass of temperate forest west of the Andes and mesic forest shows that the model can capture local vegetation dynamics, paving the way to use the model in simulating past vegetation.

The potential climate drivers of postglacial forest cover and treeline along the eastern Andes of northern Patagonia (lat. 40º – 45ºS) are provided in Chapter 3. After successfully modeling present-day vegetation using the new parameterization of the critical local tree species, the model was used to further discriminate the significant drivers of past forest cover and treeline dynamics. I applied monthly anomalies from GENMOM (Genesis Modular Ocean Model) a coupled atmosphere-ocean model on monthly CRU (Climate Research Unit) climate data, to derive the paleoclimate data for each time slice (15, 9, 6, 3 and 0 ka BP) used in driving the postglacial simulations. The paleoclimate data did come with its challenges. First, the coarse spatial resolution of the climate data, did not capture the local climate of the Patagonian Andes very well. I was able to overcome this challenge by applying the GENMOM anomalies to downscaled CRU climate data (1 km). Secondly, the radiation data that was used with the GENMOM anomalies were derived from LPJ-GUESS modern-day simulation, because the topographically derived solar radiation was underestimating the region's monthly solar radiation. The idea for Chapter 3 was conceived by Cathy Whitlock and Ben Poulter but was implemented by me. The foresight about the implementation was developed at the

PAGES workshop at the Harvard Forest in 2015 and the PALEON summer school at Land O'Lakes Wisconsin in 2017.

The northern Patagonia forest-steppe ecotone represents a critical region for exploring changes in forest vegetation cover and composition in response to past climate changes. However, an abrupt change in limiting conditions (e.g., precipitation) at the end of a forest gradient (e.g., semi-arid belt) will produce a significant response, such as a shift in the dominant keystone species (Kitzberger 2012). I focused on time intervals from late-glacial to pre-industrial (15, 9, 6, 3, and 0 ka BP) as opposed to the evolution of climate and vegetation over time because the GENMOM dataset was available only as time intervals. I used Canonical Correspondence Analysis (CCA) and machine learning (Random Forest) to better understand the drivers of past ecological variability, under the premise that the CCA algorithm employed a selection of linear combinations of measured explanatory variables to maximize the dispersion of response variables (Green et al. 1990). Use of RF helps overcome the issue of a large number of correlated explanatory variables because it uses a small amount of the predictor variables at each stage of analysis.

Finally, in Chapter 4, I provided a summary of the significant results from each chapter and discussed how they had enhanced our understanding of the biogeographical and ecophysiological control of modern-day and past forest cover, and the advantages of assessing model performance with pollen reconstruction. My findings emphasize the contribution of climate and CO_2 to the changes in vegetation type and structure from the late-glacial to the present-day.

References

Blois, J. L., J. W. Williams, M. C. Fitzpatrick, S. T. Jackson, and S. Ferrier. 2013. Space can substitute for time in predicting climate-change effects on biodiversity. Proc Natl Acad Sci U S A **110**:9374-9379.

Dale, V. H., L. A. Joyce, S. McNulty, R. P. Neilson, M. P. Ayres, M. D. Flannigan, P. J. Hanson, L. C. Irland, A. E. Lugo, C. J. Peterson, D. Simberloff, F. J. Swanson, B. J. Stocks, and B. M. Wotton. 2001. Climate Change and Forest Disturbances: Climate change can affect forests by altering the frequency, intensity, duration, and timing of fire, drought, introduced species, insect and pathogen outbreaks, hurricanes, windstorms, ice storms, or landslides. BioScience **51**:723-734.

Flato, G., J. Marotzke, B. Abiodun, P. Braconnot, S. C. Chou, W. Collins, P. Cox, F. Driouech, S. Emori, V. Eyring, C. Forest, P. Gleckler, E. Guilyardi, C. Jakob, V. Kattsov, C. Reason, M. Rummukainen, T. F. Stocker, D. Qin, G.-K. Plattner, M. Tignor, S. K. Allen, J. Doschung, A. Nauels, Y. Xia, V. Bex, and P. M. Midgley. 2013. Evaluation of Climate Models. Pages 741-866 Climate Change 2013: The Physical Science Basis. Contribution of Working Group I to the Fifth Assessment Report of the Intergovernmental Panel on Climate Change.

Green, R. H., R. H. G. Jongman, C. J. F. Braak, and O. F. R. V. Tongeren. 1990. Data Analysis in Community and Landscape Ecology. Biometrics **46**.

IPCC. 2013. Climate Change 2013: The Physical Science Basis. Contribution of Working Group I to the Fifth Assessment Report of the Intergovernmental Panel on Climate Change. Cambridge University Press, Cambridge, United Kingdom and New York, NY, USA.

IPCC. 2018. Summary for Policymakers. In: Global warming of 1.5°C. An IPCC Special Report on the impacts of global warming of 1.5°C above pre-industrial levels and related global greenhouse gas emission pathways, in the context of strengthening the global response to the threat of climate change, sustainable development, and efforts to eradicate poverty. World Meteorological Organization,, Geneva, Switzerland.

Kaplan, J. O. 2003. Climate change and Arctic ecosystems: 2. Modeling, paleodata-model comparisons, and future projections. Journal of Geophysical Research **108**.

Kitzberger, T. 2012. Ecotones as Complex Arenas of Disturbance, Climate, and Human Impacts: The Trans-Andean Forest-Steppe Ecotone of Northern Patagonia. Pages 59-88 *in* R. Myster, editor. Ecotones Between Forest and Grassland. Springer, New York.

Smith, B., I. C. Prentice, and M. T. Sykes. 2001. Representation of vegetation dynamics in the modelling of terrestrial ecosystems: comparing two contrasting approaches within European climate space. Global Ecology and Biogeography **10**:621-637.

Steffen, W., A. Persson, L. Deutsch, J. Zalasiewicz, M. Williams, K. Richardson, C. Crumley, P. Crutzen, C. Folke, L. Gordon, M. Molina, V. Ramanathan, J. Rockstrom, M. Scheffer, H. J. Schellnhuber, and U. Svedin. 2011. The anthropocene: from global change to planetary stewardship. Ambio **40**:739-761.

CHAPTER TWO

MANUSCRIPT IN CHAPTERS TWO

DRIVERS OF MODELED FOREST COVER CHANGE IN SOUTHERN SOUTH AMERICA ARE LINKED TO CLIMATE AND CO_2

Contribution of Authors and Co-Authors

Manuscript in Chapter 2

Author: Ayodele Gilbert Ogunkoya
Contributions: Contributions: Defined the experimental design, parametrized the Plants Functional Types (PFTs) and plant species used in LPJ-GUESS DGVM, downscaled the climate used for simulations, performed the modeling simulations, analyzed the output from the model simulation and wrote the manuscript.

Co-Author: Benjamin Poulter

Contribution: Supported this research under the National Science Foundation grant GSS 1461590 helped define the experimental design, discussed the results and implication and edited the manuscript.

Co-Author: Jed Kaplan

Contribution: Participate in parametrization of PFTs and plants species used in LPJ-GUESS simulation, discussed the results and edited the manuscript

Co-Author: Cathy Whitlock

Contribution: Supported this research under the National Foundation grant, commented on the manuscript

Co-Author: William Nanavati

Contribution: Commented on the manuscript

Co-Author: David Roberts

Contribution: Discussed the results and commented on the manuscript.

Manuscript Information Page

Ayodele Ogunkoya, Jed O. Kaplan, Cathy Whitlock, William Nanavati, Benjamin Poulter, David Roberts

Status of Manuscript:
__x__ Prepared for submission to a peer-reviewed journal
____ Officially submitted to a peer-review journal
____ Accepted by a peer-reviewed journal
___ Published in a peer-reviewed journal

Abstract

Widespread changes in forest structure and distribution have been documented in Patagonia over the past century. Reconstructions of forested area in Patagonia over the last 75 to 100 years show an expansion of forests at high and low elevation. At low elevation, expansion has coincided with the implementation of fire suppression, potentially shifting the vegetation from open woodlands to dense forest, especially along the forest/steppe margin. In contrast, at high elevation, a combination of climate and fire suppression is thought to be responsible for forest expansion. We employed LPJ-GUESS, a Dynamic Global Vegetation Model (DGVM) to investigate the role of climate, atmospheric carbon dioxide (CO_2), and fire on simulated forest cover during the 20th century. We established a series of experimental simulations to evaluate the individual and interactive effects of climate, CO_2, and fire, running combinations of fixed and dynamic CO_2 with historical climate data (1901-2016). We simulated current potential vegetation composition and distribution for southern Chile and southwestern Argentina (40^{o}S-45^{o}S). Simulating observed climate and observed CO_2 from 1930 to 2010 showed an increase in forest cover under changing climate and CO_2 because of higher carbon assimilation and net primary production. The model results were compared with a remote sensing derived biomass map and 'greening' indices from the normalized difference vegetation index and revealed agreement in greening at the high and low elevations. The simulations also captured the distribution of temperate rainforest west of the Andes and the high-elevation forest but underestimated forest cover along the eastern forest-steppe transition. At low CO_2, biomass was low, thereby reducing available fuel for burning and suggesting that high CO_2 is necessary to accurately simulate present-day productivity. The use of pre-industrial climate (PI) and PI CO_2 caused a decrease in fire frequency and reduction of

simulated biomass that does not match present-day distributions. Climate is the primary driver and CO_2 fertilization is the secondary driver of forest expansion. CO_2 also mitigates climate-induced drought stress due to increases in water-use efficiency.

Introduction

Climate, fire, and atmospheric CO_2 induce vegetational changes at the landscape scale (Bradshaw and Sykes, 2014). Their interactions are complicated because, fuel load, types, and moisture (element of a fire regime) are controlled by climate (Martin Calvo et al. 2014), while interannual variation in atmospheric CO_2 (Friedlingstein and Prentice 2010) constrains forest productivity by limiting the rate of photosynthetic activities (Martin Calvo et al. 2014). Also, CO_2 responds to climate anomalies (e.g., El Niño Southern Oscillation [ENSO]) because there are higher than average CO_2 concentrations during El Niño years and trees are sensitive to interannual climate variation (Friedlingstein and Prentice 2010). Biomass production depends on atmospheric CO_2 concentration and therefore CO_2 determines fuel load in part (Martin Calvo et al. 2014). In turn, fire releases stored litter carbon into the atmosphere creating a complex feedback mechanism between vegetation, fire regime, and climate (van der Werf et al. 2010). Ecosystems thus respond to changes in climate, CO_2, and fire, either by increasing biomass or decreasing biomass production. A process-based ecosystem model can assist in examining these interactions because different drivers of forest productivity (e.g., CO_2, fire, and climate) can be changed one variable at a time (Martin Calvo and Prentice 2015).

The northern Patagonia region of southern South America (Fig. 2.1) represents a very interesting area to explore the interaction of climate, CO_2, and fire because of the strong effect of the Andes on climate on the vegetation, and the role of humans on ignition. The north-to-

south orientation of the Andes influences the west-to-east moisture gradient, which in turn affects forest distribution (Veblen et al. 1996). Moreover, the strong topographic gradients drive intricate vegetation patterns, with the mean elevation of the Andes decreasing from approximately 3000 m at 35°S to less than 1000 m at 56°S (Veblen et al. 1996). Because of the decrease in mean annual temperature and growing season length along the latitudinal gradient (north to south), species richness decreases with total above-and below-ground biomass. Across the longitudinal trans-Andean gradient annual precipitation decreases from west to east (Arroyo et al. 1996, Veblen et al. 1996). The history of climate and fire on the forest-steppe ecotone has been extensively studied using fossil pollen and charcoal records (e.g. Markgraf et al. 1996, Whitlock et al. 2007, Iglesias et al. 2014, Nanavati et al. 2019); however no study that we are aware of has used a dynamic vegetation model to evaluate the individual and combined effect of climate, CO_2, and fire on the northern Patagonia trans-Andean gradient.

Fire in this region is driven by both anthropogenic and natural ignitions (e.g., lightning). Consequently, in the more hyper-humid forest, fire events are rare, and the primary disturbances regimes are the fine-scale tree fall dynamics and the coarse-scale disturbance from volcanic activity. In the *Nothofagus* dominated mesic forest, infrequent coarse-scale disturbance (e.g., extreme drought events) causes tree mortality (Veblen et al. 1996). In dry forest receiving moderate rainfall levels (forest-steppe) fire events occur because abundant fuels desiccate frequently, while at the steppe, the lack of abundant fuel reduces fire activities (Kitzberger 2012).

Considerable vegetation change during the 20th century has been described in northern Patagonia based on information from dendroecology, remotely sensed data, repeat

photography, and landscape models (Veblen and Lorenz 1988, Kitzberger and Veblen 1999, Gowda et al. 2011, Paritsis et al. 2018). Repeat photography shows a significant increase in the *Austrocedrus chilensis* woodland of the Patagonia steppe between 1913 and 1985 as a result of changes in fire and grazing (Veblen and Lorenz 1988). Changes in patch composition and landscape structure from the wet *Nothofagus dombeyi* forest to the semi-arid woodlands of *Austrocedrus chilensis* at woodlands from 1940 and 1970 have been attributed to the reduction in fire frequency. Gowda et al. (2011) used historical land cover maps from the 1940s in combination with 30 years of LANDSAT data to quantify the change in forest cover along the northern Patagonia forest-steppe transition and attributed the change to human-related activities (i.e., fire, intensive grazing) and structural feature of the landscape (i.e., aspect and slope).

In this paper, we used the Lund-Potsdam-Jena General Ecosystem Simulator (LPJ-GUESS) DGVM, a dynamics process-based model that simulates forest stands accounting for eco-physiological activities (i.e., competition, disturbance) between individual trees and populations. The use of a DGVM allows the exploration of different climate-fire scenarios that might influence vegetation cover and biomass and the role of fire in altering these effects. We address the following questions:

1. How well does LPJ-GUESS represent the present-day Patagonia vegetation gradients in terms of forest cover and biomass?
2. Can the model reproduce observed trends in forest cover and biomass over the 20th century?
3. What is the role of climate, atmospheric CO_2, and fire in forest expansion in the last 116 years?

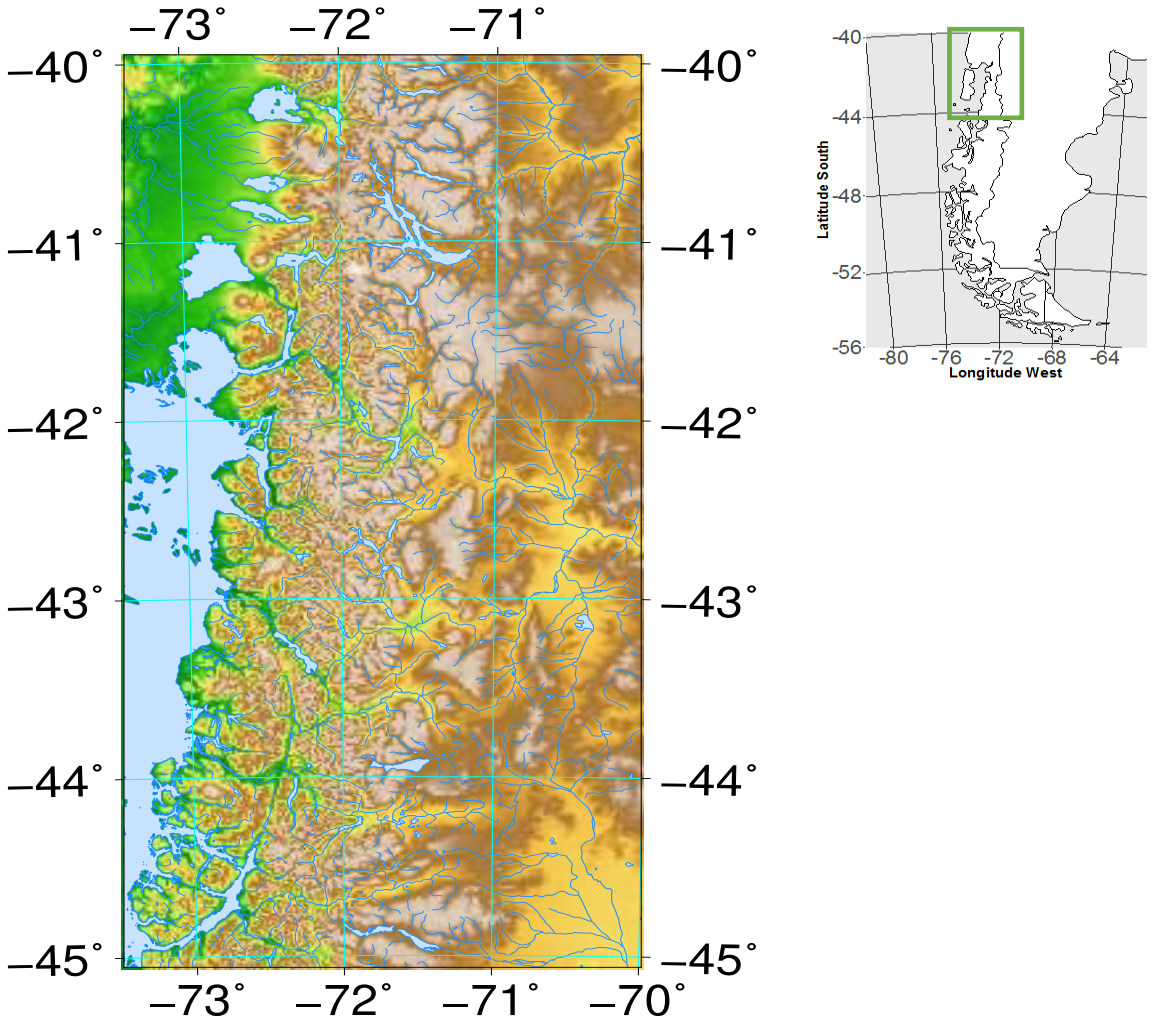

Fig. 2.1: Map showing the topography of the study area. The Andes influence the west-to east precipitation and vegetation gradient in the region. The west is wetter than the east as a result of orographic precipitation.

To answer these questions, we combined (1) detrended gridded meteorological pre-industrial climate (PI; 1901-1930 repeated to run the simulations for 1901-2016), (2) gridded observed meteorological climate (1901-2016), (3) pre-industrial CO_2 (280 ppm), and (4) observed CO_2 (1901-2016) into six specific simulations. We implemented a land masking system to control for fire in some simulation. By using a set of pair-wise combination, we were able to separate the non-linear relationships between climate, CO_2 and fire.

Study Area

The dramatic environmental gradient in northern Patagonia (40 to 45°S) is shaped by the shifting latitudinal position of the Southern Westerlies wind (SWW) during the year and the interception of frontal storms by the north-south-trending Andes. Seasonal position and strength of the SWW is determined by the intensity and location of subtropical atmospheric high-pressure systems, which are accompanied by moisture-laden cyclones (Garreaud et al. 2009). On the leeward westernmost slope of the Andes in northern Patagonia, annual precipitation ranges from >3000 mm/yr at the Andean crest to < 100 mm/yr in the steppe. In the temperate rainforest west of the Andes, the average annual temperature is 11.1°C, average austral winter temperature is 7.6°C (June, July, and August of 1901 - 2016) and the average austral summer temperature is 15.0°C (December, January, and February of 1901 - 2016). However, at high elevation (~1500 m), the average annual temperature is 2.6°C, average austral winter temperature is -2.4°C, average austral summer temperature is 7.9°C. East of the Andes, at low elevation (~800 m), the average annual temperature is 7.4°C, and the average austral winter temperature is 1.85°C; average austral summer temperature is 13.2°C. The Andes act as an effective barrier in blocking the movement of the SWW from the west, causing orographic precipitation at high elevations and dry conditions on the eastern Argentinian flank of the Andes (Fig. 2.2; Paruelo et al. 1998).

The dominant tree species in the temperate rainforest are the shade-intolerant conifer *Fitzroya cupressoides* and *Nothofagus* species accompanied by shade-tolerant trees including *Laureliopsis philipiana*, and *Saxegothaea conspicua* (Kitzberger and Veblen 2003). Subalpine forest at elevations >1000 m are dominated by *Nothofagus pumilio*. With the eastward decline in precipitation, *Nothofagus dombeyi* forms a homogeneous forest composition with a 3- to 6-m

tall, dense bamboo (*Chusquea culeou*) understory. At intermediate precipitation levels (1,500 – 1000 mm yr), the conifer *Austrocedrus chilensis* co-dominates with *Nothofagus dombeyi*. With increasing aridity (< 1,000 mm yr) to the east, pure open stands of *Austrocedrus chilensis* become dominant with xeric shrubs such as *Aristotelia chilensis* and *Lomatia hirsuta*. At the forest-steppe ecotone, *Austrocedrus chilensis* form open woodlands with steppe grasses and small shrubs such as *Discaria* articulate and *Mulinum spinosum*. *Nothofagus antarctica* dominates nutrient-limited sites, xeric sites close to the steppe, along stream and bogs with high ground water, disturbed sites, and places exposed to strong winds, and high insolation (north-facing slopes) (Kitzberger and Veblen 2003).

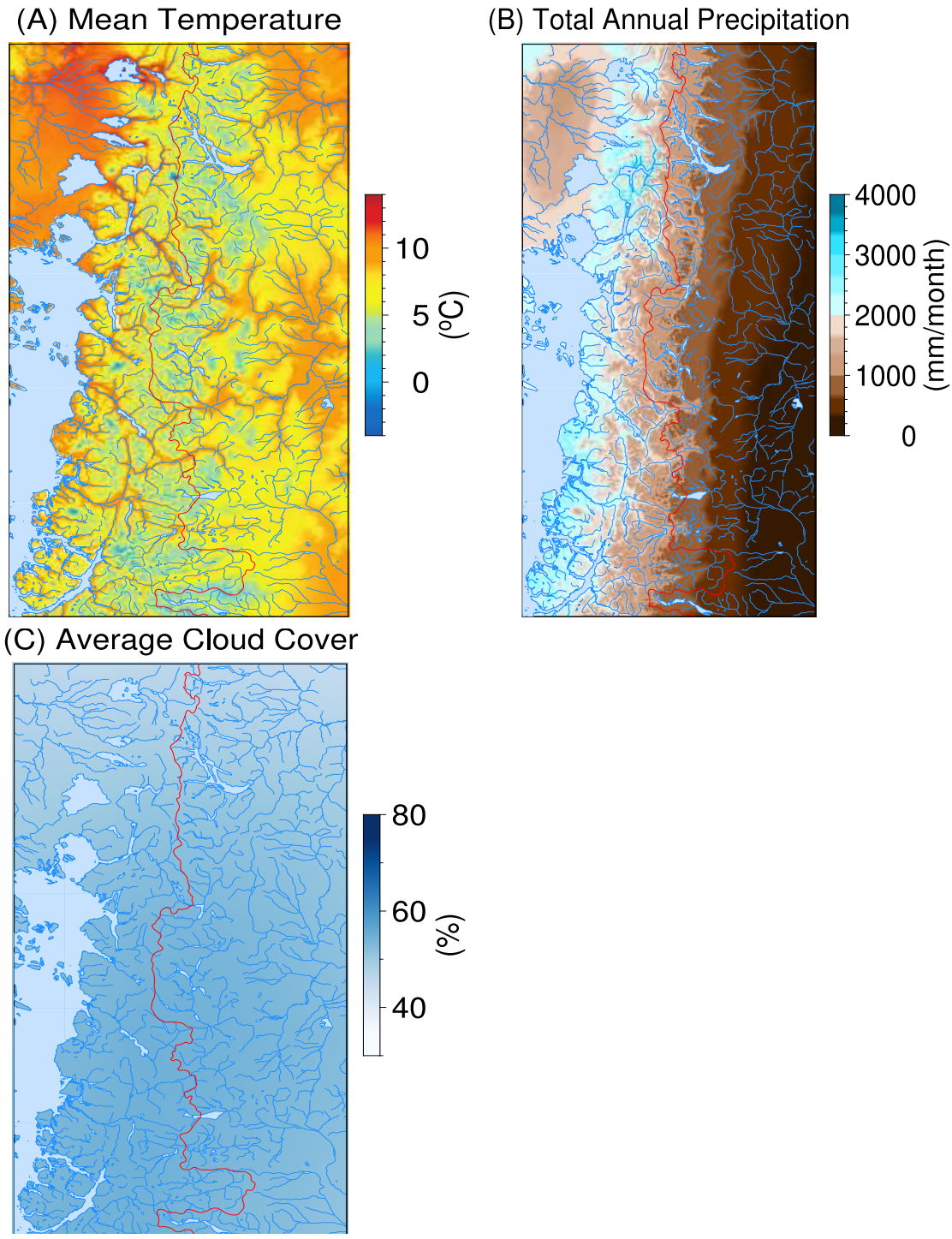

Figure 2.2 Spatial distribution of downscaled (1981-2010) CRU climate data (1 km resolution) (a) mean temperature (degrees Celsius). (b) annual precipitation (mm/month). (C) mean cloud cover (%). The red line shows the border between Chile and Argentina.

Methods

LPJ-GUESS was run with monthly climate data from the climate research unit (CRU; 1901 to 2016) to simulate the vegetation of northern Patagonia. The model was parameterized with the major plant functional types (PFTs) and local tree species that dominate the study area. For model evaluation, we compared the simulated above and below biomass from the model (2000 – 2013) with remotely sensed derived above-ground biomass (AGB; 2000-2013), as well as trends in vegetation greenness and remotely-sensed burned area. A paired t-test on 20000 randomly selected site was used to determine whether differences between CO_2, fire, and climate were significant on simulated biomass.

Ecosystem model description

LPJ-GUESS is a DGVM that follows the BIOME3 model (Haxeltine and Prentice 1996). It is designed to model both regional and global vegetation, using a forest gap model in its implementation of plant biophysical properties such as demography and plant resource competition (Prentice 1983, Bugmann 2001). Model outputs from the model such as biomass, nitrogen balance, vegetation structure and composition, have been compared with observational data, such as ecosystem flux, field observation, and data inventory associated with net primary productivity (e.g. Jung et al. 2007, Hickler et al. 2008, De Kauwe et al. 2014), and remote-sensing data (e.g. Tang and Beckage 2010, Lindeskog et al. 2013, Blanke et al. 2016). Sensitivity analyses and model-data comparisons suggest that LPJ-GUESS performs very well when compared with other terrestrial vegetation models (e.g. Piao et al. 2013, Sitch et al. 2015). In LPJ-GUESS, each grid cell is represented by latitude and longitude, and individual Plant Functional Types (PFTs) and tree species are simulated in multiple patches

(1000 m^2) within each grid cell. Establishment of each Plant Functional Types (PFTs) and tree species occurs yearly as long as there is space within the grid cell and the simulated climate is within the prescribed bioclimatic limits of the PFT or tree species.

The model simulates soil water content using a two-layer soil hydrology scheme with each layer of fixed thickness (0.5 upper and 1.0 m lower respectively) and with percolation between layers, including surface and sub-surface runoff (Haxeltine and Prentice 1996). The model also integrates a process-based fire model called Glob-FIRM (Global FIRe Model) to simulate burned area, linking fire with fuel load and fuel moisture, factors that in turn depend on climate and simulated vegetation. Ignitions are assumed to be unlimited, and the area burned is related to fire season length. The fire effects depend on the length of fire season and PFT or tree-species specific fire resistance value. In our simulation, we assumed that the smallest area burned in a grid cell is equal to 1000 m^2 (Thonicke et al. 2001b).

Plant Functional Types and species parameterization

We estimated the bioclimatic parameters associated with the establishment of the six-tree species and two plant functional types (PFTs) groupings specific to the region, and two grasses (high and low elevation; Table 2.1). The bioclimatic parameters are minimum coldest month mean temperature for survival (T_{cmin_surv}), (2) minimum coldest month mean temperature for establishment (T_{cmin_est}), (3) maximum coldest month mean temperature for establishment (T_{cmax_est}), (4) minimum warmest month mean temperature for establishment (T_{wmin_est}) and (5) minimum growing degree days sum on a 5-degree Celsius base (GDD_5). GDDs were estimated as a function of monthly mean temperature (Wang et al., 2006) using the equation below:

$$GDD5 = \sum_{1}^{12}(Tm - 5)\ X\ Nd \quad Tm \geq 5^{\circ}C \qquad (1)$$

Where GDD_5 is the annual sum of monthly temperature above 5°C, T_m is the monthly mean temperature ($T_m \geq 5^{\circ}C$), and Nd is the number of days in a month. In the model, PFTs or tree species will not establish in a particular grid cell if the average value of the last 20 years for these variables does not exceed the threshold given in Table 2.1 (Venevsky et al. 2002). Following a workshop in Bariloche, Patagonia in spring 2016, we estimated bioclimatic parameters for each tree species and PFTs based on distribution map associated with the classification of southern South America vegetation belts published by the World Wildlife Fund (WWF) (Olson et al. 2001) and Worldclim with a resolution of (~ 1 km) (Hijmans et al. 2005). The vegetation maps (WWF & Worldclim) classify each PFT and tree species into bioclimatic zones that are strongly associated with the distribution of each PFT and tree species. This climate database together with monthly means meteorological data from the Climate Research Unit (CRU) datasets was used create a bioclimatic classification for northern Patagonia which was used to construct the northern Patagonian bioclimatic natural vegetation distribution maps. The bioclimatic zone for each PFT and tree species was subsequently extracted from the vegetation map and overlay on the CRU climate data. We then choose boundary values between 5% and 95% CI of these variables (Table 2.1) that correspond to the observed limit of each of the PFT and tree species.

Table 2.1: Species parameters and bioclimatic limits used in the simulation: GDD_5; minimum growing degree-day sum (5°C base), T_{cmin_est} (T_{cmax_est}): minimum(maximum) coldest month mean temperature. T_{wmin_est}: minimum warmest month mean temperature, $T_{cmin\_surv;}$ minimum coldest month temperature, D_T; Drought tolerance. We use '- ' to indicate that no limit is applied.

Species	DD_5	T_{cmin_est}	T_{cmax_est}	T_{wmin_est}	T_{cmin_surv}	D_T
High elevation 300 to 1931 m] grasses (e.g., Asteraceae)	100	-	0	-	-	-
Low elevation [0 to 299 m] grasses (e.g., Stipa speciose, Euphorbia collina)	1500	0.6	-	11.6	-1.3	-
Mixed evergreen shrubs (e.g., Lomatia hirsuta, Schinus Patagonicus)	700	-0.33	5	10.8	-3.2	0.59
Broadleaved evergreen warm temperate tree (e.g., Eucryphia cordifolia, Weinmannia trichosperma)	1500	1.73	7.9	10.1	0.23	0.70
Austrocedrus Chilensis	1350	0.6	6.3	11.6	-1.3	0.58
Fitzroya cupressoides	600	6.4	0.18	9.3	-1.4	0.65
Chusque culeou	700	-1.6	4.3	8.6	-3.7	0.62
Nothofagus dombeyi	1000	0.53	8.15	10.9	-1.4	0.63
Nothofagus pumilio	400	-1.6	4.3	8.6	-3.7	0.62
Nothofagus betuloides	1100	0.53	8.15	10.9	-1.4	0.68
Nothofagus antarctica	700	-0.36	4.8	10.3	-2.9	0.58

We also focused on fitting parameters related to limiting factors for growth for each tree species and PFT based on the literature (Veblen et al. 1996, Donoso 2006, Avaria 2013). For example, the variables related to growing season length (characterized by growing degree days, (GDDs) and growing season drought; Sykes et al. 1996) were considered the most limiting factors for Austrocedrus chilensis. The bioclimatic parameters are listed in Table 1.

The parameters used for tree species were based on information about the composition and distribution of native forest in southwestern Argentina and southern Chile (Pollmann and Veblen 2004).

Environmental data and simulation protocol

Present-day vegetation cover was modeled using six experimental scenarios (Table 2.2) to determine the role of climate, CO_2, and fire. The study was set up using current era climate data for the "historical period" 1901-2016. LPJ-GUESS began the simulation from "bare ground," (i.e., LPJ-GUESS assumes no vegetation in the grid cells), and the model was run on 100 replicate patches within each grid cell at 1 km^2 (0.008333°) resolution. Each patch has a stochastic element for establishment, mortality, and patch-replacing disturbance, thus allowing the model to represent a quasi-stable landscape pattern and process. The first phase in the simulation is a 1,000 years spin-up to achieve equilibrium in pre-industrial stable vegetation structure and carbon pools. For this phase, the first 30 years of detrended historical climate data (1901 – 1930) were used repeatedly as model input with pre-industrial atmospheric CO_2 content. The detrending of the climate data (1901 - 1930) was done to remove long-term trends in order to emphasize short-term changes in the climate data, (i.e., variations related to ENSO and SAM).

Table 2.2. The simulations comprise six combinations of the input conditions.

Climate	Fire	CO_2	LAND MASK
HISTORICAL (S1)	on	Historical	off
HISTORICAL (S2)	on	Historical	on
HISTORICAL (S3)	off	Historical	on
HISTORICAL (S4)	on	Pre-industrial	off
PRE-INDUSTRIAL (S5)	on	Pre-industrial	off
PRE-INDUSTRIAL (S6)	on	Historical	off

The historical period was simulated following the spin up and was run from 1901 to 2016 with observed changes in atmospheric CO_2 and climate. The original meteorological data consisted of monthly time series corresponding to mean air temperature, total precipitation and cloud cover percentage at a spatial resolution of 0.5° for the model domain from climate database CRU TS 4.01 provided by the Climate Research Unit (CRU), University of East Anglia. The CRU climate data were spatially downscaled and biased-corrected to match the spatial resolution (1 km^2) and historical period of overlap (1960-1990) from the WorldClim-Global Climate Database (http://www.worldclim.org/) (see Zhang et al. 2017 for details of the methods). We compared the performance of the downscaled CRU precipitation and temperature climate data with the Northern Patagonia Climate Grid data (NPCG; Bianchi et al. 2016). Our results showed good agreement with the NPCG climate data (Fig. S1). The soil texture data used in the simulation were based on the WISE30sec database (0.00833º spatial resolution; Batjes 2015), and were used to provide sand, silt and clay content for estimating water-holding capacity and thermal diffusivity at 1 km resolution.

Experimental design

The different scenarios consider the effects of different drivers on vegetation patterns and trends over time (observed CO_2, observed climate, pre-industrial (PI) CO_2 and PI climate; Table 2.2). For the pre-industrial climate, we cycled detrended CRU climate data for the period (1901-1930), for 116 years (1901-2016); for the observed climate we used CRU historical climate data from 1901–2016. A land-masking system was implemented into LPJ-GUESS to ensure that fire did not occur in urban or agricultural areas using data from the land cover data from the Global Land Cover 2000 (GLC2000) for South America (European Commission, Joint Research Center,2003), which consists of 55 land cover classes at 1 km^2 spatial resolution (Bartholomé and Belward 2007). We classified urban and agricultural grid cells as masked and scaled each 1 km^2 pixel to range between 0 and 1 accordingly. The simulated fire is limited to those areas that were not masked. To assess how well the model represents the biomass gradient in Patagonia (Objective 1), we evaluated it against a biomass map derived from various satellite observations of surface reflectance and vegetation height. For more information see Avitabile et al. (2016). A Pearson correlation coefficient was computed to assess the relationship between the simulated and remotely-sensed biomass. For objective 2, we used Global Inventory Modeling and Mapping Studies third-generation NDVI (GIMMS NDVI3g) at 8 km resolution for the period of January 1981 to December 2016 based on the Advanced Very High-Resolution Radiometer (AVHRR) sensor to understand regions of browning and greening in the vegetation. The NDVI data are a composite of daily values each half-month (Tucker et al. 2010). NDVI is widely used as a proxy for vegetation productivity and vegetative response to seasonal climate variability (Zhu et al. 2016). Trend

analysis on GIMMS NDVI was performed using Trend Estimation on Annual Aggregated Time Series (AAT) based on Forkel et al. (2013).

We used the modeled carbon in vegetation biomass (Objective 3) from the S1 scenario (historical climate, changing CO_2, land masking on, with fire 'on') and S4 scenario (historical climate, PI CO_2 (280 ppm), no land masking, with fire 'on') to evaluate the effect of CO_2 on forest cover. The difference between the simulations isolates the impact of increasing CO_2 on forest cover compared to the PI level. The same logic was applied to isolate the effect of fire and climate on forest cover. The fire effect was calculated by the difference between S2 (historical climate, changing CO_2, land masking on, with fire 'on') and S3 (historical climate, historical CO_2, land masking on, with fire 'off'). While S1 and S6 (PI climate, historical CO_2, land masking off, with fire 'on') and S4 (historical climate, PI CO_2, land masking off, with fire 'on') and S5 (PI climate, PI CO_2, land masking off, with fire 'on') were used to calculate the effects of climate. Analysis of the interactions and the statistical significance of their effects was determined using paired t-tests of difference between the means as estimated for the entire study region. The six experimental set-up (Table 1) allows the full evaluation of the individual and combined effect of climate, CO_2, and fire incidence on above-and belowground biomass.

Lastly, we used results from Glob-Firm to compare the similarity of the annual burned area from MODIS and LPJ-GUESS DGVM outputs for the period of 2001 to 2014. The Terra and Aqua combined MCD64A1 Collection 6 sensor Burned Area data product is a monthly, Level-3 gridded 500-m product containing per-pixel burning and quality information. For more information on the MODIS burned area product see Giglio et al. (2018)

Results

Overall, the model results show that between 1930 and 2010 there was an increase in biomass based on the S2 (historical climate, historical CO_2, land masking on, with fire 'on') simulation (Fig. 2.5b & Table 2.3). This increase in biomass is coincident with changes in CO_2, increasing temperature, and decreasing precipitation (Fig S5; Veblen et al. 2011). In contrast, the PI CO_2 decrease forested area under these observed climate changes. However, PI climate reduced forest distribution under PI CO_2, but the effect of PI climate alone on biomass was minor compared to the effect of PI CO_2. However, the absence of fire increased forest biomass under changing climate, increasing CO2, land masking on and fire off.

Table 2.3: This table shows the quantile summary (kg C m^{-2}) for all the scenarios used in these analyses.

Scenarios	0%	25%	50%	70%	100%
HISTORICAL (S1)	0.00	0.19	2.22	15.7	28.39
HISTORICAL (S2)	0.00	0.19	0.65	9.88	29.13
HISTORICAL (S3)	0.00	0.19	0.65	10.27	29.06
HISTORICAL (S4)	0.00	0.13	1.67	13.57	24.59
PRE-INDUSTRIAL (S5)	0.00	0.08	0.42	12.16	23.14
PRE-INDUSTRIAL (S6)	0.00	0.13	0.53	14.17	26.65

Spatial distribution of biomass

The spatial distribution of forests simulated by S2 (historical climate, historical CO_2, masking on, with fire 'on') and remotely sensed above-ground biomass (AGB) are shown in Fig. 2.4. The model captured the general observed distribution of present-day vegetation from the temperate rainforest west of the Andes to the mesic forests on the east. The model results underestimate the sharp lower treeline boundary on the eastern side of the Andes and instead showed low simulated biomass (Fig. 2.3). Simulated biomass ranged from 0 to 29.5 kg C m^{-2}, whereas remotely sensed observed above-ground biomass ranged between 0 to 48 kg C m^{-2}. There was a positive correlation between the two variables (R^2 = 0.71; simulated mean = 5.68 kg C m^{-2}, observed mean = 7.72 kg C m^{-2}). Overall, there was a strong positive correlation between simulated and observed biomass especially in the temperate forest west of the Andes and the mesic forest at high elevations on both sides of the Andes (Fig. 2.4a & b).

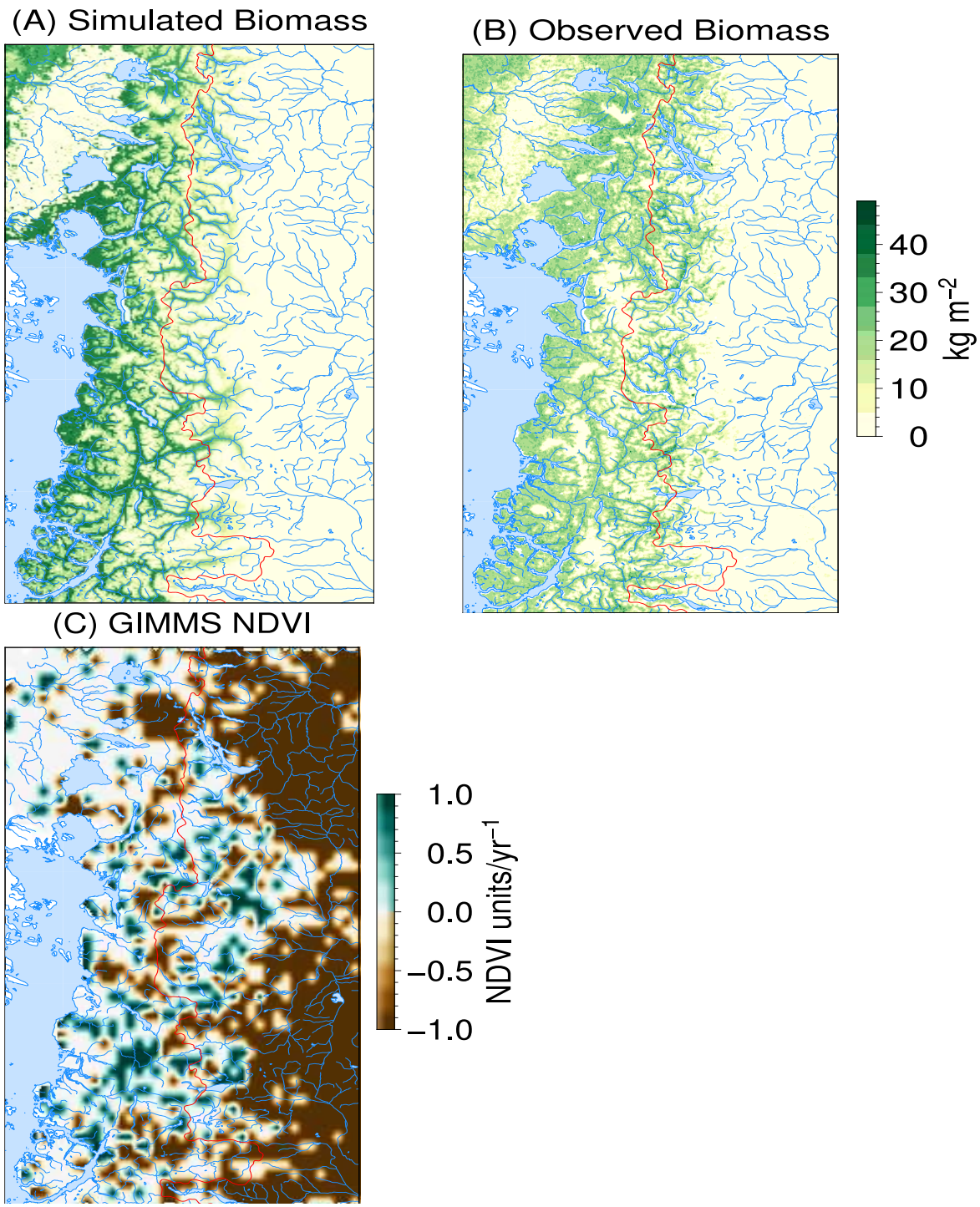

Figure 2.3: Spatial distribution of (A) simulated above and below ground biomass based on S2 (historical climate, historical CO_2, masking on, fire 'on'), and (B) Avitabile et al. (2016) observed biomass (Kg C m^{-2}), (C) Trends in annual mean NDVI in northern Patagonia from 1982 to 2016. Trend significance is estimated using Forkel et al. (2013) Annual Aggregated Time series (AAT). The simulated above ground biomass is based on S2 (historical climate, historical CO_2, masking on).

The analysis of annual aggregated time series (AAT) GIMMS NDVI dataset from 1982-2016 shows a greening trend (mean = +0.17 NDVI units/y^{-1}, $P < 0.05$, standard deviation (SD) = 0.38) for 9.12% of the spatial pixels. However, an observed browning trend (mean = -0.51 NDVI units/y^{-1}, $P < 0.05$, SD = 0.500) was detected for 46% of the spatial pixels. The mean trend for the entire region was -0.001027 NDVI/yr^{-1} (Fig. 2c). The high browning percentage was concentrated in steppe vegetation while the greening trend occurred in the mesic forest (Fig. 2.4c).

In S2 (historical climate, historical CO_2, masking on, with fire 'on'), high biomass at the mesic forest (high elevation) and forest-steppe ecotone was accompanied by a decrease in the burned-area fraction from 1901-2016. However, the burned-area fraction increased with latitude along the steppe from north to south (Fig. 2.5b). In the steppe, mixed patches of high and low burned area are consistent with previous studies that show fuel discontinuity at the steppe (see Fig 2.5b, c & d Kitzberger and Veblen 1999). Under S2 scenario there was an increase in biomass and decreased burned-area, the soil water content was low at the forest-steppe ecotone but increased at the steppe, likely due to increased effective moisture from the South Atlantic polar front (Kitzberger and Veblen 2003) (Fig. 2.5c & d).

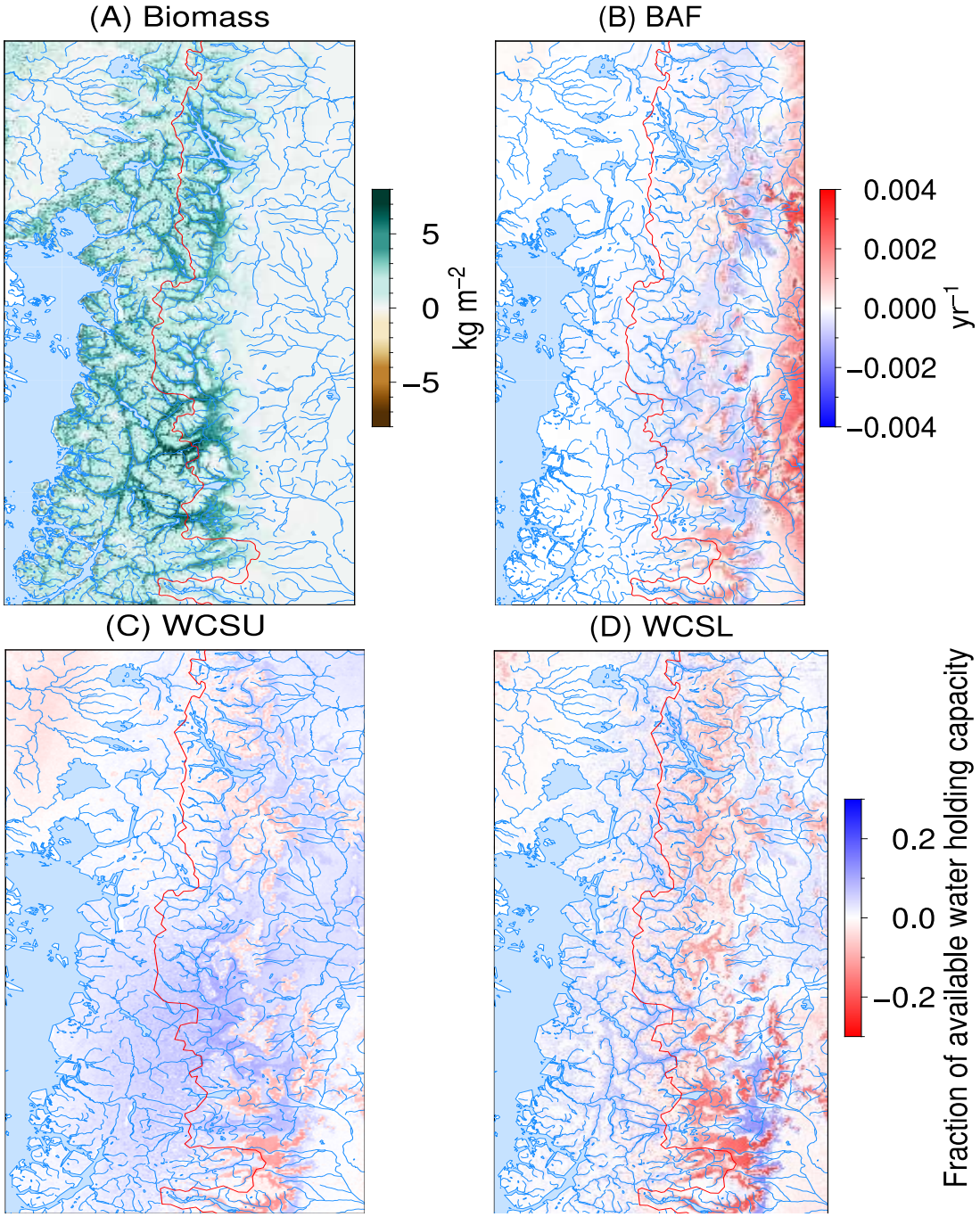

Figure 2.4: Changes in metric between 1930 and 2010 from S2 scenario (historical climate, historical CO_2, fire 'on'). Positive values suggest increases and negatives values suggest decrease (A) average tree biomass (Kg C m^{-2}). (B) average burned-area fraction (C) Upper soil moisture (fraction of available water holding capacity), see legend for (d), and (D) Lower soil moisture (same unit as (C)).

Spatial differences in biomass patterns between all simulations

Overall, the inclusion of masked area and fire 'on' in S2 (historical climate, increasing CO_2, masking on, with fire 'on') results in an average 25.8% increase in simulated biomass between 1930 and 2010. However, the exclusion of masked area and fire 'on' (S1) increased biomass by 22.6% while the S3 scenario, with masked area 'on' and fire 'off' increased simulated biomass by 24.8%. Furthermore, S1, S2, and S3 all show the same spatial pattern of biomass distribution with increased biomass at the temperate forest west of the Andes, mesic forest (high elevation), but the highest biomass gain was at the forest-steppe ecotone (Fig. 2.6a b & c).

On average, PI CO_2 under warming historical climate (S4) increase simulated tree biomass by 10.4%. In the S4 simulation, there was an increase in biomass in the mesic forest (high elevation), and at the forest-steppe ecotone, but the most substantial decline in biomass occurred at the temperate forest west of the Andes. The use of S5 (PI climate and low CO_2) produced a realistic reduction in simulated biomass by -1.6% from the temperate forest west of the Andes, to the Patagonia steppe, and also from north to south in the study area (Fig. 2.6e). However, the use of PI climate with changing CO_2 (S6) increased the simulated biomass by 9.6%. While in S6, the most substantial gain in biomass occurred mainly at the temperate forest west of the Andes (Fig. 2.6f & Table 2.3).

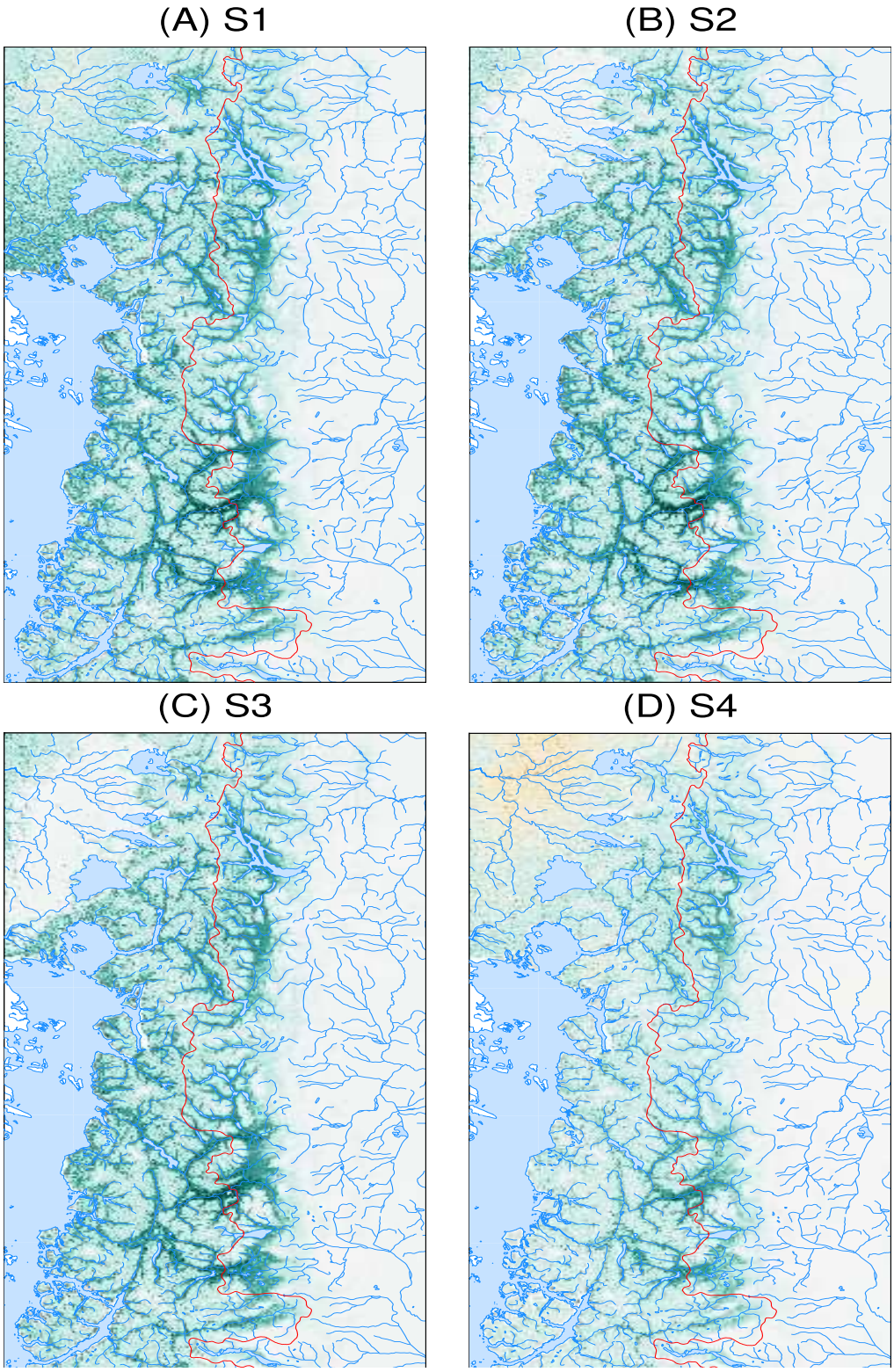
(A) S1
(B) S2
(C) S3
(D) S4

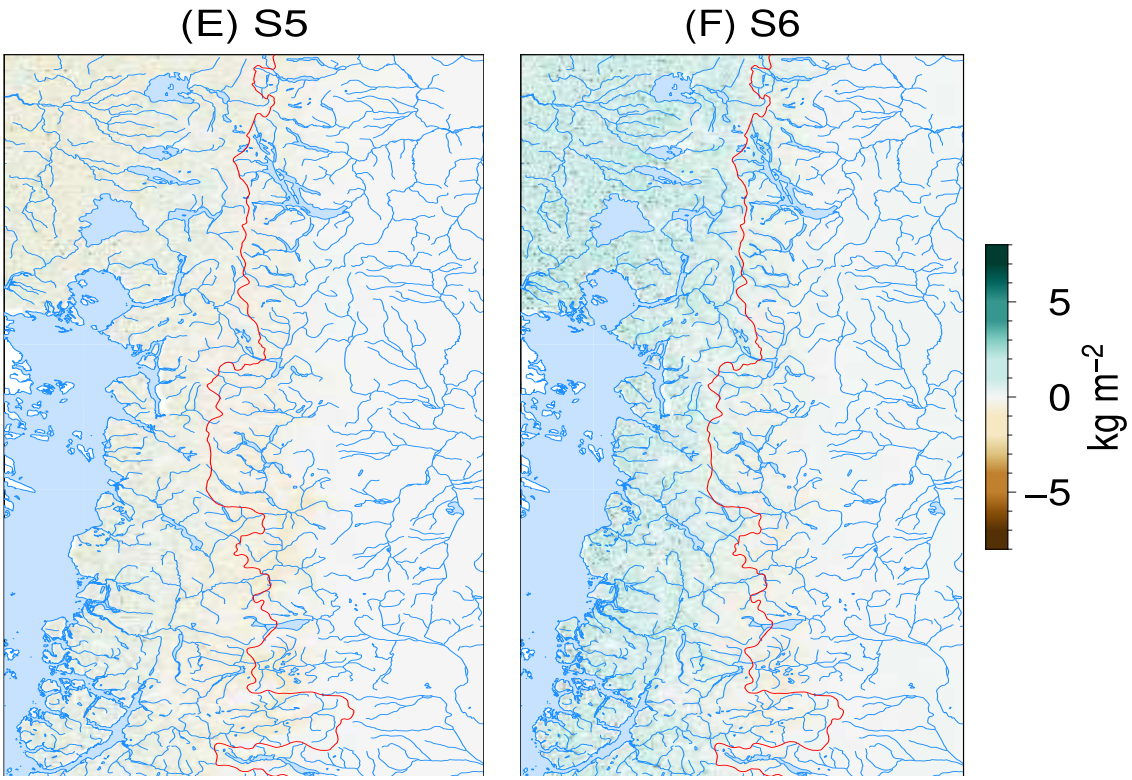

Figure 2.5: Mean tree biomass: Changes between 1930 and 2010. Positive values suggest high biomass and negative values suggests low biomass A) S1 (historical climate, historical CO_2), B) S2 (historical climate, historical CO2, masking on), C) S3 (historical climate, historical CO_2,masking on, fire off), D) S4 (historical climate, PI CO_2), E) S5 (PI climate, PI CO_2), and F) S6 (PI climate, historical CO_2).

Spatial differences in burned-area patterns between all simulations

Fig. 2.7 shows the results of simulated LPJ-GUESS burned area for S2 and the observed burned area from MODIS. The model overestimates burned-area when compared with the result from MODIS BA but the simulations showed the same temporal pattern as the MODIS data. Fire plays a significant role in the reduction of biomass in S5 (PI climate and PI CO_2, agriculture mask off, fire 'on'), but the reduction in forested area is less than that caused by the PI CO_2 under PI climate (Fig. 2.8e). The small area burned or absence of fire in all the simulations in temperate forest west of the Andes and the mesic forest at high elevations is

mainly related to water availability because high effective moisture increases soil water content and makes the forest naturally fire resistant (Fig. 2.8a, b, d, e & f). Moving into the steppe, the magnitude of fire increased because of seasonally dry summers that increased fuel desiccations (Fig. 2.8).

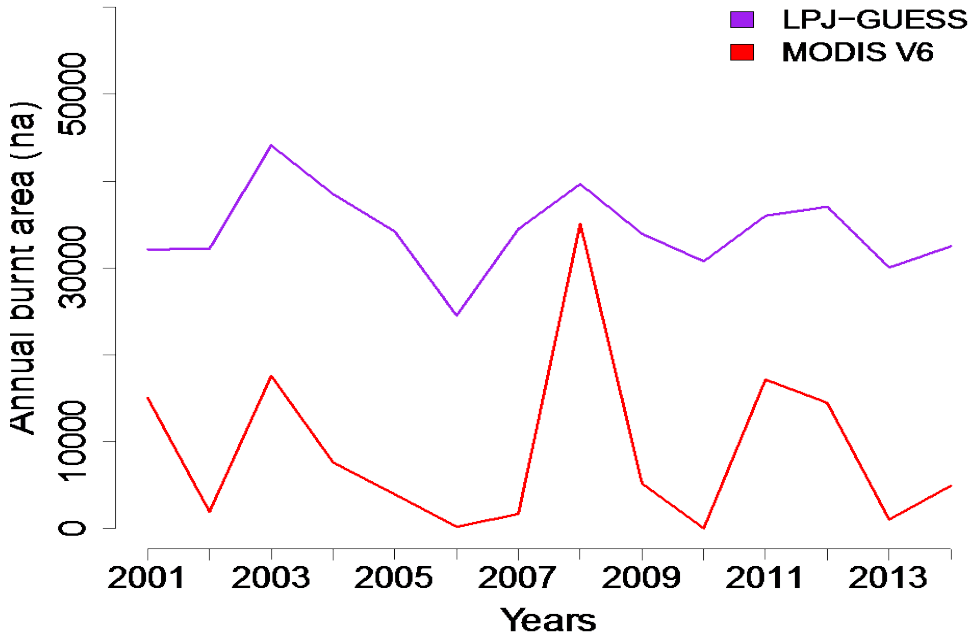

Figure 2.6: Mean annual burned area during 2001- 2014 in northern Patagonia. MODS V6 observations and LPJ-GUESS burned-area simulation: S2 (historical climate, historical CO_2, masked on, with fire 'on').

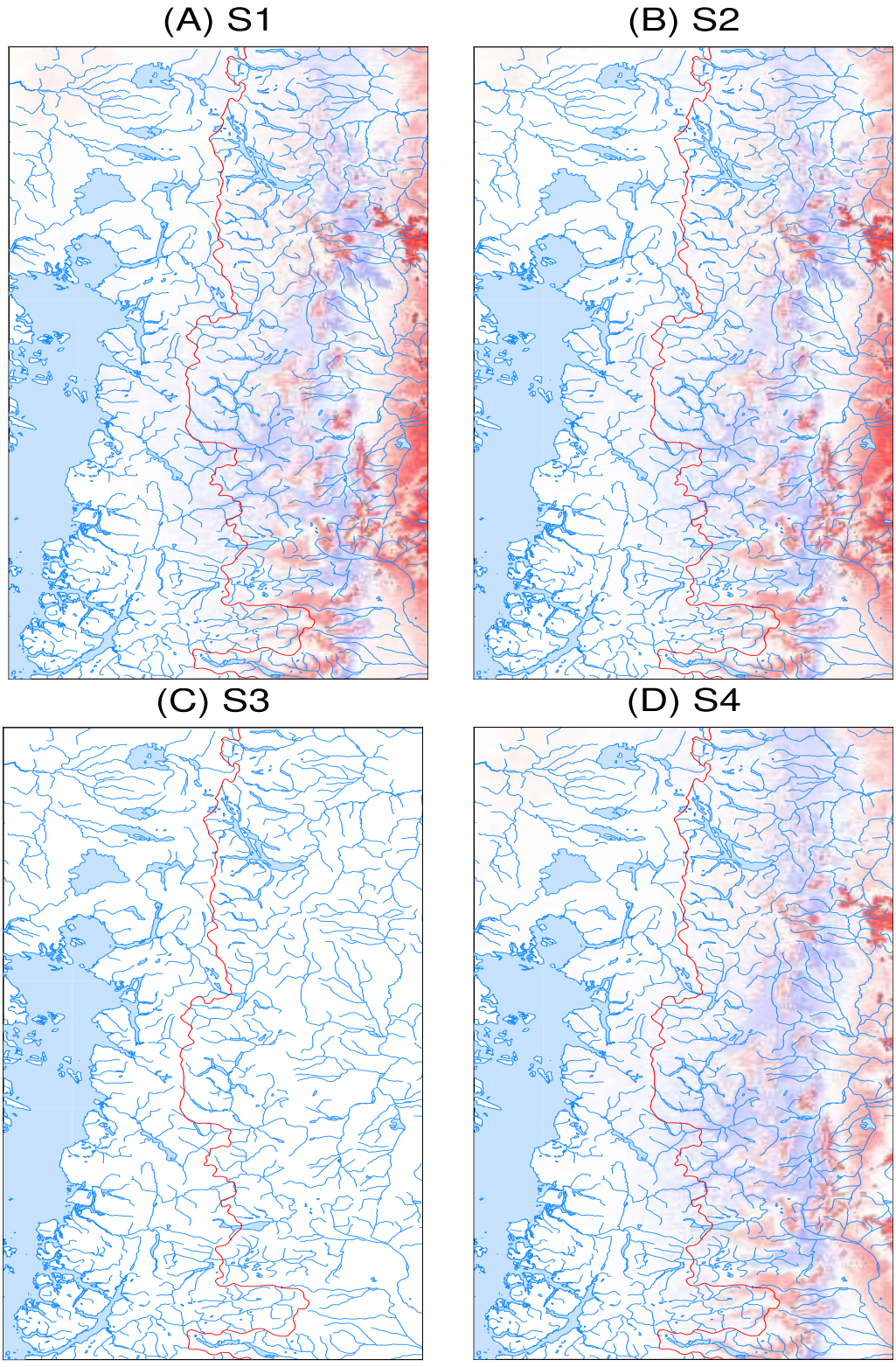
(A) S1
(B) S2
(C) S3
(D) S4

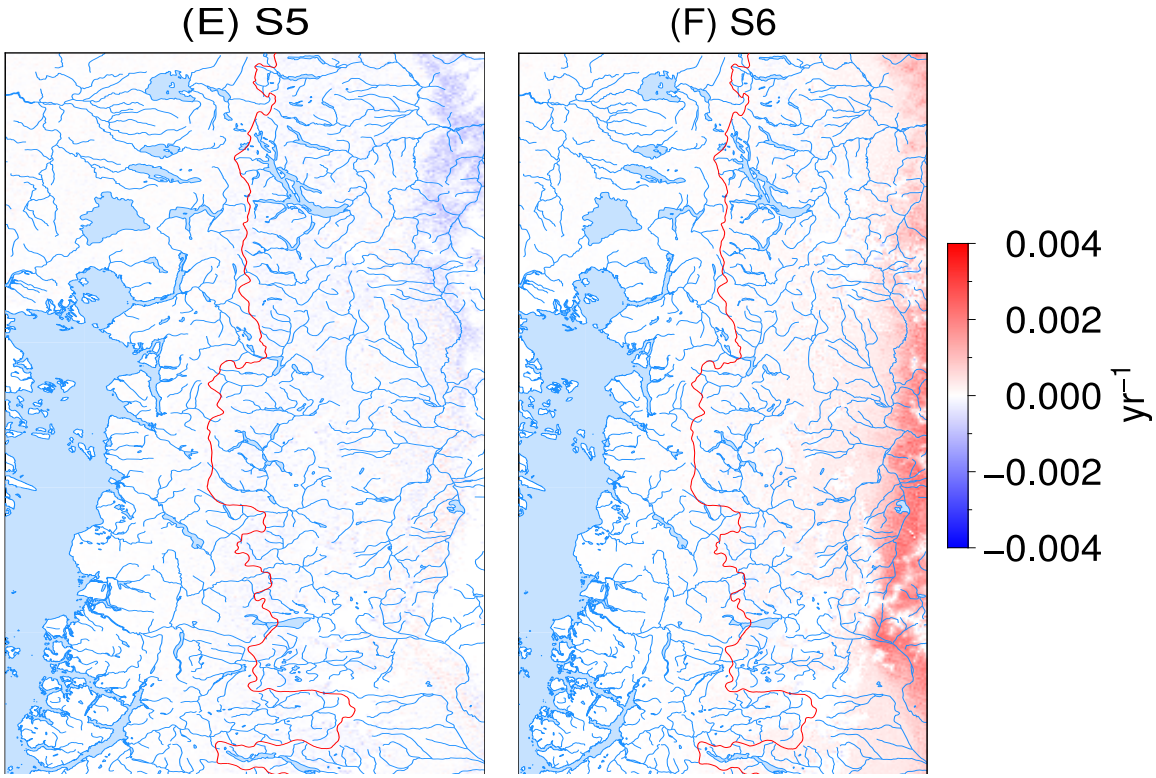

Figure 2.8: Mean burned area fraction. Changes between 1930 and 2010. Positive values suggest region of high fire activity and negative values suggests regions of low fire activity. A) S1(historical climate, historical CO_2), B) S2 (historical climate, historical CO2, masking on), C) S3 (historical climate, historical CO_2,masking on, fire 'off'), D) S4 (historical climate, PI CO_2), E) S5 (PI climate, PI CO_2), and F) S6 (PI climate, historical CO_2).

Effect of atmospheric CO_2, fire and climate on simulated biomass

To assess the effect of CO_2 on simulated biomass, two sets of combinations (S1 - S4 & S6 – S5) was analyzed. The difference between S1 (historical climate, increasing CO_2, agriculture mask off, with fire 'on') and S4 (historical climate and PI CO_2, agriculture mask off, with fire 'on') overall shows increased in forest productivity (Fig. 2.9a). The results of the paired *t*-test between S1 and S4 indicated that the inclusion of changing CO_2 in S1 was responsible for the increase in average biomass (M= 1.03 kg m^{-2}; t (19999) = 100.31, P <0.01) due to CO_2 fertilization. Consequently, the effect of low CO_2 thus reduces more biomass at

the forest-steppe compared to the temperate forest west of the Andes, and the mesic forest (high elevation). Also, the difference between S6 (PI climate, changing CO_2) and S5 (PI climate, PI CO_2) shows increases (M= 0.93 kg m^{-2}; t (19999) = 94.65, P <0.01) in biomass caused by CO_2 fertilization which increase the biomass stock (Fig. 2.9b). The result shows that the inclusion of changing CO_2 caused the observed increase in forest productivity. The spatial difference between S2 (historical climate, increasing CO_2 agriculture mask on, with fire 'on') and S3 (historical climate, increasing CO_2, agriculture mask on, with fire 'off') revealed biomass loss throughout the study region (Fig. 2.9c). The inclusion of fire reduced forest cover compared to the absence of fire (M = -0.21 kg m^{-2}; t (19999) = -29.93, P <0.01).

The effect of climate was analyzed based on two combinations (S4 – S5 & S1 – S6). The comparison between the mean of S4 (historical climate and PI CO_2) and S5 (PI climate and PI CO_2) showed increase in biomass under changing climate (M = 0.82 kg m^{-2}; t (19999) = 76.47, P <0.01), Nonetheless, the contribution of climate to biomass reduction, as evidenced in Fig. 2.9d, was a decrease in biomass in the temperate forest west of the Andes. However, biomass increased at the mesic forest and the forest-steppe ecotone. The effect of climate based on the difference between S1 (historical climate and historical CO_2) and S6 (PI climate and changing CO_2) revealed the same spatial pattern as S4 – S5 (Fig. 2.9d & e). The presence of changing climate increased simulated average biomass (M= 0.918 kg m^{-2}; t (19999) = 76.74, P <0.01)

(A) S1 – S4

(B) S6 – S5

(C) S2 – S3

(D) S4 – S5

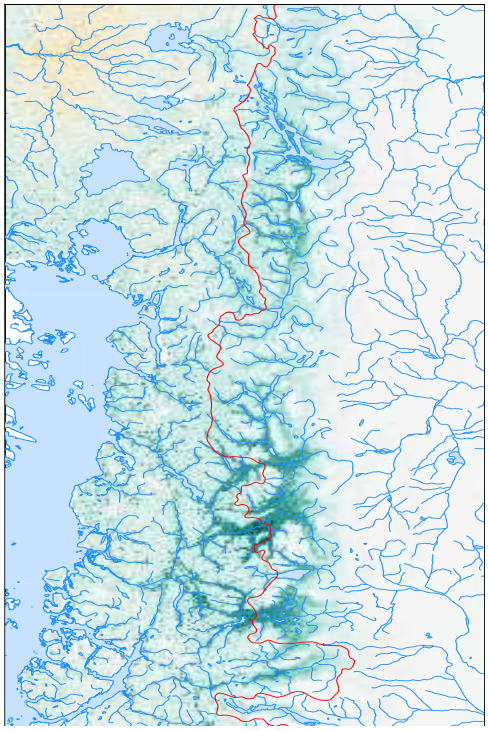

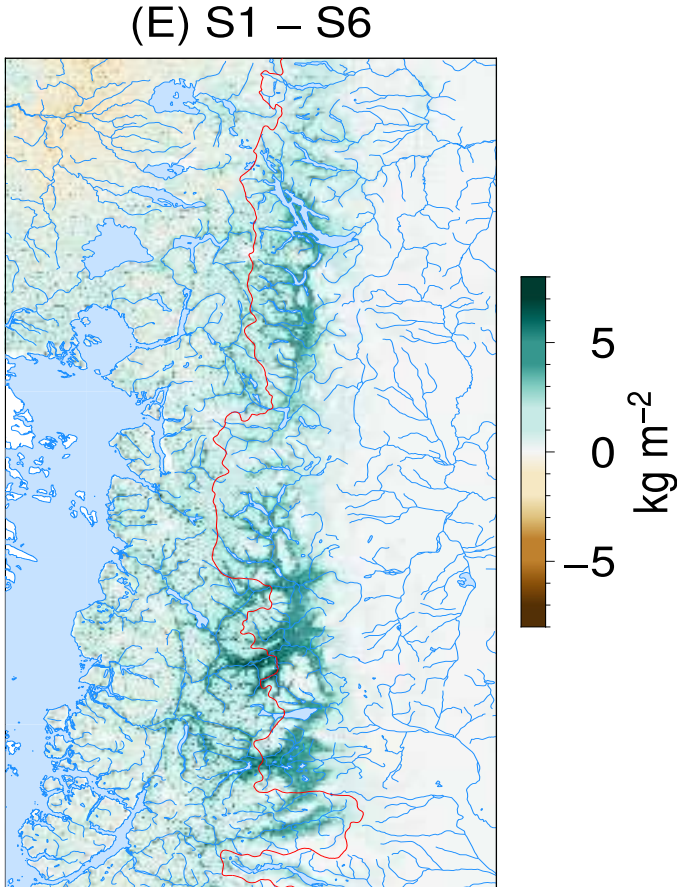

Figure 2.8: Effect of CO_2, fire, and climate on forest cover. The figure show changes in metric between 1930 and 2010. A & B; The effect of CO_2: A (S1: historical climate, historical CO_2) minus S4 (historical climate, low CO_2); B (S6: PI climate, changing CO_2 minus S5: PI climate, PI CO_2). C) The effect of fire (S2: historical climate, historical CO_2, masking on, with fire 'on') minus S3 (historical climate, historical CO_2, masking on, with fire 'off'). D & E: Effect of climate; D (S4: historical climate, low CO_2) minus (S5: PI climate, low CO_2) E (S1: historical climate, historical CO_2) minus (S6: PI climate, historical CO_2). Positive values suggest region of increasing biomass and negative values suggests region of decreasing biomass.

Discussion

Our study provides the first attempt to use a DGVM to simulate drivers of modeled forest cover change in southern South America. As revealed by these new findings the incorporation of 20th century atmospheric CO_2 concentrations, climate, and fire in LPJ-GUESS assessed their relative influence on the simulated vegetation structure and dynamics

of the Patagonia study area (Fig. 2.6a). However, the interactions at high and low elevation in these transitions have seldom been considered before. The results suggest that climate, CO_2, and fire play a crucial role in determining the long-term vegetation dynamics. Our results shows (Fig. 2.6a) that (1) changing climate accompanied by a steep increase in atmospheric CO_2 concentration likely increase forest growth, because the high rate of photosynthesis increased water use efficiency (WUE), and (2) fires are a relatively frequent disturbance at the forest-steppe ecotone (Fig 2.8). Our result is broadly consistent with other forest models that respond very positively to steep increases in CO_2 with an increase in forest productivity (Pan et al. 1998, Ciais et al. 2008, Kirschbaum et al. 2012, Hickler et al. 2015). Also, results from dendrochronology analysis in northern Patagonia shows variation in fire frequency responds to regional climate variability (Kitzberger and Veblen 2003).

Changes in forest cover

The results from S4 (historical climate and low CO_2), S5 (PI climate and low CO_2), and S6 (PI climate and historical CO_2 ; Fig. 2.6d, e & f) scenarios show low biomass and support studies that examine the factors (e.g., CO_2) that limit woody forest expansion into grasslands (Bond 2008, Hirota et al. 2011). The significant greening and browning trends (1982 – 2016) occur in 9.12% and 46% of the natural vegetation of northern Patagonia, with 44% of the remaining pixels showing no significant change. The strong greening trend occurred in the mesic forest (high elevation) and forest-steppe (low elevation), while strong browning trend was more pronounced at the semi-arid steppe (Fig. 2.4c).

The differences between 1930 and 2010 from S2 (historical climate and historical CO_2) revealed that biomass increased from the temperate rainforest west of the Andes to the forest-

steppe ecotone. The increase in biomass at the forest-steppe ecotone, coincided with a decrease in the fraction of burned area and decrease in soil moisture at the forest-steppe (Fig. 2.5b, c, & d). Our results suggest that CO_2 fertilization, and changing climate, combined with reduction in fire frequency caused forests to expand. The observed increase in forest cover and a decrease in fire frequency are consistent with previous research in northern Patagonia that shows changes in land cover as result of intensive grazing and land management practices (Veblen and Lorenz 1987, Veblen and Lorenz 1988, Kitzberger and Veblen 1999, Gowda et al. 2011). However, in this study, climate and CO_2 drive the increase in forest cover while empirical results from previous studies using dendrochronology analysis attributed forest expansion to intentional fire suppression and more effective fire management at the forest-steppe ecotone (Veblen and Lorenz 1988). Despite the observed decline in precipitation and increase in temperature in northwestern Patagonia since the 1940's based on CRU data analysis Figure 5S (Veblen et al. 2011), forested area has increased in this region because of reduced fire frequency (Kitzberger and Veblen 1999). The steep increase in CO_2 may have contributed to the biomass increase observed in our simulation because our model lacks effective fire management indicating woody biomass growth under elevated CO_2.

In LPJ-GUESS, photosynthesis is coupled with stomatal conductance, and increases greatly with increasing CO_2 provided that other nutrients are not limiting (e.g., water; Sitch et al. 2003). LPJ-GUESS has been shown to be less sensitive to elevated CO_2 (eCO_2) compared to other DGVMs. In the free air CO_2 enrichment (FACE) and chamber experiments to determine the global response of biomass to eCO_2, LPJ-GUESS under-estimated biomass under eCO_2 (375 ppm to 625 ppm) compared with the empirical result from FACE and other dynamic vegetation models (Terrer et al. 2019).

In general, the model captured the closed canopy forests west of the Andes and the mesic forest but did not create the sharp change in forest cover transition from forest to steppe grasses at the forest-steppe ecotone. The poor result in the east might be attributed to the two-layer soil hydrology architecture of the model which lacked ground water storage for a semi-arid ecosystem (Wramneby et al. 2008). A lack of ground water storage might reduce the capacity of steppe vegetation to extract the water required for photosynthesis during the dry season from October to March (Hickler et al. 2004). The results from S5 (PI climate and low CO_2) and S6 (PI climate and historical CO_2) show a low burned-area and low biomass yield (Fig. 2.8e & f). The low burned-area in S5 and S6 suggested that climate variability is significant to promote fire. This observation agrees with the ecological studies in the region. For example, the successful establishment of *Austrocedrus* at xeric sites near the steppe is probably linked to interannual and decadal climate variability in the region (Villalba and Veblen 1998, Kitzberger and Veblen 1999).

Influence of CO_2, fire, and climate on Patagonia forest

In this study, the spatial analysis and paired t-tests show a difference in magnitude of these factors (CO_2, fire and climate) on biomass, with climate and CO_2 being stronger influence than fire (Fig. 2.9b & c). The effect of CO_2, fire and, climate on simulated forest cover supports previous studies that compared the influence of glacial climate (low CO_2) and modern climates on global biome distribution (Martin Calvo et al. 2014, Martin Calvo and Prentice 2015). The effect of low CO_2 on forest cover has been well documented based on growth chamber and modeling studies to have reduced tree biomass (Gerhart and Ward, 2010). The effect of PI CO_2 (S1 – S4) on modern climate is more visible at the forest-steppe ecotone, where biomass

was low. The observed low biomass at the forest-steppe ecotone is consistent with a study of a semi-arid ecosystem in northeastern Colorado, USA (LeCain et al. 2003), which suggested that, at low CO_2 steppe grasses experienced water stress that reduced the rate of photosynthesis and productivity. The comparison between S1 (changing climate, changing CO_2) & S4 (changing climate, PI CO_2), and S6 (PI climate, changing CO_2) & S5 (PI climate, PI CO_2) shows the physiological effect of CO_2 fertilization on forest productivity. With the physiological effects of CO_2 turned on, the model projected an increase in biomass for both paired comparisons.

The physiological effect of CO_2 on vegetation productivity has mainly been observed in modeling studies due to limited observation data (Hickler et al. 2015). The comparison of the scenario (S1 & S4) and (S6 & S5) of keeping CO_2 fixed at a certain level (PI: 280 ppmv), thereby switching off both the effects on photosynthesis and stomatal conductance, but maintaining the climatic effect of CO_2 was used to capture the uncertainty associated with the potential physiological effects of CO_2, as shown in this study. Our study shows the effects of CO_2 fertilization as a driver of these observed increases in biomass and supports previous results that have demonstrated the potential impact of eCO_2 on vegetation productivity. For example, Ciais et al. (2008) used the ORCHIDEE model to simulate carbon accumulation in the European forest between 1950 and 2000. They found substantial increases in NPP and potential harvest, which was, in part, attributed to CO_2 fertilization and regional climate trends.

Other studies on global vegetation have shown that at low CO_2 levels, photorespiration increases with temperature (Martin Calvo and Prentice 2015). Average biomass production by modern C_3 plant may vary between 40-70% when grown at low (180 - 220 ppm) vs moderate (350 - 380 ppm) CO_2 (Gerhart and Ward 2010). These results and our

S5 simulation show that fire amplifies this interaction between climate and CO_2 leading to a large reduction in biomass under a combination of PI climate and PI CO_2 (Fig. 2.9b). This combination reduces the ability of the forest to expand due to the extreme reduction in forest productivity.

Fire controls biomass dynamics in an ignition-limited ecosystem such as the Patagonia mesic forest (Veblen and Lorenz 1988, Kitzberger and Veblen 1999, Veblen et al. 1999a, Kitzberger et al. 2016). In northern Patagonia, high woody biomass in the forest-steppe compared to the steppe provides more contiguous fuel biomass, and stand-replacing fire would support Nothofagus forest (Veblen et al. 1992, Kitzberger and Veblen 1999). The removal of fire caused biomass to increase in those areas occupied by forest under S3 (historical climate, changing CO_2, masking on, with fire 'off'). Also, the presence of fire increased biomass in S2 (historical climate, changing CO_2, masking on, with fire 'on'). The comparison between S2 & S3 shows that the presence of fire decrease biomass (Fig. 2.9 c). Under S2, forested area increased (25.8%) compared to S3 (24.8%), because, in the absence of fire, there is a longer rate of biomass turnover but an increase in average biomass.

This causes higher respiratory losses associated with reduced productivity because fire tends to maintain productivity by the continuous turnover of vegetation in the landscape (Martin Calvo et al. 2014). Veblen and Lorenz (1988) analyzed forest stands at the forest-steppe ecotone and observed that Nothofagus dombeyi and Austrocedrus chilensis regenerated vigorously after a stand-replacing fire at the mesic site and reduction in high-severity fire frequency shifted the dominant vegetation from a short-lived resprouting shrub (e.g., *Nothofagus antarctica*) to long-lived obligate seeders (e.g., *Nothofagus dombeyi*). Nonetheless, our simulation using historical climate and changes in CO_2 show that fire amplified the

biomass response to CO_2 under changes in climate variability (e.g., ENSO). This result is consistent with Bond and Keeley (2005). Fire studies at the forest-steppe thus show the importance of changes in fire regime in altering fire frequency (Kitzberger and Veblen 1999). Fewer fires in scenario S1, S2, and S3 resulted in high biomass and forest expansion (Fig. 2.6a, b & c).

When only including annual climate variation, the model predicted a reduction in forest cover at the temperate rainforest west of the Andes, but the average biomass increased in the pairwise comparison between S4 (changing climate, PI CO_2) - S5 (PI climate, PI CO_2) and S1 (changing climate, changing CO_2) – S6 (PI climate, changing CO_2 (Fig. 2.9 d & e). The reduction of precipitation in dry years caused drought and reduction in biomass in the temperate rainforest west of the Andes. Drought (Fig. S5 b) occurs during poleward displacement of the southern Westerlies with their cyclonic storms during summer (Holz et al. 2012) and through increased evapotranspiration when variability in near-surface temperature places vegetation under increase water stress (Fig. S5 a; Bartholomeus et al. 2008).

Conclusion

This is the first study that uses a DGVM to access the influence of CO_2, fire, and climate on northern Patagonia forest. Research presented here suggests that LPJ-GUESS can realistically simulate historical responses of northern Patagonia forest to changes in CO_2, climate, and fires. The similarity between the simulated biomass and observed biomass of temperate rainforest west of the Andes and mesic forests east of the Andes shows that the model can capture local vegetation and dynamics. Significant findings from this study are:

1. Under current climate condition and rising CO_2, the model predicts that forest cover will increase, with an increase in forest biomass at high and low elevations.
2. Low CO_2 decreased forested area under these observed changing climate. While PI climate reduced forest distribution under increasing CO_2, but the effect of PI climate alone on biomass was minor compared to the effect of low CO_2.
3. In our study, the largest percentage of fire occurred at the steppe followed by the forest-steppe ecotone, this is due to high biomass desiccations at the steppe and the frequency of fire depends on available fuel load as well a gradual change in temperature under increasing drought.
4. In terms of magnitude, the influence of climate is the strongest and CO_2 fertilization is the secondary driver of forest expansion. CO_2 also mitigates climate-induced drought stress due to increases in water-use efficiency.

Further Considerations

In order to improve the accuracy of LPJ-GUESS at the patch level, it will be necessary to improve the parameterization of the key taxa. This will include more sensitivity analyses on some critical parameters, such as distance to seed source as well as the establishment conditions that differ widely in closed forests as compared to forest expansion. These factors may not be important in long-term studies but have a strong effect in the time frame of this study (100 years), particularly for species such as Nothofagus pumilio that exhibited clear difficulties in reestablishing in area lost 100 years ago through fire and land-use change. Moreover, there are limited model simulations that study long-term forest cover trends and how environmental factors such as climate and CO_2 affects regional vegetation through fire

(Martin Calvo and Prentice 2015, Wu et al. 2017, Dionizio et al. 2018). In southern South America, as far as we are aware that there is no DGVM simulation or previous research that uses ecosystem model to simulate the response of the vegetation to past and future environmental effects. This new parametrization of the important regional tree species can thus be used to model the past and future vegetation in the study area.

Acknowledgements

This work was supported by the National Science Foundation [grant numbers GSS 1461590]. We thank T. Kitzberger, J. Paritsis, J. Gowda for their helpful suggestions in improving the manuscript. We also thank Laura Burkle for her comments on the manuscript.

References

Arroyo, M. T. K., M. Riveros, A. Peñaloza, L. Cavieres, and A. M. Faggi. 1996. Phytogeographic Relationships and Regional Richness Patterns of the Cool Temperate Rainforest Flora of Southern South America. Pages 134-172 in R. G. Lawford, E. Fuentes, and P. B. Alaback, editors. High-Latitude Rainforests and Associated Ecosystems of the West Coast of the Americas. Springer New York.

Avaria, C. E. 2013. Simulating current regional pattern and composition of Chilean native forests using a dynamic ecosystem model. Lund University, Sweden.

Avitabile, V., M. Herold, G. B. Heuvelink, S. L. Lewis, O. L. Phillips, G. P. Asner, J. Armston, P. S. Ashton, L. Banin, N. Bayol, N. J. Berry, P. Boeckx, B. H. de Jong, B. DeVries, C. A. Girardin, E. Kearsley, J. A. Lindsell, G. Lopez-Gonzalez, R. Lucas, Y. Malhi, A. Morel, E. T. Mitchard, L. Nagy, L. Qie, M. J. Quinones, C. M. Ryan, S. J. Ferry, T. Sunderland, G. V. Laurin, R. C. Gatti, R. Valentini, H. Verbeeck, A. Wijaya, and S. Willcock. 2016. An integrated pan-tropical biomass map using multiple reference datasets. Glob Chang Biol 22:1406-1420.

Bartholomé, E., and A. S. Belward. 2007. GLC2000: a new approach to global land cover mapping from Earth observation data. International Journal of Remote Sensing 26:1959-1977.

Bartholomeus, R. P., J.-P. M. Witte, P. M. van Bodegom, J. C. van Dam, and R. Aerts. 2008. Critical soil conditions for oxygen stress to plant roots: Substituting the Feddes-function by a process-based model. Journal of Hydrology 360:147-165.

Batjes, N. H. 2015. World soil property estimates for broad-scale modellling (WISE30sec,ver.1.0). Report 2015/01, ISRIC - World Soil Information, Wageningen.

Bianchi, E., R. Villalba, M. Viale, F. Couvreux, and R. Marticorena. 2016. New precipitation and temperature grids for northern Patagonia: Advances in relation to global climate grids. Journal of Meteorological Research 30:38-52.

Blanke, J. H., M. Lindeskog, J. Lindström, and V. Lehsten. 2016. Effect of climate data on simulated carbon and nitrogen balances for Europe. Journal of Geophysical Research: Biogeosciences 121:1352-1371.

Bond, W. J. 2008. What Limits Trees in C4 Grasslands and Savannas? Annual Review of Ecology, Evolution, and Systematics 39:641-659.

Bond, W. J., and J. E. Keeley. 2005. Fire as a global 'herbivore': the ecology and evolution of flammable ecosystems. Trends Ecol Evol 20:387-394.

Bugmann, H. 2001. A Review of Forest Gap Models. Climatic Change 51:259-305.

Ciais, P., M. J. Schelhaas, S. Zaehle, S. L. Piao, A. Cescatti, J. Liski, S. Luyssaert, G. Le-Maire, E. D. Schulze, O. Bouriaud, A. Freibauer, R. Valentini, and G. J. Nabuurs. 2008. Carbon accumulation in European forests. Nature Geoscience 1:425-429.

De Kauwe, M. G., B. E. Medlyn, S. Zaehle, A. P. Walker, M. C. Dietze, Y. P. Wang, Y. Luo, A. K. Jain, B. El-Masri, T. Hickler, D. Warlind, E. Weng, W. J. Parton, P. E. Thornton, S. Wang, I. C. Prentice, S. Asao, B. Smith, H. R. McCarthy, C. M. Iversen, P. J. Hanson, J. M. Warren, R. Oren, and R. J. Norby. 2014. Where does the carbon go? A model-data intercomparison of vegetation carbon allocation and turnover processes at two temperate forest free-air CO2 enrichment sites. New Phytol 203:883-899.

Dionizio, E. A., M. Heil Costa, A. D. d. A. Castanho, G. Ferreira Pires, B. Schwantes Marimon, B. Hur Marimon-Junior, E. Lenza, F. Martins Pimenta, X. Yang, and A. K. Jain. 2018. Influence of climate variability, fire and phosphorus limitation on vegetation structure and dynamics of the Amazon–Cerrado border. Biogeosciences 15:919-936.

Donoso, C. 2006. Especies arbóreas de los bosques templados de Chile y Argentina: autoecología. Marisa Cuneo Eds, Santiago de Chile:.

Forkel, M., N. Carvalhais, J. Verbesselt, M. Mahecha, C. Neigh, and M. Reichstein. 2013. Trend Change Detection in NDVI Time Series: Effects of Inter-Annual Variability and Methodology. Remote Sensing 5:2113-2144.

Friedlingstein, P., and I. C. Prentice. 2010. Carbon–climate feedbacks: a review of model and observation based estimates. Current Opinion in Environmental Sustainability 2:251-257.

Garreaud, R. D., M. Vuille, R. Compagnucci, and J. Marengo. 2009. Present-day South American climate. Palaeogeography, Palaeoclimatology, Palaeoecology 281:180-195.

Gerhart, L. M., and J. K. Ward. 2010. Plant responses to low [CO2] of the past. New Phytol 188:674-695.

Giglio, L., L. Boschetti, D. P. Roy, M. L. Humber, and C. O. Justice. 2018. The Collection 6 MODIS burned area mapping algorithm and product. Remote Sens Environ 217:72-85.

Gowda, J. H., T. Kitzberger, and A. C. Premoli. 2011. Landscape responses to a century of land use along the northern Patagonian forest-steppe transition. Plant Ecology 213:259-272.

Harris, I., P. D. Jones, T. J. Osborn, and D. H. Lister. 2014. Updated high-resolution grids of monthly climatic observations - the CRU TS3.10 Dataset. International Journal of Climatology 34:623-642.

Haxeltine, A., and I. C. Prentice. 1996. BIOME3: An equilibrium terrestrial biosphere model based on ecophysiological constraints, resource availability, and competition among plant functional types. Global Biogeochemical Cycles 10:693-709.

Hickler, T., A. Rammig, and C. Werner. 2015. Modelling CO2 Impacts on Forest Productivity. Current Forestry Reports 1:69-80.

Hickler, T., B. Smith, I. C. Prentice, K. MjÖFors, P. Miller, A. Arneth, and M. T. Sykes. 2008. CO2fertilization in temperate FACE experiments not representative of boreal and tropical forests. Global change Biology 14:1531-1542.

Hickler, T., B. Smith, M. T. Sykes, M. B. Davis, S. Sugita, and K. Walker. 2004. Using a generalized vegetation model to simulate vegetation dynamics in northeastern USA. Ecology 85:519-530.

Hirota, M., M. Holmgren, E. H. Van Nes, and M. Scheffer. 2011. Global Resilience of Tropical Forest and Savanna to Critical Transitions. Science 334:232.

Holz, A., T. Kitzberger, J. Paritsis, and T. T. Veblen. 2012. Ecological and climatic controls of modern wildfire activity patterns across southwestern South America. Ecosphere 3.

Iglesias, V., C. Whitlock, V. Markgraf, and M. M. Bianchi. 2014. Postglacial history of the Patagonian forest/steppe ecotone (41–43°S). Quaternary Science Reviews 94:120-135.

Jung, M., G. Le Maire, S. Zaehle, S. Luyssaert, M. Vetter, G. Churkina, P. Ciais, N. Viovy, and M. Reichstein. 2007. Assessing the ability of three land ecosystem models to simulate gross carbon uptake of forests from boreal to Mediterranean climate in Europe. Biogeosciences Discussions 4:1353-1375.

Kirschbaum, M. U. F., M. S. Watt, A. Tait, and A.-G. E. Ausseil. 2012. Future wood productivity of Pinus radiata in New Zealand under expected climatic changes. Global change Biology 18:1342-1356.

Kitzberger, T. 2012. Ecotones as Complex Arenas of Disturbance, Climate, and Human Impacts: The Trans-Andean Forest-Steppe Ecotone of Northern Patagonia. Pages 59-88 in R. Myster, editor. Ecotones Between Forest and Grassland. Springer, New York.

Kitzberger, T., G. L. W. Perry, J. Paritsis, J. H. Gowda, A. J. Tepley, A. Holz, and T. T. Veblen. 2016. Fire–vegetation feedbacks and alternative states: common mechanisms of temperate forest vulnerability to fire in southern South America and New Zealand. New Zealand Journal of Botany 54:247-272.

Kitzberger, T., and T. T. Veblen. 1999. Fire-induced changes in northern Patagonian landscapes. Landscape Ecology 14:1-15.

Kitzberger, T., and T. T. Veblen. 2003. Influence of climate on fire in northern Patagonia, Argentina. Pages 296-321 in T. T. Veblen, W. L. Baker, G. Montenegro, and T. W.

Swetnam, editors. Fire regimes and climatic chnage in temperate ecosystem of the western Americas. Springer-Verlag, New York, USA.

LeCain, D. R., J. A. Morgan, M. A. R., and J. A. Nelson. 2003. Soil and Plant Water Relations Determine Photosynthetic Responses of C_3 and C_4 Grasses ina Semi-arid Ecosystem under Elevated CO_2. Annals of Botany 92:41-52.

Lindeskog, M., A. Arneth, A. Bondeau, K. Waha, J. Seaquist, S. Olin, and B. Smith. 2013. Implications of accounting for land use in simulations of ecosystem services and carbon cycling in Africa. Earth System Dynamics Discussions 4:235-278.

Markgraf, V., E. Romero, and C. Villagran. 1996. History and paleoecology of South American Nothofagus forests. Pages 354-386 in T. T. Veblen, R. S. Hill, and J. Read, editors. Ecology and Biogeography of Nothofagus Forests. Yale University Press, New Heaven.

Martin Calvo, M., and I. C. Prentice. 2015. Effects of fire and CO2 on biogeography and primary production in glacial and modern climates. New Phytol 208:987-994.

Martin Calvo, M., I. C. Prentice, and S. P. Harrison. 2014. Climate versus carbon dioxide controls on biomass burning: a model analysis of the glacial–interglacial contrast. Biogeosciences 11:6017-6027.

Nanavati, W. P., C. Whitlock, V. Iglesias, and M. E. de Porras. 2019. Postglacial vegetation, fire, and climate history along the eastern Andes, Argentina and Chile (lat. 41-55 degrees S). Quaternary Science Reviews 207:145-160.

Olson, D. M., E. Dinerstein, E. D. Wikramanayake, N. D. Burgess, G. V. N. Powell, E. C. Underwood, J. A. D'Amico, I. Itoua, H. E. Strand, J. C. Morrison, C. J. Loucks, T. F. Allnutt, T. H. Ricketts, Y. Kura, J. F. Lamoreux, W. W. Wettengel, P. Hedao, and K. R. Kassem. 2001. Terrestrial Ecoregions of the World: A New Map of Life on Earth. BioScience 51:933-938.

Pan, Y., J. M. Melillo, A. D. McGuire, D. W. Kicklighter, L. F. Pitelka, K. Hibbard, L. L. Pierce, S. W. Running, D. S. Ojima, W. J. Parton, D. S. Schimel, and V. m. Other. 1998. Modeled responses of terrestrial ecosystems to elevated atmospheric CO2: a comparison of simulations by the biogeochemistry models of the Vegetation/Ecosystem Modeling and Analysis Project (VEMAP). Oecologia 114:389-404.

Paritsis, J., J. Landesmann, T. Kitzberger, F. Tiribelli, Y. Sasal, C. Quintero, R. Dimarco, M. Barrios-García, A. Iglesias, J. Diez, M. Sarasola, and M. Nuñez. 2018. Pine Plantations and Invasion Alter Fuel Structure and Potential Fire Behavior in a Patagonian Forest-Steppe Ecotone. Forests 9.

Paruelo, J. M., A. B. Beltran, E. G. Jobbagy, O. E. Sala, and R. A. Golluscio. 1998. The climate of Patagonia: general patterns and controls on biotic processes. Ecologia Austral 8:85-101.

Piao, S., S. Sitch, P. Ciais, P. Friedlingstein, P. Peylin, X. Wang, A. Ahlstrom, A. Anav, J. G. Canadell, N. Cong, C. Huntingford, M. Jung, S. Levis, P. E. Levy, J. Li, X. Lin, M. R. Lomas, M. Lu, Y. Luo, Y. Ma, R. B. Myneni, B. Poulter, Z. Sun, T. Wang, N. Viovy, S. Zaehle, and N. Zeng. 2013. Evaluation of terrestrial carbon cycle models for their response to climate variability and to CO2 trends. Glob Chang Biol 19:2117-2132.

Pollmann, W., and T. T. Veblen. 2004. Nothofagus Regeneration Dynamics in South-Central Chile: A Test of a General Model. Ecological Monographs 74:615-634.

Prentice, I. C. 1983. Pollen Mapping of Regional Vegetation Patterns in South and Central Sweden. Journal of Biogeography 10:441-454.

Sitch, S., P. Friedlingstein, N. Gruber, S. D. Jones, G. Murray-Tortarolo, A. Ahlström, S. C. Doney, H. Graven, C. Heinze, C. Huntingford, S. Levis, P. E. Levy, M. Lomas, B. Poulter, N. Viovy, S. Zaehle, N. Zeng, A. Arneth, G. Bonan, L. Bopp, J. G. Canadell, F. Chevallier, P. Ciais, R. Ellis, M. Gloor, P. Peylin, S. L. Piao, C. Le Quéré, B. Smith, Z. Zhu, and R. Myneni. 2015. Recent trends and drivers of regional sources and sinks of carbon dioxide. Biogeosciences 12:653-679.

Sitch, S., B. Smith, I. C. Prentice, A. Arneth, A. Bondeau, W. Cramer, J. O. Kaplans, S. Levis, W. Lucht, M. T. Sykes, and K. Thonicke. 2003. Evaluation of ecosystem dynamics,plant geography and terrestial carbon cycling in the LPJ dynamic global vegetation model. Global change Biology 9:25.

Sykes, M. T., I. C. Prentice, and W. Cramer. 1996. A bioclimatic model for the potential distributions of north European tree species under present and future climates. Journal of Biogeography 23:203-233.

Tang, G., and B. Beckage. 2010. Projecting the distribution of forests in New England in response to climate change. Diversity and Distributions 16:144-158.

Terrer, C., R. B. Jackson, I. C. Prentice, T. F. Keenan, C. Kaiser, S. Vicca, J. B. Fisher, P. B. Reich, B. D. Stocker, B. A. Hungate, J. Peñuelas, I. McCallum, N. A. Soudzilovskaia, L. A. Cernusak, A. F. Talhelm, K. Van Sundert, S. Piao, P. C. D. Newton, M. J. Hovenden, D. M. Blumenthal, Y. Y. Liu, C. Müller, K. Winter, C. B. Field, W. Viechtbauer, C. J. Van Lissa, M. R. Hoosbeek, M. Watanabe, T. Koike, V. O. Leshyk, H. W. Polley, and O. Franklin. 2019. Nitrogen and phosphorus constrain the CO2 fertilization of global plant biomass. Nature Climate Change 9:684-689.

Thonicke, K., S. Venevsky, S. Sitch, and W. Cramer. 2001. The role of fire disturbance for global vegetation dynamics: coupling fire into a Dynamic Global Vegetation Model. Global Ecology & Biogeography 10:661-677.

Tucker, C. J., J. E. Pinzon, M. E. Brown, D. A. Slayback, E. W. Pak, R. Mahoney, E. F. Vermote, and N. El Saleous. 2010. An extended AVHRR 8-km NDVI dataset compatible with MODIS and SPOT vegetation NDVI data. International Journal of Remote Sensing 26:4485-4498.

van der Werf, G. R., J. T. Randerson, L. Giglio, G. J. Collatz, M. Mu, P. S. Kasibhatla, D. C. Morton, R. S. DeFries, Y. Jin, and T. T. van Leeuwen. 2010. Global fire emissions and the contribution of deforestation, savanna, forest, agricultural, and peat fires (1997–2009). Atmospheric Chemistry and Physics 10:11707-11735.

Veblen, T. T., C. Donoso, T. Kitzberger, and A. J. Rebertus. 1996. Ecology of Southern Chilean and Argentinean Nothofagus Forests.in T. T. Veblen, R. S. Hill, and J. Read, editors. The Ecology and Biogeography of Nothofagus Forests. Yale University Press, New Haven, USA.

Veblen, T. T., A. Holz, J. Paritsis, E. Raffaele, T. Kitzberger, and M. Blackhall. 2011. Adapting to global environmental change in Patagonia: What role for disturbance ecology? Austral Ecology 36:891-903.

Veblen, T. T., T. Kitzberger, and A. Lara. 1992. Disturbance and Forest Dynamics Along a Transect from Andean Rain-Forest to Patagonian Shrubland. Journal of Vegetation Science 3:507-520.

Veblen, T. T., T. Kitzberger, R. Villalba, and J. Donnegan. 1999. Fire History in Northern Patagonia: The Roles of Humans and Climate Variation. Ecological Monography 69:47-67.

Veblen, T. T., and D. C. Lorenz. 1987. Post-Fire Stand Development of Austrocedrus-Nothofagus Forests in Northern Patagonia. Vegetatio 71:113-126.

Veblen, T. T., and D. C. Lorenz. 1988. Recent Vegetation Changes along the Forest/Steppe Ecotone of Northern Patagonia. Annals of the Association of American Geographers 78:93-111.

Venevsky, S., K. Thonicke, S. Sitch, and W. Cramer. 2002. Simulating fire regimes in human-dominated ecosystems: Iberian penisula case study. Global change Biology 8:984-998.

Villalba, R., and T. T. Veblen. 1998. Influences of large-scale climatic variability on episodic tree mortality in northern Patagonia. Ecology 79:2624-2640.

Whitlock, C., P. I. Moreno, and P. Bartlein. 2007. Climatic controls of Holocene fire patterns in southern South America. Quaternary Research 68:28-36.

Wramneby, A., B. Smith, S. Zaehle, and M. T. Sykes. 2008. Parameter uncertainties in the modelling of vegetation dynamics—Effects on tree community structure and ecosystem functioning in European forest biomes. Ecological Modelling 216:277-290.

Wu, C., S. Venevsky, S. Sitch, Y. Yang, M. Wang, L. Wang, and Y. Gao. 2017. Present-day and future contribution of climate and fires to vegetation composition in the boreal forest of China. Ecosphere 8.

Zhang, Z., N. E. Zimmermann, A. Stenke, X. Li, E. L. Hodson, G. Zhu, C. Huang, and B. Poulter. 2017. Emerging role of wetland methane emissions in driving 21st century climate change. Proc Natl Acad Sci U S A 114:9647-9652.

Zhu, Z., S. Piao, R. B. Myneni, M. Huang, Z. Zeng, J. G. Canadell, P. Ciais, S. Sitch, P. Friedlingstein, A. Arneth, C. Cao, L. Cheng, E. Kato, C. Koven, Y. Li, X. Lian, Y. Liu, R. Liu, J. Mao, Y. Pan, S. Peng, J. Peñuelas, B. Poulter, T. A. M. Pugh, B. D. Stocker, N. Viovy, X. Wang, Y. Wang, Z. Xiao, H. Yang, S. Zaehle, and N. Zeng. 2016. Greening of the Earth and its drivers. Nature Climate Change 6:791-795.

CHAPTER THREE

CLIMATE DRIVERS OF LATE-GLACIAL TO POSTGALACIAL FOREST COVER ALONG THE EASTERN ANDES OF NORTHERN PATAGONIA (LAT. 40 - 45^{0}S)

Contribution of Authors and Co-Authors

Manuscript in Chapter 3

Author: Ayodele Gilbert Ogunkoya
Contributions: Contributions: Defined the experimental design, parametrized the Plants Functional Types (PFTs) and plant species used in LPJ-GUESS DGVM, downscaled the climate used for simulations, performed the paleo-modeling simulations, analyzed the output from the model simulation and wrote the manuscript.

Co-Author: Benjamin Poulter
Contribution: Supported this research under the National Science Foundation grant GSS 1461590 helped define the experimental design, discussed the results and edited the manuscript.

Co-Author: Jed Kaplan
Contribution: Participate in parametrization of PFTs and plants species used in LPJ-GUESS

Co-Author: Cathy Whitlock
Contribution: Supported this research under the National Foundation grant, commented on the manuscript and discussed the results

Co-Author: William Nanavati
Contribution: Commented on the manuscript

Co-Author: David Roberts
Contribution: Contributed to the development of the statistical methods and commented on the manuscript.

Co-Author: Steve Hostetler
Contribution: Provided the GENesis Modular Ocean Model (GENMOM) reconstructed climate data

Manuscript Information Page

Ayodele Ogunkoya, Jed O. Kaplan, Cathy Whitlock, William Nanavati, Benjamin Poulter, David Roberts, Steve Hostetler

Status of Manuscript:
__x__ Prepared for submission to a peer-reviewed journal
____ Officially submitted to a peer-review journal
____ Accepted by a peer-reviewed journal
___ Published in a peer-reviewed journal

Abstract

The past influences of climate on the vegetation of northern Patagonian have been thoroughly documented using dendrochronology and high-resolution pollen and charcoal based reconstructions. Here, we investigate for the first time the influence of climate on past changes in the forest cover and upper and lower treeline dynamics for five-time intervals (15, 9,6,3, and 0 ka BP) using a dynamic global vegetation model (DGVM), LPJ-GUESS. Past climate anomalies were derived from the GENesis Modular Ocean Model (GENMOM), a coupled atmosphere-ocean model. Modeled above - and below-ground biomass from two plant functional types and seven tree species were mapped for each time interval representing quasi-steady state conditions. The results from the model were compared with the published reconstructions of forest cover and treeline change in the region. The causes and controls of forest cover and treeline dynamics changes were analyzed using ordination techniques (Canonical Correspondence Analysis) and machine-learning algorithms (Random Forests). In general, the LPJ-GUESS simulations of biomass agree with pollen-based vegetation reconstruction. The model also shows a general increase in fire activity from 15 to 0 ka BP that matches quantitative charcoal-based fire history reconstructions. However, the model and published data differ concerning the climate factors responsible for the forest cover changes over the Holocene. Vegetation reconstructions identify a decrease in annual and winter insolation and strengthening of the Southern Westerlies at mid-latitudes at 6 ka BP to explain an increase in forest cover. Whereas CCA, attributes the increase in forest cover to a combination of increased winter temperature and longer growing seasons, constrained by higher moisture availability. Increased air temperature and effective moisture in the model increased tree establishment and seedling survival rate. Simulations of lower and upper treeline

show west-to-east fluctuations through time. The west-to-east shifts as analyzed by Random Forest (RF) identifies summer and winter precipitation as predictors of treeline dynamic. The model results suggest that precipitation alone can account for the observed changes in treeline dynamics which are in agreement with empirical studies from northern Patagonia that analyzed factors controlling growth and establishment at treeline.

Introduction

Forest-steppe ecotones around the world are highly sensitive to climate, disturbance, and land-use, and their dynamics have been studied extensively to understand how dry forest cover might respond to future climate change (Kitzberger 2012, Iglesias and Whitlock 2014, Mátyás and Sun 2014, Stan and Sanchez-Azofeifa 2019). Erdős et al. (2018) defined the forest-steppe ecotone as "a natural or near-natural vegetation complex of arboreal and herbaceous components (typically distributed in a mosaic pattern), where co-existence of forest and grassland is enabled primarily by the semi-humid to semi-arid climate, complemented by complex interactions of biotic and abiotic factors operating at a multiple scales". In terms of composition, structure, and function, the forest-steppe ecotone represents a series of complex ecosystems outside the tropics (Erdős et al. 2014). However, compared with non-tropical systems, forest-steppe ecotones are also regions of high forest productivity and carbon sequestrations (Schultz 2005). Despite the advances in research on the forest-steppe ecotones (Leach and Givnish 1999, Kitzberger 2012, Erdős et al. 2014), there are still significant knowledge gaps about the interactions of macroclimate and nonclimatic factors (e.g., soil, topography, disturbance land-use) on these terrestrial ecosystems. For example, recent research on the forest-steppe in Eurasia by Erdős et al. (2018) documents that at a certain

threshold in climate change (e.g., rise in global temperature and reduction in precipitation), the ecotone will shift in dominant species, change structure or shift its latitudinal or longitudinal position, but few studies exist to test this hypothesis..

Fire is an inherent constituent of the natural ecosystem that varies in severity across the forest-steppe ecotone transition and produces vegetational changes in landscape composition and structure (Veblen et al. 1999b). In northern Patagonia, the geographic region of southern South America between 40-45°S, the fire regime across the steppe transition has been altered due to land management practices resulting in changes in ignition frequency (Kitzberger 2012). The changes in ignition frequency (i.e., a decrease in fire return time) have altered the vegetational composition from non-sprouting obligate seed reproducing tree species to re-sprouting shrubs (i.e., *Nothofagus antarctica*, *Discaris spp.*) contributing to the observed reduction in the dominant Nothofagus dombeyi forest (Mermoz et al. 2005).

The northern Patagonian forest-steppe ecotone represents a key region for exploring long-term changes in vegetation cover and composition in response to past climate change and disturbance. This is due to the effect of human activities (i.e. landscape fragmentation, intensive grazing) and changing climate on the forest-steppe ecotone. The vegetation and fire history of northern Patagonia has been reconstructed from pollen and charcoal records. Early palynological research at the forest-steppe ecotone (e.g., Heusser 1966, 1974, Markgraf 1983) described past changes in Argentina. More recent studies suggest that insolation-driven changes in temperature and precipitation over the last 15 ka BP have been the primary drivers of forest composition and distribution through time (Whitlock et al. 2006, Whitlock et al. 2007, Iglesias et al. 2014, Nanavati et al. 2019). Pollen analysis suggests that during the late-glacial to early Holocene transition, shrubs colonized the landscape at 11, ka BP. However, the

climate became wetter/cooler, and steppe vegetation was replaced by an open forest dominated by *Nothofagus type*. During the late-glacial/early Holocene, fire activity was at a minimum but increased at 9 ka BP, when summers were dry enough to support fire and winters was sufficiently wet to promote *Nothofagus type* expansion. The late Holocene (3 ka BP) exhibited an oscillation between *Nothofagus* forest during humid periods while drier periods promoted *Austrocedrus chilensis*, associated with the onset and strengthening of the El Nino Southern Oscillation (ENSO) (Whitlock et al. 2006, Iglesias et al. 2011, de Porras et al. 2012, Iglesias et al. 2012, Iglesias et al. 2014, Nanavati et al. 2019).

Dynamic global vegetation modeling offers an opportunity to explore the influence of different environmental parameters, plant taxa, and essential vegetation properties, such as net primary productivity (NPP), leaf area index (LAI), and disturbance through time (Miller et al. 2008, Allen et al. 2010). In this study, we used a DGVM parameterized with regional native plant species and Plant Functional Types (PFTs) to further understand the drivers of postglacial forest cover change and treeline dynamics in northern Patagonia. We focused on five-time intervals from late-glacial to pre-industrial (15, 9, 6, 3, and 0 ka BP). We used the model-predicted biomass of each simulated plant taxa and the reconstructed climate data to determine the climate drivers of species distribution using Canonical Correspondence Analysis (CCA; Ter Braak 1986, 1987). We then used Random Forest (RF) machine learning (Breiman 2001), applying RF to the simulated biomass (above and below ground biomass) at each time interval to understand the drivers of the ecotone position. The use of LPJ-GUESS allows for modeling at a fairly high spatial (1 km) and temporal resolution (daily). This study provides the first use of LPJ-GUESS to simulate postglacial vegetation of northern Patagonia. Within this context, the main objectives of this study are (1) to determine significant predictors of

forest distribution, and (2) to identify drivers of forest treeline (upper and lower) change during the last 15 ka BP. We hypothesize that variations in seasonal insolation will be the primary driver of forest cover and treeline dynamics, by modulating changes to temperature and precipitation.

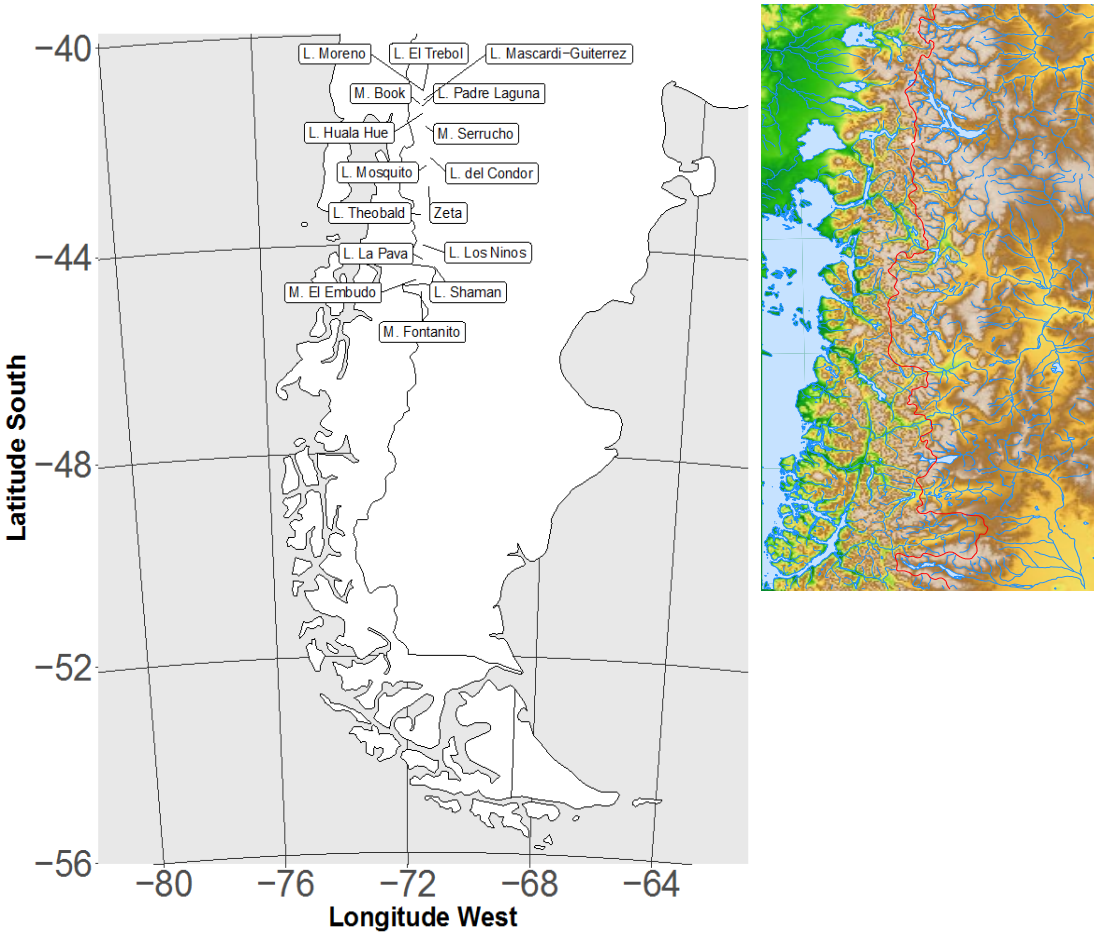

Figure 3.1: Map of southern South America showing the location of the 16 selected sites along the forest-steppe ecotone (40 – 45 °S). The LPJ-GUESS simulated values of these sites were used to develop the Canonical Correspondence Analysis (CCA) model, change in biomass, and fire. The inserted map is the topography of the study area showing the Andes and Northern Patagonia.

Data and Methods

Regional Background

Northern Patagonia (Fig. 3.1) is seasonally influenced by the Southern Westerlies atmospheric circulation (Miller, 1976). The Andes exhibit a highly complex orography resulting in wetter conditions on the westside and drier conditions on the east (Paruelo et al. 1998). Annual precipitation is highest on the western slopes of the Andes, which may receive > 3500 mm yr^{-1}. Precipitation decreases to < 500 m in the east (Kitzberger 2012). The latitudinal position of the Southern Westerlies is controlled by the strength of the southeastern Pacific subtropical high-pressure system and a subpolar low-pressure trough centered along the Antarctic Circle (Mayr et al., 2005). Annual and seasonal precipitation is a result of frontal systems migrating eastward along the storm tracks from the Pacific tracking the jet stream (Garreaud et al. 2009). Northern Patagonia has a Mediterranean type climate, with wet winters and relatively dry summers. Mean July (coldest month) temperature varies from -1 to 8°C, while the mean warmest month (January) varies from 7 to 22°C. Winters are cold and wet as the southeastern Pacific subtropical high-pressure system shifts north and SWW storms predominate. Austral summers are dry and warm as the southeastern Pacific subtropical high-pressure system shifts the Southern Westerlies Winds (SWW) southward. Over two-thirds of the annual precipitation falls during the austral winter (June, July, and August) when the Southern Westerlies lay further towards the equator (Moreno, 2004).

The distribution of vegetation reflects the latitudinal changes in precipitation modified by altitude, slope, and aspect. At elevations between 1100 and 1200 m (west of east of the Andean crest), slopes are dominated by the *Nothofagus pumilio* and *Nothofagus*

antarctica shrubland. At elevations between 1000 and 1500 m, 40 to 50 m tall *Nothofagus dombeyi* dominates with 2 to 5 m tall *Chusquea culeou* (Bamboo) in the understory and other arboreal taxa such as *Saxegothaea conspicua* and *Laurelia philippiana* occur together. Further to the east with the decline in precipitation (1500 to 1000 mm yr^{-1}) *Austrocedrus chilensis* and *Nothofagus dombeyi* coexist within a matrix of forest that includes shrubs such as *Lomatia hirsuta*, *Schinus patagonicus*, *Chusquea culeou* etc. With a further decrease in precipitation (< 1000 mm yr^{-1}) farther east under more xeric condition (< 500 mm yr^{-1}) *Austrocedrus chilensis* forms pure stands and woodlands with shrubs and small trees (e.g., *Berberis*). At lower treeline (700 m elevation) *Nothofagus antarctica* dominate with xerophytic shrubs (*Maytenus sp*), Rhamnaceae (e.g., *Colletia Discaria*). With the decline in precipitation to < 300 mm yr^{-1} bunchgrasses (e.g., *Stipa speciosa*, *Festuca pallescens*) and cushion shrub (*Mulinum spinosum*) dominate the sparse steppe (Veblen et al. 1996).

Model experiments

To simulate the postglacial vegetation change in northern Patagonia, we generated a paleoclimate scenario by applying climate anomalies, i.e., the differences in monthly mean temperature or ratio for monthly mean precipitation and insolation from GENMOM (Genesis Modular Ocean Model) (Fig. 3.2), a coupled atmosphere-ocean climate model (AGCM) (Alder and Hostetler 2015). GENMOM couples the GENESIS atmospheric model (Pollard and Thompson 1997) and Modular Ocean Model (MOM2; Pacanowski 1996). GENMOM captures the significant structure of global and regional climate (Hostetler et al. 2006, Tabor et al. 2014). The version of GENMOM dataset used in this study has a "spatial resolution which corresponds to a grid of 96 longitudes (3.75°) by 48 Gaussian latitudes (~ 3.71°)".

GENMOM simulates the atmospheric condition using "18 vertical sigma levels with mid-layers ranging from 0.993 at the surface to 0.005 at the tropopause" (Alder and Hostetler 2015). Boundary conditions specified in GENMOM during the paleoclimate simulation were the orbital configuration, atmospheric composition (concentrations of CO_2, CH_4, and N_2O), terrestrial ice-sheet configuration, and global sea-level depression. Eight equilibrium time slices at 3000-year intervals for the past 21,000 years forced by changes in Earth-Sun geometry, atmospheric greenhouse gases (GHGs), continental ice sheets, and sea level were then run until the simulation approached quasi-equilibrium to generate paleoclimate datasets. Further details of the model configuration and paleo-simulation performed are given by Alder and Hostetler (2015). Our study looks at five of the time intervals simulated by GENMOM, 15, 9, 6, 3 and 0 ka BP. The differences between the paleoclimate simulations and control (0 kyr ago; 1800s) and a "baseline" climate [CRU datasets] (Harris et al. 2014) representing 20th-century climate variability were used to calculate climate anomalies into LPJ-GUESS for each period. Atmospheric carbon dioxide concentrations for each five-time interval correspond to the value used in GENMOM simulation (15 ka BP = 220 ppmv; 9 ka BP = 260 ppmv; 6 ka BP = 260 ppmv; 3 ka BP = 275 ppmv, and 0 ka BP = 280 ppmv).

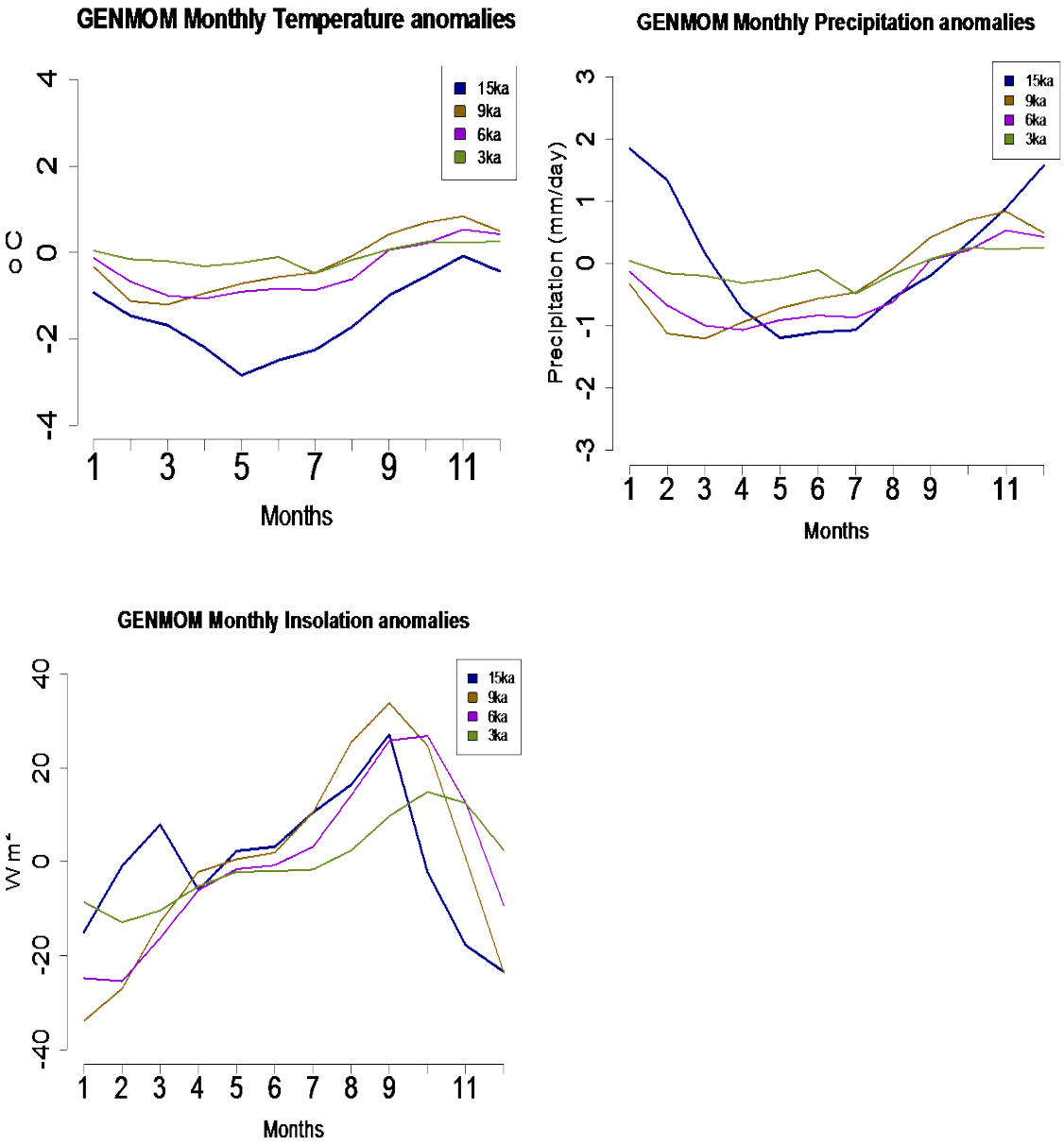

Fig. 3.2: The monthly time series show temperature, precipitation, and insolation anomalies from GENMOM used to generate paleoclimate scenarios to drive LPJ-GUESS. Positive values mean observed was greater than present-day, while negative indicates that observed was less than present-day

Dynamic vegetation model

The Lund-Potsdam Jena Dynamic Global Vegetation Model (LPJ-GUESS DGVM) (Smith et al. 2001) was parameterized with two plant functional types (PFTs; Broadleaved evergreen warm temperate tree, and Mixed Evergreen Shrubs), seven tree species (*Nothofagus dombeyi*, *Nothofagus pumilio*, *Nothofagus betuloides*, *Nothofagus antarctica*, *Chusquea culeou*, *Fitzroya cupressoides*, *Austrocedrus chilensis*) and two types of C_3 grasses based on elevation (Low [0 to 299 m] and High elevation [300 to 1931 m] grasses), For more information see Table 2.1. For each defined species and PFT, environmental constraints were defined in the form of temperature thresholds representing their respective bioclimatic tolerance. These thresholds determine the grid area where the establishment of the species or PFT is possible. Cold tolerance is defined by the minimum and maximum coldest month mean temperature (T_{cmin_est} and T_{cmax_est}), chilling requirements by the minimum coldest month temperature (T_{cmin_surv}), the minimum warmest month mean temperature (T_{wmin_est}) and the minimum growing degree days sum on 5-degree Celsius base (GDD5), which is a summation of temperatures over days with temperature higher than 5^0C.

The specific bioclimatic parameters for each of the PFT and tree species (Table 2.1) were inferred from the vegetation distribution map associated with the classification of southern South America vegetation belts published by the World Wildlife Fund (WWF) (Olson et al. 2001) and Worldclim with a resolution of (~ 1 km^2) (Hijmans et al. 2005). The vegetation maps (WWF & Worldclim) classify each PFT and tree species into bioclimatic zones that are strongly associated with the distribution of each PFT and tree species. This climate database together with monthly means meteorological data from the Climate Research Unit (CRU) datasets was used create a bioclimatic classification for northern Patagonia which

was used to construct the northern Patagonian bioclimatic natural vegetation distribution maps. The bioclimatic zone for each PFT and tree species was subsequently extracted from the vegetation map and overlay on the CRU climate data. We choose boundary values of these variables that correspond to the observed limits of the species or PFT (Table 2.1). The majority of the parameters used were based on Chilean and Argentinian species literature (Veblen et al. 1996, Donoso 2006). When there were no data to parameterize the tree species and PFTs (e.g., maximum and minimum rate of transpiration per year, optimal Ci/Ca ratio), we used global and European standard values in LPJ-GUESS for comparable taxa (Smith et al. 2001, Sitch et al. 2003, Hickler et al. 2012). The values of the limits are listed in Table 2.1.

In LPJ-GUESS grid cells are composed of multiple patches, where several plants can be present. The balance between establishment and mortality determines the fractional projective cover (FPC). Mortality is calculated as a function of age plus disturbance-related mortality (fire and windbreak). Fire regime (based on Thonicke et al. 2001b) is modeled yearly as a stochastic process. Establishment is calculated as a function of bioclimatic requirements, and net primary productivity (NPP) among all plant taxa and includes the different moisture requirements of the plants. During establishment, preference is given to woody plants over grasses, and the latter establishment depends on available space after the former has established. The survivability of a PFT or tree species during a fire relates to a fire resistance value assigned to each modeled PFT or tree species and the length of the fire season. The higher the fire resistance value, the greater the probability of surviving severe fire. To simulate species biomass for the study sites, we statistically downscaled CRU TS4.01 0.5 X 0.5° (1901-1930) resolution to 1 km^2 to match the spatial resolution of the input grid cells used for simulation (see Zhang et al. 2017 for methods) and the anomalies from GENMOM were

then imposed on each of the five equilibrium time slices (15, 9, 6, 3, and 0 ka BP). Modeled biomass changes can be ascribed to bioclimatic shifts (i.e., temperature changes), changes in plant productivity (related to precipitation) or changes in the frequency of disturbances (Brovkin et al. 2009).

Modeled parameters and predictor variables

For each time slice, we investigated (1) the drivers of modeled biomass using CCA, (2) the position of the treeline using two approaches (a simple empirical approach and the RF model), and (3) the observed trend in simulated fire and biomass during the postglacial. To accomplish this, we simulated LPJ-GUESS with CRU data derived using the anomalies from the GENMOM AGCM. To determine the cut-off value for the hypothetical treeline (upper and lower) during the late-glacial (i.e., 15 ka), we assessed the relationship between present-day simulated biomass and a pan-tropical biomass map (Avitabile et al. 2016) derived from various satellite observations of surface reflectance, and vegetation structure ($R^2 = 0.72$; mean = 7.7 kg m^{-2}) . The mean biomass was then taken as our modern value to create a north- south position of the treeline. We used the Generic Mapping Tools [GMT] (Wessel et al. 2013) mapping function to create contours at grid cells with 100 or more points with values greater than the observed biomass to capture major regions.

The climate predictor parameters that we tested using Canonical Correspondence Analysis (CCA) and RF were derived from the input climate used to drive LPJ-GUESS. We used June, July, and August (JJA) for austral winter predictors, and for austral summer predictors we used December, January, and February (DJF). The predictor variables are the mean summer temperature (MST), mean winter temperature (MWT), mean summer

precipitation (MSP), mean winter precipitation (MWP), mean summer insolation (MSI), mean winter insolation (MWI), the ratio of actual/potential evapotranspiration (METEP), growing degree days (GDDs), and the mean annual water content of the soil upper layer (SM). To determine the effect of fire on a plant community, we used the LPJ-GUESS simulated fire return interval (FRI). FRI is calculated using the fractional area of grid cells that burn during the fire season. The affected grid cells are then converted into an average fire return interval.

For each predictor parameter considered, the closest value at the spatial resolution of a 1° x 1° grid cell was chosen. To do this, we created a boundary region (30 m circular radius) representing the spatial extent of each grid cell around the longitude and latitude point locations (where values will be extracted). Maximum values for all pixels that falls within the circular buffer were extracted and used to estimate the grid points values. The data for the grid cells containing a fossil pollen site were thus taken as representative of the site's climate and fire conditions.

Statistical analysis and variable selection

In order to understand the climate drivers responsible for the observed changes in forest assemblage from the late-glacial (15 ka BP) to the pre-industrial (0 ka BP), we used 16 paleoecological sites along the forest-steppe transition zone. The sites represent the locations where modern pollen data were collected from sediments of lakes and wetlands in northern Patagonia (latitude 40 – 45˚S) (Iglesias et al. 2016). The postglacial vegetation and fire history of those sites has been discussed by (Whitlock et al. 2006, Whitlock et al. 2007, Iglesias et al. 2011, Iglesias et al. 2012, Iglesias and Whitlock 2014, Iglesias et al. 2014, Iglesias et al. 2015, Nanavati et al. 2019). The biomass from the two plant functional types, seven tree species and

two kinds of grasses at the selected sites were used as response variables. We used an ancillary function (step.cca) that makes use of a permutation approach to tests whether adding a variable explains more inertia than expected at random. This function was used to determine the best predictor variable rather than the standard R package step-wise fitting function in "vegan" which uses a statistic that resembles 'deviance' and 'AIC' in constrained ordination. The justification is that constrained ordination methods do not have a log-Likelihood, which means that they cannot have AIC and deviance. The selected explanatory variables were subsequently used to build the Canonical Correspondence Analysis (CCA) sequence [cca (formula = response variables ~ predictor variables)] for the analysis. The CCA algorithm employed a selection of linear combinations of measured explanatory variables to maximize the dispersion of response variables (Green et al. 1990). For this analysis we used the R package "vegan" version 2.5-6 (Oksanen et al. 2019).

We then used random forest (RF) as a predictive and inferential model to determine the variable of importance in predicting drivers of what controls the position of the treeline (upper and lower) from the postglacial to late-glacial to present. We used (n = 2000) randomly sampled points with simulated above-and below-ground carbon in vegetation (cVeg) as the response variable that identifies the ecotonal position. The use of RF helps overcome the issue of a large number of correlated explanatory variables because it uses a small number of the predictor variables at each stage of analysis. For this analysis, we used the R package Random Forest (Liaw and Wiener 2002).

Results

At 15 ka BP, our model predicted that the mean position of the upper and lower treeline (Fig. 3a) was located at approximately -72.08° W, further west of the control simulation [pre-industrial; 0ka; longitude ~ -71.97° E] (Fig. 3.3e). Pollen reconstruction however depicts scattered refugia with trees, which would suggest the absent of zonal vegetation during this cold period (Whitlock et al. 2006). The simulated patterns of low forest cover at 15 ka BP and the subsequent increase in forest cover at 9 ka BP generally corresponded with vegetation reconstructions based on pollen records (Whitlock et al. 2006, Iglesias et al. 2012, Iglesias et al. 2014, Nanavati et al. 2019). During the 15 ka BP, late-glacial simulated mean biomass ranged between 0 to 7 kg C m^{-2} relative to early Holocene 0 to 12.2 kg C m^{-2} (Fig. 3.4). At this time, the dominant simulated tree species were *Nothofagus* pumilio, *Chusquea culeou*, *Nothofagus antarctica* and, PTFs were High elevation grasses and Mixed evergreen shrubs (e.g., *Lomatia hirsuta*; Fig. S1). Between 15 and 9 ka BP, simulated biomass increased from 7 kg C m^{-2} at 15 ka BP to 12.2 kg C m^{-2} at 9 ka BP (Fig. 3.4). At this time (15 ka BP) mean lower and upper treeline positions were west of the present-day position (Fig. 3.3b). The dominant simulated tree species at 9 ka BP were the *Nothofagus dombeyi*, *Nothofagus pumilio*, and *Nothofagus antarctica* (Fig. S2).

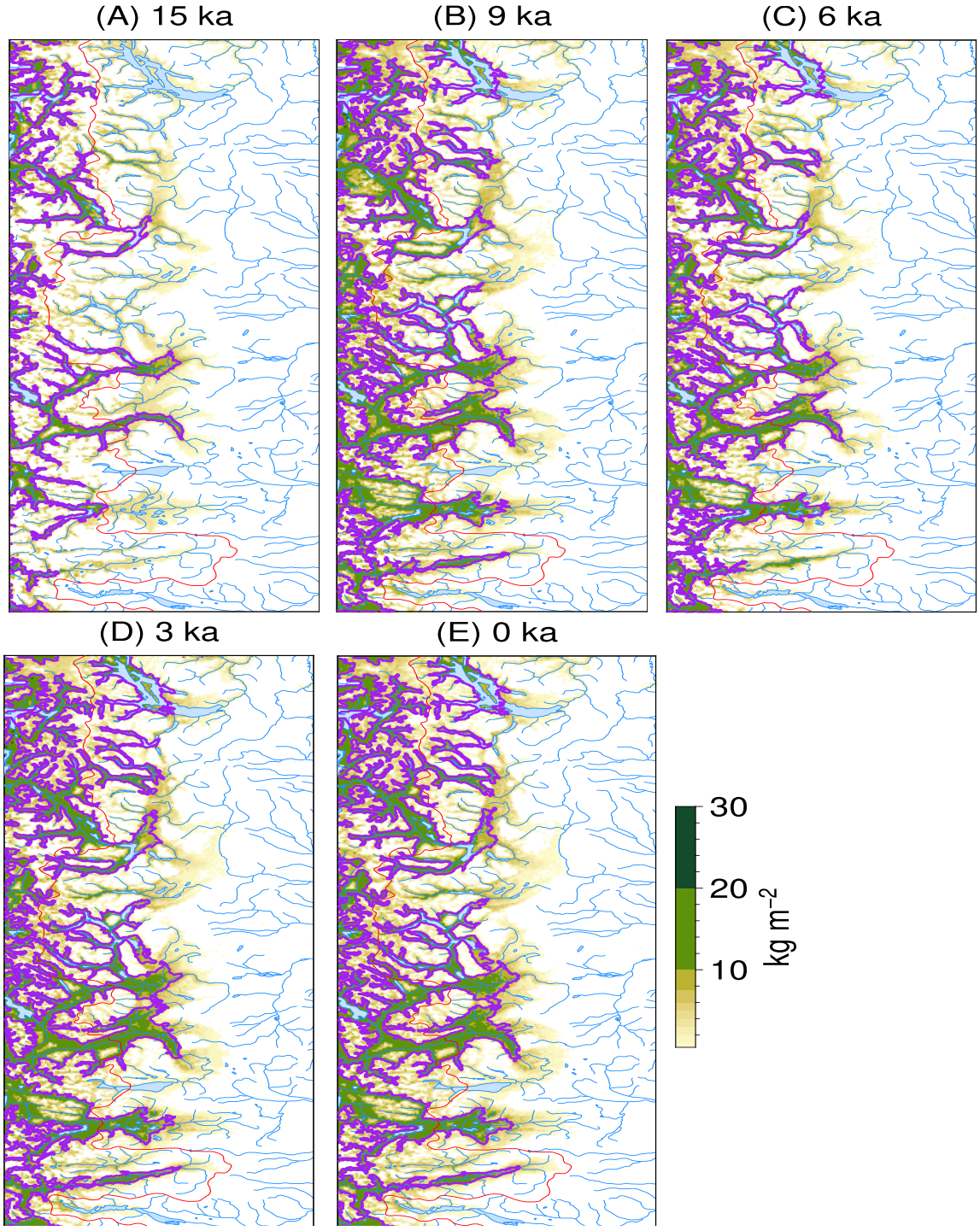

Fig. 3.3: Spatial biomass map showing the changes in treeline position (purple line) from 15 to 0 ka. The position of the treeline was determined using a cutoff mean of 7.7 kg C m^{-2} based on the Pearson Coefficient difference in mean between LPJ-GUESS simulated modern-day biomass and remote sensing biomass data. The total biomass was an aggregation of simulated trees and shrubs.

The transition from 9 to 6 ka BP witnessed a slight decrease in mean simulated biomass at 6 ka BP (10.5 kg C m^{-2}) compared to 9 ka BP (12.2 kg C m^{-2}) (Fig. 3.4) but no change in the mean upper and lower treeline position was observed (Fig. 3.3b & c). During this period (6 ka BP), the dominant simulated tree species were *Austrocedrus* chilensis, *Nothofagus dombeyi*, *Nothofagus pumilio*, and *Nothofagus antarctica* (Fig. S3). The simulated biomass increased from 10.5 kg C m^{-2} at 6 ka BP to 12.3 kg C m^{-2} at 3 ka BP with no change in the mean upper and lower treeline position (Fig. 3.3d). The biomass at 3 ka BP thus shows an upward trend in biomass compared to 6 ka BP (Fig. 3.4) and simulated Austrocedrus chilensis was much higher compared than other time intervals (Fig. S4). The increase in *Austrocedrus chilensis* was also accompanied by an increase in simulated *Nothofagus dombeyi*, *Nothofagus pumilio*, and *Nothofagus antarctica*. At 0 ka BP (Fig. 3.3e) the mean simulated biomass decrease slightly from 12.3 kg C m^{-2} at 3 ka BP to 11 kg C m^{-2} at 0 ka BP. There was no change in the treeline position relative to 9 ka BP position at 0 ka BP. During this period the dominant species were *Austrocedrus chilensis*, *Nothofagus dombeyi*, *Nothofagus pumilio*, *Nothofagus antarctica* (Fig. S5).

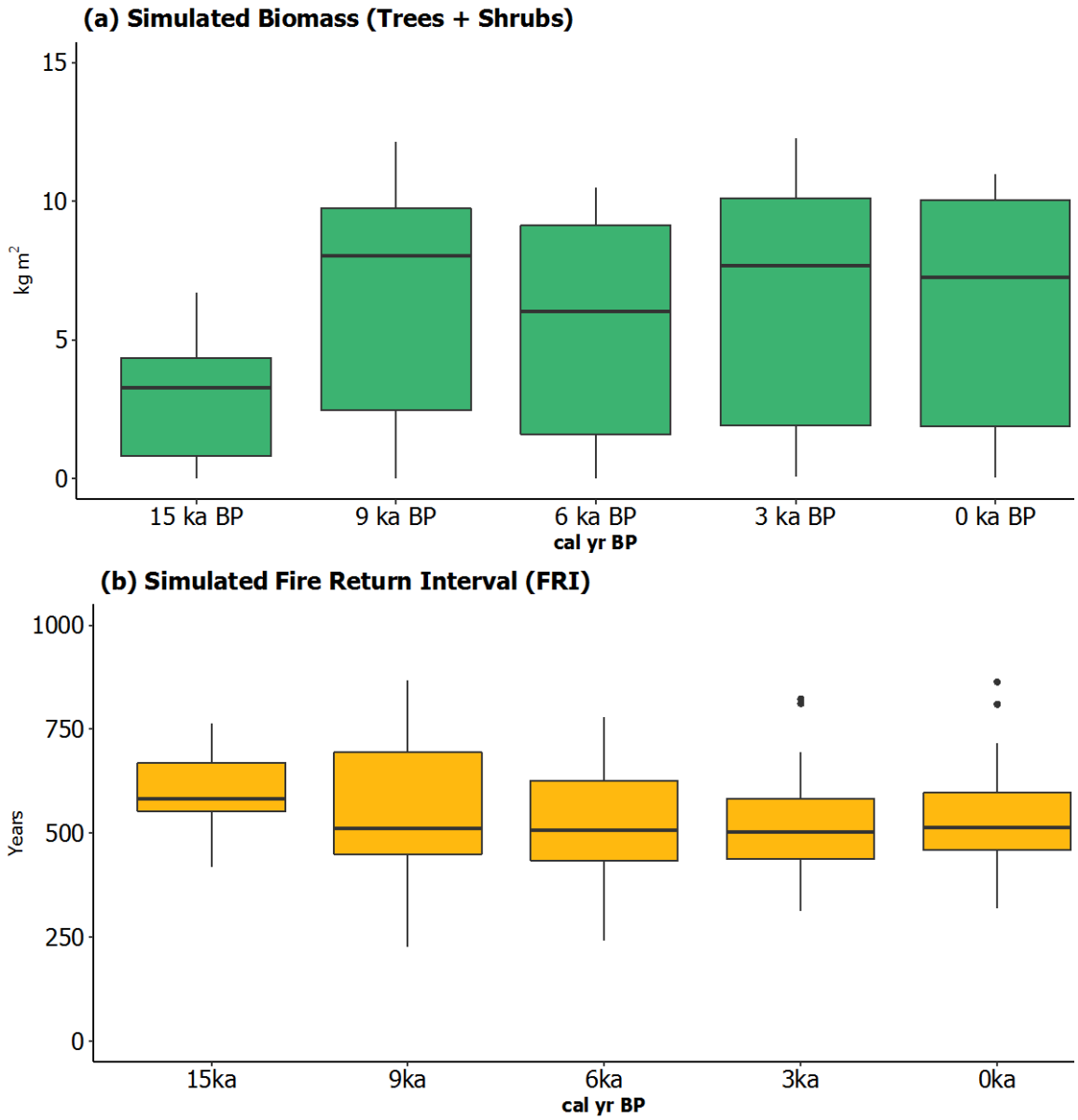

Fig. 3.4: Simulated biomass (trees + shrubs) and fire return interval (FRI) using LPJ-GUESS from the locations of published 16 pollen and charcoal sites from north-south along the forest-steppe ecotone. The boxplots shows the median (i.e., band inside the box), first and third quartiles (lower and upper values defining the box) and lowest and highest (i.e., whiskers) for each period.

The postglacial trend in Northern Patagonia fire activity

Figure 3.4 and the simulated fire maps document changing spatial and temporal patterns in biomass burning over the last 15, 000 years (Fig. 3.4 & 3.5). The modeled fire return interval (FRI) for the study region at 15 ka BP shows low fire activity compared to other time intervals (Fig. 3.5a). Conversely, at 15 ka BP simulated median FRI was ~580 years which matches with charcoal records that show little or no fire. The late-glacial to early-Holocene transition witnessed an increase in fire activities that was associated with an increased forest biomass and warmer summer temperatures (Fig. 3.4 & Fig. 3.5). During this period charcoal records show high fire activity. At 9 ka BP the model simulated FRI shows an increase in fire activity (511 years) compared to 15 ka BP ~580 years.

During the middle Holocene (6 ka BP), the model simulated an increase in fire activity (506 years) compared to 9 ka BP (511 years; Fig. 3.4). During this period fire activity was relatively low due to high *Nothofagus* abundance as inferred from charcoal records. During the late Holocene (3 ka BP) simulated fire activity steeply increased (~503 years) compared to 6 ka BP (506 years) (Fig. 3.4 & 3.5). Charcoal records documents the highest fire activity during this period. This shortening in FRI from 9 to 0 ka BP implies that biomass burning was steadily increasing throughout the Holocene. However, the high simulated FRI value does not match the relatively low FRI that are derived from charcoal records (Whitlock et al. 2006). This is because FRI in the model is calculated as a function of grid cells that burned during a single fire season. The number of grid cells that burn is a function of climate variability, which control vegetation productivity i.e. fuel load (Thonicke et al. 2001a).

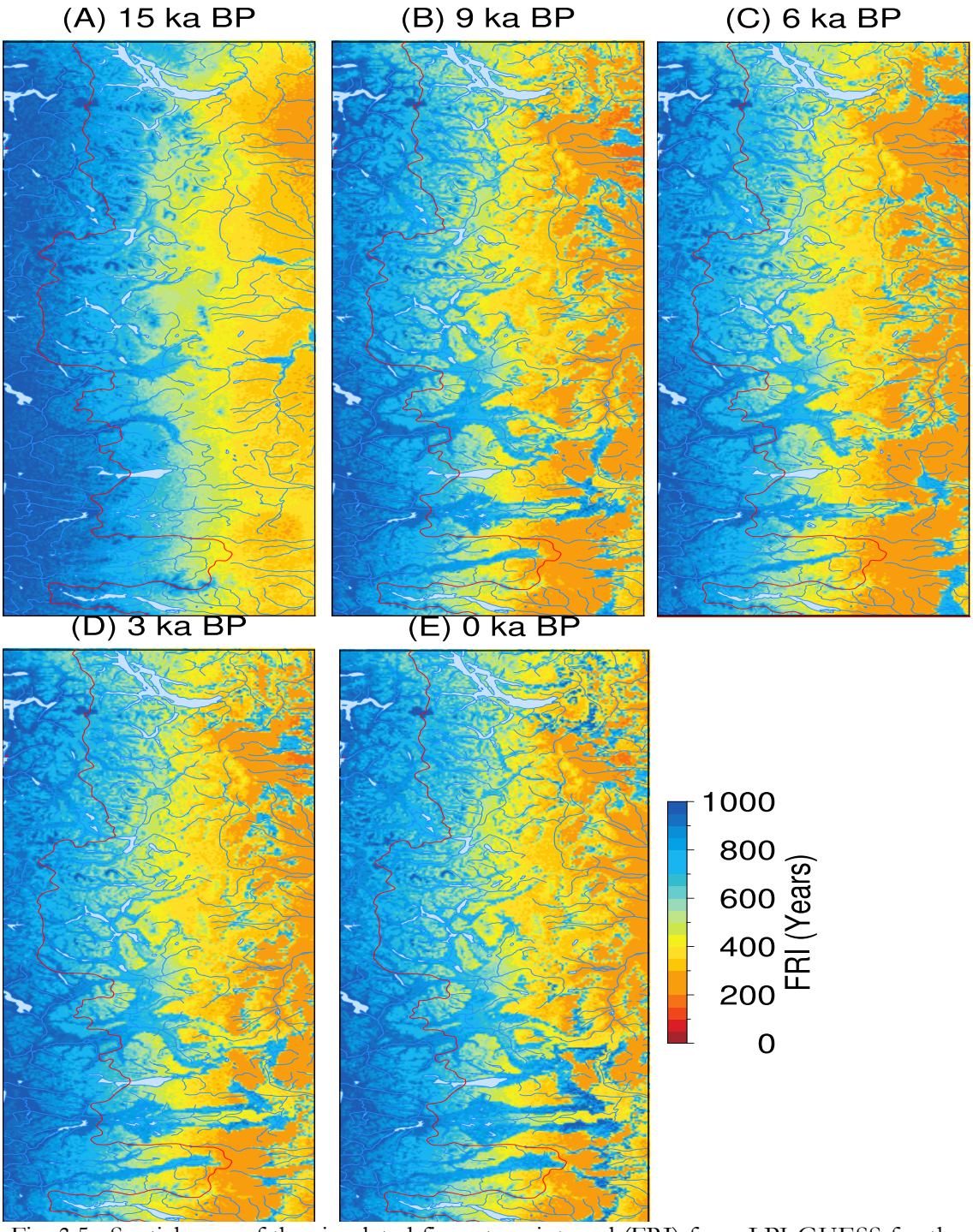

Fig. 3.5: Spatial map of the simulated fire return interval (FRI) from LPJ-GUESS for the entire study area (a) 15, (b) 9, (c) 6, 3 and (d) 0 ka BP. FRI is calculated using the fractional area of grid cells that burn during the fire season. The affected grid cells are then converted into an average fire return interval.

Control of observed biomass change and treeline dynamic

The results of the Canonical Correspondence Analysis (CCA) on plant functional types (PFTs), tree species and two types of grasses provided the tool for understanding the hierarchy of explanatory variables responsible for changes in species community assemblage during the late-glacial and postglacial periods.

During late-glacial to early Holocene transition (15 - 9 ka), the CCA model explained 52% of the total inertia (i.e., variance) using mean winter temperature, soil moisture and mean summer precipitation. The inertia explained by first two axes was 46.2% and 5.3% of the observed variance (Fig. 3.6a). We found that mean winter temperature highly constrained species distribution, for both 15 and 9 ka BP, and the greatest influence of soil moisture was at 9 ka BP because of the increase in precipitation.

At the transition from early Holocene to middle-Holocene (9 – 6 ka), the total inertia explained by our model was 53% using mean winter temperature, soil moisture, and ratio of actual/potential evapotranspiration. However, the first two axes together explained 40.6% and 12.2% of the variation (Fig. 3.6b). The changes in forest cover were driven by increased in winter temperature but soil moisture availability also played in role. Evapotranspiration increased with increasing temperature.

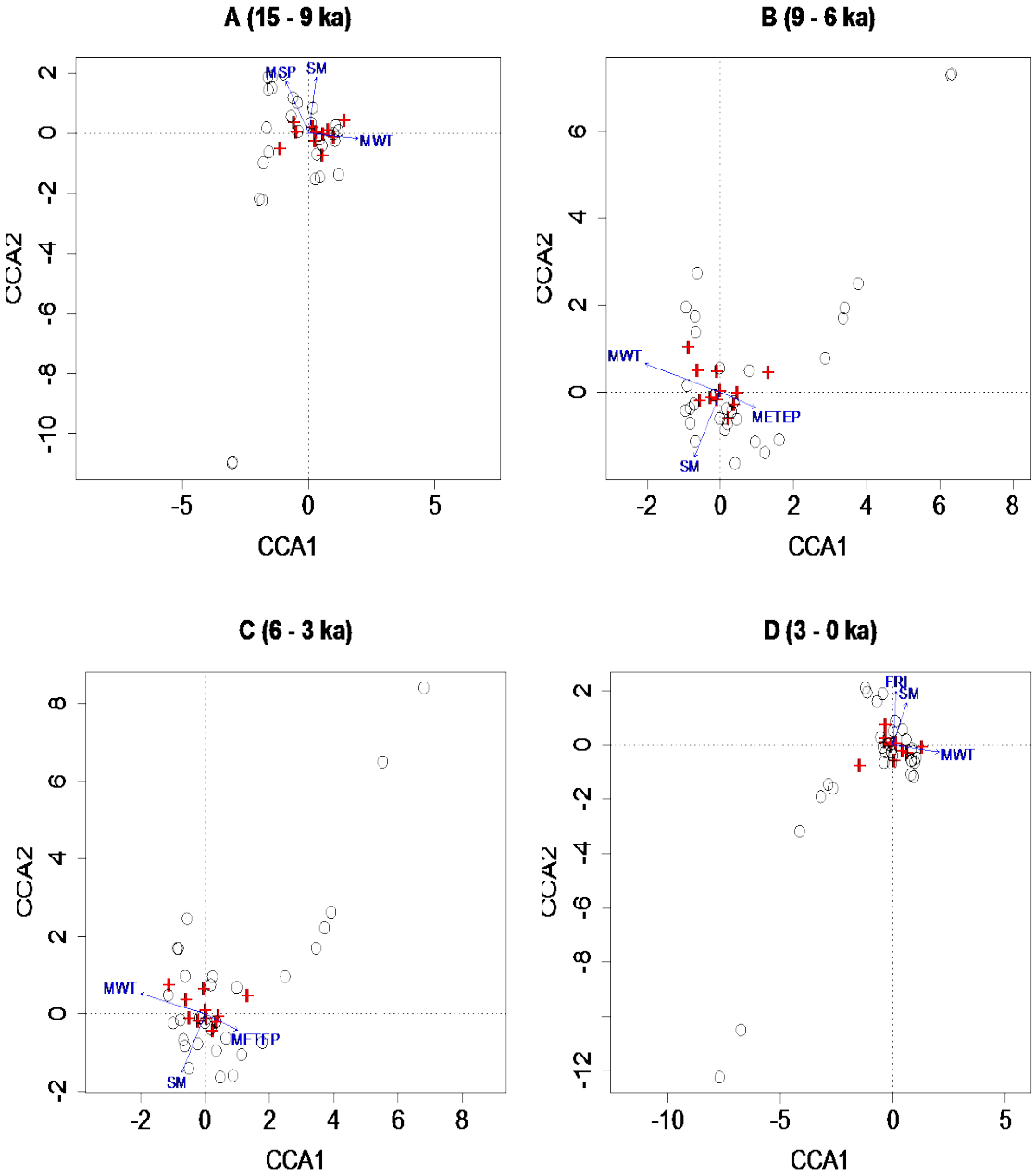

Fig. 3.6: Canonical Correspondence Analysis (CCA) triplot depicting the relationship between selected climate and fire variables and the variation of coverage among two Plant Functional Types, seven tree species, and two type of grasses. (a) late-glacial to early Holocene (15 – 9 ka BP); (b) Early Holocene to middle Holocene (9 – 6 ka BP); (c) Middle Holocene to late Holocene (6 – 3 ka BP); (d) Late Holocene to pre-industrial (3 – 0 ka BP). MWT (mean winter temperature), SM (Soil moisture), METEP (ratio of actual/potential evapotranspiration), FRI (fire return interval). Species are shown as red crosses and sites as black circles

During the middle-Holocene to late-Holocene transition (6 - 3 ka), the total inertia explained was 49% using mean winter temperature, soil moisture and ratio of actual/potential evapotranspiration), and the first two axes taken together explained 38% and 11.1% of variation (Fig. 3.6c). The result was the same as 9 – 6 ka BP transition.

Lastly, during the late-Holocene to pre-industrial transition (3 - 0 ka) the overall total inertia explained was 46% using mean winter temperature, fire return interval, and soil moisture. The first two axes combined together displayed 34.4% and 11.0% of the variation (Fig. 3.6d). The influence of mean winter temperature decreased because of increased temperature. Tree and shrub distribution was strongly limited by the increase in fire which decreased their distribution at 0 ka BP.

The Random Forest treeline driver analysis was used to determine the explanatory variables that predicts the position of the ecotone. At 15 ka BP mean summer precipitation, mean winter temperature followed by the mean winter precipitation emerged as the best predictor of biomass dynamics (R^2 = 97.5%). At 9 ka BP mean summer precipitation was selected as the best predictor of treeline tree establishment, followed by soil moisture and mean winter precipitation (R^2 = 97.7%). Mean summer precipitation mean winter precipitation, and mean winter temperature together explained the observed changes in biomass at the upper and lower treeline (R^2 = 98.1%) at 6 ka BP. During the 3 ka, it can be seen that mean summer precipitation, mean winter precipitation, and mean winter temperature were the strongest drivers of biomass (R^2 = 98.7%). Among all the potential predictors, mean summer and winter precipitation were the primary modulator of the upper and lower treeline during the late-glacial and postglacial (Fig. 3.7).

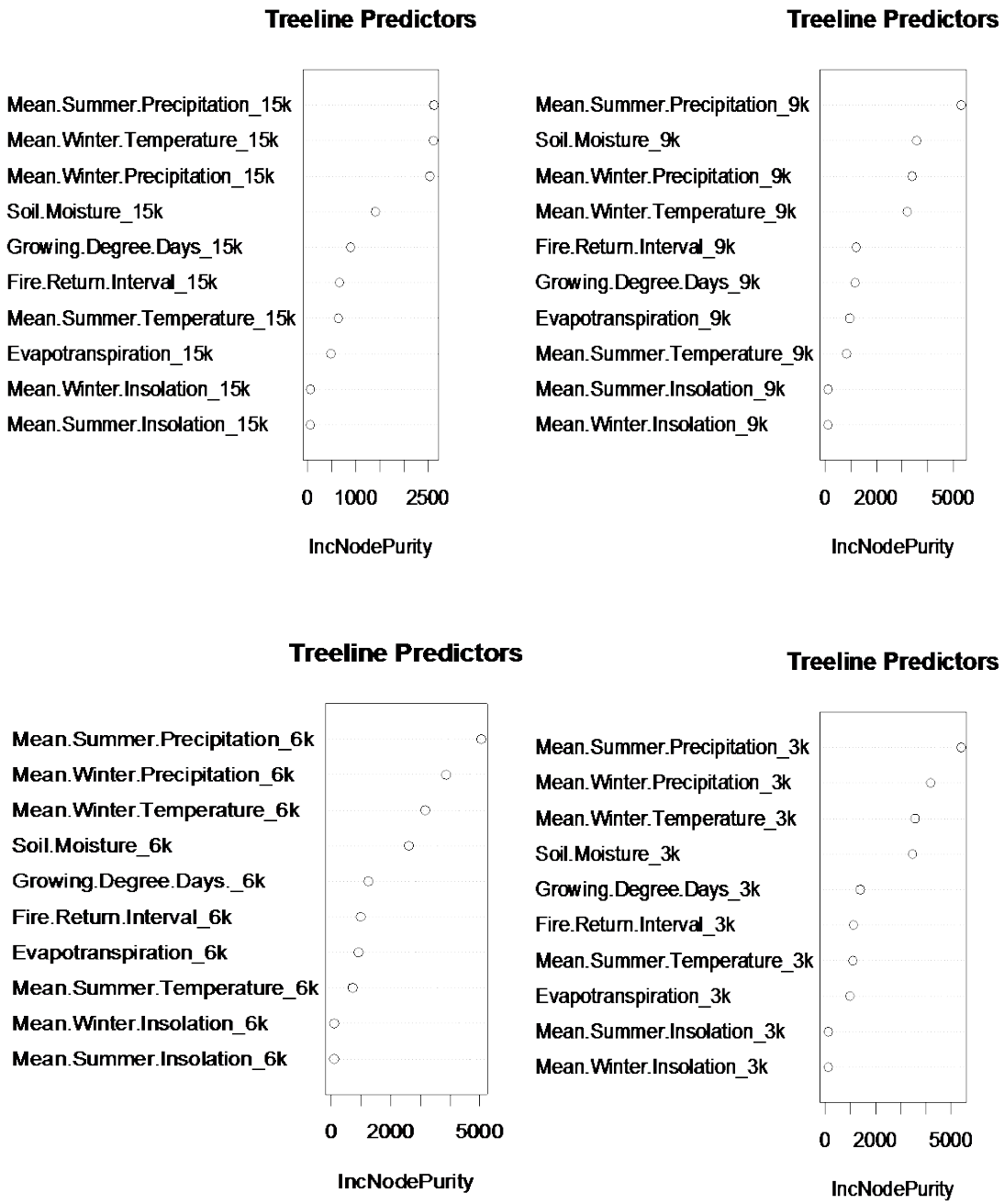

Fig. 3.7: Predictors of both upper and lower treeline establishment based on the Random Forest model during the postglacial periods. The explanatory variable with the highest purity is the best predictor of the treeline establishment.

Discussion

The simulated total tree and shrub abundance during the late-glacial and Holocene reflects shifts in the west -to-east position of the forest-steppe borderline (Fig. 3.3). The model results and changes over time are generally consistent with vegetation reconstructions based on pollen records from the region (Iglesias et al. 2011). Pollen records indicate that prior to 9 ka BP, the forest-steppe ecotone was located west of its present position, and in all likelihood, trees were relegated to discontinuous isolated refugia and no ecotone existed. The simulated forest-steppe ecotone at 15 ka BP was dominated by High Elevation grasses at a time when pollen records show high levels of *Poaceae*, *Chenopodiacea*e, *Asteraceae*, and *Apiaceae*. The general north-to-south trend across northern Patagonia (40º – 45˚S) suggests that fire activity increased during the postglacial, with variability at early Holocene (9 ka BP) and middle Holocene (6 ka BP) followed by more fire in the late Holocene (Fig. 3.4). Most pollen records, however, show the most significant forest cover at 6 and 3 ka BP with a continued rise over the last millennia because of the cooler and wetter conditions and increased interannual climate variability, along with decreasing winter and increasing summer insolation (Whitlock et al. 2006, Nanavati et al. 2019). Our quantitative analyses of the drivers of vegetation distribution suggested that increases in winter temperature drove the observed change in spatial vegetation composition through the late-glacial to postglacial (Fig. 5). Our results also supports de Porras et al. (2012) who observed that the change from cold tolerant grass and shrub to present-day forest-steppe ecotone vegetation at central Chilean Patagonia was the result of the increase in temperature at the start of the Holocene. Our result agrees with empirical studies of drivers of treeline dynamics in northern Patagonia which show that climate variability (e.g.,

precipitation) controls the upward and downward shifts of upper and lower treeline (Villalba and Veblen 1997, Daniels and Veblen 2004, Lara et al. 2005).

Vegetation and fire trend during the late-glacial and postglacial periods

The simulated biomass and fire during the postglacial periods are in good agreement with pollen and charcoal records from the region(Whitlock et al. 2006, Markgraf et al. 2007, Whitlock et al. 2007, Iglesias et al. 2011, Markgraf et al. 2013, Iglesias and Whitlock 2014, Nanavati et al. 2019). During the late-glacial period, low biomass was accompanied by little fire (Fig. 3.5a), as a result of cold dry conditions (Fig. 3.2) (Whitlock et al. 2006, de Porras et al. 2012, Markgraf et al. 2013, Iglesias et al. 2014, Nanavati et al. 2019) and also to low atmospheric CO_2 concentration (220 ppmv) (Kaplan et al. 2002, Prentice and Harrison 2009). The general reduction in simulated biomass at 15 ka BP is consistent with modeled reduction in global annual net primary production (aNNP) simulated by Kaplan et al. (2002) for the last 21 ka BP. During the 15 ka BP, simulated fire was low as a result of limited tree establishment. Although charcoal data at 15 ka BP indicate negligible fire (Iglesias and Whitlock 2014), simulated fire distribution for that period shows small areas of fire in the steppe (Fig. 3.5a). In general, however, the simulated biomass and fire results show a good agreement with pollen and charcoal results at 15 ka.

The late-glacial to early-Holocene transition was characterized by an increase in biomass and fire activities as a result of increased soil moisture and temperature (Fig. 3.2). During this period, effective moisture increased, which was attributed to a shift from polar air masses to humid Pacific air masses as the SWW shifted south from their glacial position (Vilanova et al. 2019). Nanavati et al. (2019) suggest that the increased in fire and tree cover

during the transition was a result of rising temperature induced by increased winter and annual insolation (i.e., their figure 5). During this transition, the pollen data show an increase in woody vegetation (e.g., *Nothofagus-type*) (Whitlock et al. 2007, Iglesias et al. 2011, Iglesias and Whitlock 2014). The highest biomass simulated during the late-glacial to postglacial period was during the early Holocene, which we attribute to wetter conditions, increased in temperature and a increased in atmospheric CO_2 concentration (from 220 to 260 ppmv), increased biomass productivity (Harrison and Prentice 2003). With the temperature increased the forest established in a north-south time transgressive pattern (Iglesias et al. 2018). During the early Holocene, fire increased as a result of increased winter temperatures and precipitation, and fuel desiccation during dry summers. Charcoal peak analysis by Whitlock et al. (2006) suggests that the fire episodes were lower at 9 ka BP (c. 70 years) compared to the late-glacial and attributed more fire principally to a poleward shift or weakening of the Southern Westerlies, superimposed with higher winter insolation compared to present levels.

The middle Holocene was characterized by wetter conditions than early Holocene (Fig. 3.2). Between 9 and 6 ka BP, a steady decrease in winter insolation and increase in summer insolation (Alder and Hostetler 2015) led to a strengthening of the Southern Westerlies at mid-latitude and reduced seasonality of precipitation (Whitlock et al. 2006). Simulated biomass was lower slightly at 6 ka BP compared to 9 ka BP (10 vs. 12.2 kg C m^{-2}). Whereas pollen reconstructions suggest that this period had high forest cover (Whitlock et al. 2006, Iglesias et al. 2012, Markgraf et al. 2013, Iglesias et al. 2014), the slight reduction in simulated biomass at 6 ka BP is attributed to colder conditions (decreased winter temperature), which reduced growing season length thereby constraining photosynthetic activity and reducing simulated biomass (Fig. 3.2). The influence of climate on biomass at 6

ka BP was more pronounced than the role of atmospheric CO_2 because both periods use the same CO_2 concentration for simulations (260 ppmv vs. 260 ppmv). During the middle Holocene, pollen records document an increase in tree (e.g., *Nothofagus-type*, *Austrocedrus chilensis*) suggesting higher forest cover compared to 9 ka BP, coupled with reduced fire (Whitlock et al. 2006, Iglesias et al. 2011, Iglesias and Whitlock 2014, Nanavati et al. 2019). During this period, the mean simulated mean fire return interval was slightly lower compared to 9 ka BP showing a good agreement with charcoal reconstructions of fewer fires at 6 ka BP.

During the late Holocene (3 ka BP), simulated biomass increased from its 6 ka BP level and fire increased (Fig. 3.4). This period was characterized by an increase in summer and decrease in winter insolation to present levels (Alder and Hostetler 2015). Climate anomalies, such as ENSO and probably SAM, strengthening during this period, thereby influencing seasonal precipitation and temperature (Kitzberger et al. 1997, Holz and Veblen 2012, Holz et al. 2017, Mundo et al. 2017). According to results from pollen records the late Holocene was characterized by an increase in *Austrocedrus chilensis* and decrease in *Nothofagus* abundance at some sites (Whitlock et al. 2006, Whitlock et al. 2007, Iglesias et al. 2011, Nanavati et al. 2019). The abundance of these two species fluctuates with climate with *Nothofagus* dominating during humid periods, and *Austrocedrus chilensis* becoming abundant during dry periods. At intermediate moisture levels, both species are present, with fire playing an important role in their relative abundance (Iglesias et al. 2014). The highest peak in fire activity was observed during the late Holocene in most charcoal records from northern Patagonia (Whitlock et al. 2007). The increase in fires has been attributed to climate variability related to ENSO and a reduction in effective moisture during the growing season (Villalba et al. 2003).

Climate influence on late-glacial and postglacial species distribution and treeline

Temperature together with growing degree days significantly impact the physiological activities of plants, including photosynthesis, respiration, and phenology which in turn affects biome composition. During the late-glacial period, trees were likely growing in isolated refugia, and following ice recession, and as temperature and effective moisture increased, populations started to expand (Whitlock et al. 2006, Markgraf et al. 2013, Iglesias et al. 2014). The late-glacial climate was not suitable for a closed forest (Markgraf et al. 2013). Low winter temperatures (Fig. 3.2) would have limited the growing season, thereby favoring development of grass over tree establishment. The colder and drier climate would have also increased frost events resulting in less favorable bioclimatic conditions. With increasing winter temperature at 9ka, biomass levels increased throughout Patagonia (Markgraf et al. 2007), and winters became warmer and wetter (Fig. 3.6b). Given higher biomass simulated, tree establishment increased and successively replaced grasses further east establishing the lower treeline. Due to the decrease in seasonality caused by higher winter and lower summer insolation during the early Holocene compared to present day, fire activities increased (Whitlock et al. 2006). At the transition from 9 – 6 ka BP the climate became wetter and cooler than before (Fig. 3.2), the contribution of soil moisture to species distribution increased as a result of increased effective moisture (Fig. 3.6b). During this period, the SWW weakened and was displaced southward. Paleoclimate model simulations (Alder and Hostetler 2015) note a higher winter insolation and lower summer insolation compared to present-day at this time. The increase in effective moisture support the distribution of species and increase in biomass.

At the transition from middle Holocene to late-Holocene (6 – 3 ka BP), species distribution increased (e.g., *Austrocedrus chilensis*, *Nothofagus type*), due to the increase in winter

temperature (Fig. 3.6c), which lengthened the growing season. The results of simulated biomass and the climate drivers of species distribution for 9 - 6 ka BP and 6 – 3 ka BP shows little difference. This is unsurprising given the relatively small climate changes (e.g., temperature and precipitation) between 9 - 6 and 6 - 3 ka BP. The model did not simulate any significant difference between the two transition periods. However, the most notable and consistent change between 9 - 6 and 6 - 3 ka were the high abundance of forest cover in northern Patagonia at 6 ka BP. Pollen records show a transition from early Holocene forest dominated by *Nothofagus dombeyi* to one co-dominated by *Austrocedrus chilensis* in the late Holocene (Whitlock et al. 2006, Iglesias and Whitlock 2014, Nanavati et al. 2019). Paleoclimate model simulations (Alder and Hostetler 2015) incorporate lower winter insolation and higher summer insolation compared to previous at this time, and we think this was the main driver for increasing forest cover at 3 ka BP. During this period (6 -3 ka BP) SWW strengthened and shifted to the present-day position increasing effective moisture. Simulated fire increased (3 ka BP), and charcoal records shows high frequency in fire activity throughout northern Patagonia (Whitlock et al. 2007). The transition from the late Holocene to the pre-industrial period (3 to 0 ka) highlighted the role of fire in reducing forest expansion into the steppe (Fig. 3.6d; Gowda et al. 2011).

The simulated range of treeline variation is based on precipitation changes from the late-glacial to late Holocene (Fig. 3.7). The role of climate in controlling species distribution and hence upper and lower treeline position is less understood because the influence of microclimatic conditions and nonclimatic conditions (e.g., soil, topography) may mask the effect of other environmental drivers (e.g., cold-induced photoinhibition, disturbance, plant-plant interaction) (Cullen et al. 2001, Bekker 2005, Danby and Hik 2007). Our results show

that treeline dynamics (lower and upper) are sensitive to changes in limiting factors, and even a slight increase or decrease in precipitation will alter tree growth at treeline. These findings support previous studies indicating the role of precipitation in controlling the position of upper and lower treeline (Villalba and Veblen 1997, Daniels and Veblen 2004, Lara et al. 2005). Lara et al. (2005) analyzed tree radial growth and seedling establishment of *N. pumilio* at both mesic and xeric sites in northern Patagonia. They found that at the mesic treeline, establishment were promoted by higher growing season precipitation while at xeric treeline, establishment were promoted by a cooler-wetter growing season. Also, Daniels and Veblen (2004) found periods when both the upper and lower treelines respond to the same climate variation. For example, 1957 to 1976 was considered a cooler-wetter period, and during this period, both the upper and lower treeline were controlled by a warmer growing season. Whereas, 1977 – 1996 was regarded as a warmer-drier period, and during this interval, both upper and lower treeline establishment were controlled by wetter summer.

In northern Patagonia, changes in precipitation appear to play the most critical role in treeline dynamics. An increase in summer precipitation is seen from the late-glacial to the Holocene using the RF model, which shows that summer precipitation is crucial for driving treeline forest growth. In terms of parameters that control the upper and lower treelines more directly, summer and winter precipitation translate into an increase in soil availability and lengthening of the growing season. However, in the model simulations, change in precipitation appears to account for all of the climatically induced changes in upper and lower treeline dynamics, whereas temperature has little effect.

Conclusion

This study is the first study that used a DGVM to model the postglacial vegetation cover for northern Patagonia. Over the last 15 ka BP, the climate of northern Patagonia has changed markedly with increased in temperatures and effective moisture which have ultimately changed the vegetation (Whitlock et al. 2006, Iglesias et al. 2012, Markgraf et al. 2013, Iglesias and Whitlock 2014, Iglesias et al. 2014, Nanavati et al. 2019). The natural changes in climate altered species abundance and the position of the forest-steppe border.

Significant findings from this study are:

1. Our result shows that a Dynamic Global Vegetation Model can simulate late-glacial and postglacial vegetation forest cover and treeline (upper and lower) position. These simulations can be used to explore changes in treeline and vegetation through time as a point of comparison with paleoecological data.
2. The trends in biomass and fire from the model matches well with published quantitative pollen and charcoal reconstructions. CCA analysis reveals that low winter temperatures were the primary climatic factor that controlled forest cover during the late-glacial period. Increased temperature and effective moisture increased growing season moisture conducive for the expansion of forest during the early Holocene (Whitlock et al. 2007, Iglesias et al. 2011, Nanavati et al. 2019).
3. The simulated model treeline dynamics (upper and lower) shows a response to changes in summer and winter precipitation, which indicated that precipitation alone could account for the changes in upper and lower treeline from the late-glacial to the late Holocene. Pollen data, however, suggests that the reduction in annual and winter

insolation combined with the strengthening of the Southern Westerlies brought increased precipitation over northern Patagonia.

4. Changes in upper and lower treeline dynamics are driven by increased moisture availability but increased in temperature at the start of the Holocene played a role in forest cover distribution.
5. The results of our study shows that the combined use of paleoecological data and dynamic vegetation modeling can shed new insights on long-term vegetation history including factors that govern fire activity and treeline dynamics.

Acknowledgements

This work was supported by the National Science Foundation [grant number GSS 1461590]. The manuscript was improved by helpful suggestion and comments from Laura Burkle.

References

Alder, J. R., and S. W. Hostetler. 2015. Global climate simulations at 3000-year intervals for the last 21 000 years with the GENMOM coupled atmosphere–ocean model. Climate of the Past **11**:449-471.

Allen, J. R. M., T. Hickler, J. S. Singarayer, M. T. Sykes, P. J. Valdes, and B. Huntley. 2010. Last glacial vegetation of northern Eurasia. Quaternary Science Reviews **29**:2604-2618.

Avitabile, V., M. Herold, G. B. Heuvelink, S. L. Lewis, O. L. Phillips, G. P. Asner, J. Armston, P. S. Ashton, L. Banin, N. Bayol, N. J. Berry, P. Boeckx, B. H. de Jong, B. DeVries, C. A. Girardin, E. Kearsley, J. A. Lindsell, G. Lopez-Gonzalez, R. Lucas, Y. Malhi, A. Morel, E. T. Mitchard, L. Nagy, L. Qie, M. J. Quinones, C. M. Ryan, S. J. Ferry, T. Sunderland, G. V. Laurin, R. C. Gatti, R. Valentini, H. Verbeeck, A. Wijaya, and S. Willcock. 2016. An integrated pan-tropical biomass map using multiple reference datasets. Glob Chang Biol **22**:1406-1420.

Bekker, M. F. 2005. Positive Feedback Between Tree Establishment and Patterns of Subalpine Forest Advancement, Glacier National Park, Montana, U.S.A. Arctic, Antarctic, and Alpine Research **37**:97-107.

Breiman, L. 2001. Machine Learning **45**:5-32.

Brovkin, V., T. Raddatz, C. H. Reick, M. Claussen, and V. Gayler. 2009. Global biogeophysical interactions between forest and climate. Geophysical Research Letters **36**:n/a-n/a.

Cullen, L. E., G. H. Stewart, R. P. Duncan, and J. G. Palmer. 2001. Disturbance and Climate Warming Influences on New Zealand Nothofagus Tree-LinePopulation Dynamics. Journal of Ecology **89**:1061-1071.

Danby, R. K., and D. S. Hik. 2007. Responses of white spruce (Picea glauca) to experimental warming at a subarctic alpine treeline. Global change Biology **13**:437-451.

Daniels, L. D., and T. T. Veblen. 2004. Spatiotemporal influences of climate on altitudinal treeline in northern Patagonia. Ecology **85**:1284-1296.

de Porras, M. E., A. Maldonado, A. M. Abarzúa, M. L. Cárdenas, J. P. Francois, A. Martel-Cea, C. R. Stern, C. Méndez, and O. Reyes. 2012. Postglacial vegetation, fire and climate dynamics at Central Chilean Patagonia (Lake Shaman, 44°S). Quaternary Science Reviews **50**:71-85.

Donoso, C. 2006. Especies arbóreas de los bosques templados de Chile y Argentina: autoecología. Marisa Cuneo Eds, Santiago de Chile:.

Erdős, L., D. Ambarlı, O. A. Anenkhonov, Z. Bátori, D. Cserhalmi, M. Kiss, G. Kröel-Dulay, H. Liu, M. Magnes, Z. Molnár, A. Naqinezhad, Y. A. Semenishchenkov, C. Tölgyesi, P. Török, and B. Jiménez-Alfaro. 2018. The edge of two worlds: A new review and synthesis on Eurasian forest-steppes. Applied Vegetation Science **21**:345-362.

Erdős, L., C. Tölgyesi, M. Horzse, D. Tolnay, Á. Hurton, N. Schulcz, L. Körmöczi, A. Lengyel, and Z. Bátori. 2014. Habitat complexity of the Pannonian forest-steppe zone and its nature conservation implications. Ecological Complexity **17**:107-118.

Garreaud, R. D., M. Vuille, R. Compagnucci, and J. Marengo. 2009. Present-day South American climate. Palaeogeography, Palaeoclimatology, Palaeoecology **281**:180-195.

Gowda, J. H., T. Kitzberger, and A. C. Premoli. 2011. Landscape responses to a century of land use along the northern Patagonian forest-steppe transition. Plant Ecology **213**:259-272.

Green, R. H., R. H. G. Jongman, C. J. F. Braak, and O. F. R. V. Tongeren. 1990. Data Analysis in Community and Landscape Ecology. Biometrics **46**.

Harris, I., P. D. Jones, T. J. Osborn, and D. H. Lister. 2014. Updated high-resolution grids of monthly climatic observations - the CRU TS3.10 Dataset. International Journal of Climatology **34**:623-642.

Harrison, S. P., and C. I. Prentice. 2003. Climate and CO2 controls on global vegetation distribution at the last glacial maximum: analysis based on palaeovegetation data, biome modelling and palaeoclimate simulations. Global change Biology **9**:983-1004.

Heusser, C. J. 1966. Late-Pleistocene pollen digrams from the Province of Llanquihue, southern Chile. Proceedings of the American Philosophical Society **110**:269-305.

Heusser, C. J. 1974. Vegetation and climate of the southern Chilean Lake District during and since the last interglaciation. Quaternary Research **4**:290-315.

Hickler, T., K. Vohland, J. Feehan, P. A. Miller, B. Smith, L. Costa, T. Giesecke, S. Fronzek, T. R. Carter, W. Cramer, I. Kühn, and M. T. Sykes. 2012. Projecting the future distribution of European potential natural vegetation zones with a generalized, tree species-based dynamic vegetation model. Global Ecology and Biogeography **21**:50-63.

Hijmans, R. J., S. E. Cameron, J. L. Parra, P. G. Jones, and A. Jarvis. 2005. Very high resolution interpolated climate surfaces for global land areas. International Journal of Climatology **25**:1965-1978.

Holz, A., J. Paritsis, I. A. Mundo, T. T. Veblen, T. Kitzberger, G. J. Williamson, E. Araoz, C. Bustos-Schindler, M. E. Gonzalez, H. R. Grau, and J. M. Quezada. 2017. Southern Annular Mode drives multicentury wildfire activity in southern South America. Proc Natl Acad Sci U S A **114**:9552-9557.

Holz, A., and T. T. Veblen. 2012. Wildfire activity in rainforests in western Patagonia linked to the Southern Annular Mode. International Journal of Wildland Fire **21**:114.

Hostetler, S., N. Pisias, and A. Mix. 2006. Sensitivity of Last Glacial Maximum climate to uncertainties in tropical and subtropical ocean temperatures. Quaternary Science Reviews **25**:1168-1185.

Iglesias, V., S. G. Haberle, A. Holz, and C. Whitlock. 2018. Holocene Dynamics of Temperate Rainforests in West-Central Patagonia. Frontiers in Ecology and Evolution **5**.

Iglesias, V., F. Quintana, W. Nanavati, and C. Whitlock. 2016. Interpreting modern and fossil pollen data along a steep environmental gradient in northern Patagonia. The Holocene **27**:1008-1018.

Iglesias, V., and C. Whitlock. 2014. Fire responses to postglacial climate change and human impact in northern Patagonia (41-43 degrees S). Proc Natl Acad Sci U S A **111**:E5545-5554.

Iglesias, V., C. Whitlock, M. M. Bianchi, G. Villarosa, and V. Outes. 2011. Holocene climate variability and environmental history at the Patagonian forest/steppe ecotone: Lago Mosquito (42°29'37.89"S, 71°24'14.57"W) and Laguna del Cóndor (42°20'47.22"S, 71°17'07.62"W). The Holocene **22**:1297-1307.

Iglesias, V., C. Whitlock, M. M. Bianchi, G. Villarosa, and V. Outes. 2012. Climate and local controls of long-term vegetation dynamics in northern Patagonia (Lat 41°S). Quaternary Research **78**:502-512.

Iglesias, V., C. Whitlock, V. Markgraf, and M. M. Bianchi. 2014. Postglacial history of the Patagonian forest/steppe ecotone (41–43°S). Quaternary Science Reviews **94**:120-135.

Iglesias, V., G. I. Yospin, and C. Whitlock. 2015. Reconstruction of fire regimes through integrated paleoecological proxy data and ecological modeling. Front Plant Sci **5**:785.

Kaplan, J. O., I. C. Prentice, W. Knorr, and P. J. Valdes. 2002. Modeling the dynamics of terrestrial carbon storage since the Last Glacial Maximum. Geophysical Research Letters **29**:31-31-31-34.

Kitzberger, T. 2012. Ecotones as Complex Arenas of Disturbance, Climate, and Human Impacts: The Trans-Andean Forest-Steppe Ecotone of Northern Patagonia. Pages 59-88 *in* R. Myster, editor. Ecotones Between Forest and Grassland. Springer, New York.

Kitzberger, T., T. T. Veblen, and R. Villalba. 1997. Climatic influences on fire regimes along a rain forest to xeric woodland gradient in northern Patagonia, Argentina. Journal of Biogeography **24**:35-47.

Lara, A., R. Villalba, A. Wolodarsky-Franke, J. C. Aravena, B. H. Luckman, and E. Cuq. 2005. Spatial and Temporal Variation in Nothofagus pumillo Growth at Tree Line along ItsLatitudinal Range (35°40'-55° S) in the Chilean Andes. Journal of Biogeography **32**:879-893.

Leach, M. K., and T. J. Givnish. 1999. Gradients in the composition, structure, and diversity of remnant oak savannas in southern Wisconsin. Ecological Monographs **69**:353-374.

Liaw, A., and M. Wiener. 2002. Classification and Regression by randomForest. R News **2**:18-22.

Markgraf, V. 1983. Late and Postglacial Vegetational and Paleoclimatic Changes in Subantarctic, Temperate, and Arid Environments in Argentina. Palynology **7**:43-70.

Markgraf, V., V. Iglesias, and C. Whitlock. 2013. Late and postglacial vegetation and fire history from Cord?n Serrucho Norte, northern Patagonia. Palaeogeography, Palaeoclimatology, Palaeoecology **371**:109-118.

Markgraf, V., C. Whitlock, and S. Haberle. 2007. Vegetation and fire history during the last 18,000 cal yr B.P. in Southern Patagonia: Mallín Pollux, Coyhaique, Province Aisén (45°41'30" S, 71°50'30" W, 640 m elevation). Palaeogeography, Palaeoclimatology, Palaeoecology **254**:492-507.

Mátyás, C., and G. Sun. 2014. Forests in a water limited world under climate change. Environmental Research Letters **9**.

Mermoz, M., T. Kitzberger, and T. T. Veblen. 2005. Landscape Influences on Occurrence and Spread of Wildfires in Patagonian Forests and Shrublands. Ecology **86**:2705-2715.

Miller, P. A., T. Giesecke, T. Hickler, R. H. W. Bradshaw, B. Smith, H. Seppä, P. J. Valdes, and M. T. Sykes. 2008. Exploring climatic and biotic controls on Holocene vegetation change in Fennoscandia. Journal of Ecology **96**:247-259.

Mundo, I. A., R. Villalba, T. T. Veblen, T. Kitzberger, A. Holz, J. Paritsis, and A. Ripalta. 2017. Fire history in southern Patagonia: human and climate influences on fire activity in Nothofagus pumilio forests. Ecosphere **8**.

Nanavati, W. P., C. Whitlock, V. Iglesias, and M. E. de Porras. 2019. Postglacial vegetation, fire, and climate history along the eastern Andes, Argentina and Chile (lat. 41-55 degrees S). Quaternary Science Reviews **207**:145-160.

Oksanen, J., F. G. Blanchet, M. Friendly, R. Kindt, P. Legendre, D. McGlinn, P. R. Minchin, R. B. O'Hara, G. L. Simpson, P. Solymos, M. H. H. Steven, E. Szoecs, and H. Wagner. 2019. Vegan: community ecology package. R package version 2.5-6.

Olson, D. M., E. Dinerstein, E. D. Wikramanayake, N. D. Burgess, G. V. N. Powell, E. C. Underwood, J. A. D'Amico, I. Itoua, H. E. Strand, J. C. Morrison, C. J. Loucks, T. F.

Allnutt, T. H. Ricketts, Y. Kura, J. F. Lamoreux, W. W. Wettengel, P. Hedao, and K. R. Kassem. 2001. Terrestrial Ecoregions of the World: A New Map of Life on Earth. BioScience **51**:933-938.

Pacanowski, R. C. 1996. MOM 2 Version 2.0 (Beta) Documentation: User's Guide and Reference Manual, Technical Report 3.2, NOAA GFDL Ocean Group, GFDL. Princeton, New Jersey.

Paruelo, J. M., A. B. Beltran, E. G. Jobbagy, O. E. Sala, and R. A. Golluscio. 1998. The climate of Patagonia: general patterns and controls on biotic processes. Ecologia Austral **8**:85-101.

Pollard, D., and S. L. Thompson. 1997. Climate and ice-sheet mass balance at the last glacial maximum from the genesis version 2 global climate model,. Quaternary Science Reviews **16**:841-863.

Prentice, I. C., and S. P. Harrison. 2009. Ecosystem effects of CO2 concentration: evidence from past climates. Climate of the Past **5**:297-307.

Schultz, J. 2005. The Ecozones of the World. Springer Berlin, Germany.

Sitch, S., B. Smith, I. C. Prentice, A. Arneth, A. Bondeau, W. Cramer, J. O. Kaplans, S. Levis, W. Lucht, M. T. Sykes, and K. Thonicke. 2003. Evaluation of ecosystem dynamics,plant geography and terrestial carbon cycling in the LPJ dynamic global vegetation model. Global change Biology **9**:25.

Smith, B., I. C. Prentice, and M. T. Sykes. 2001. Representation of vegetation dynamics in the modelling of terrestrial ecosystems: comparing two contrasting approaches within European climate space. Global Ecology and Biogeography **10**:621-637.

Stan, K., and A. Sanchez-Azofeifa. 2019. Tropical Dry Forest Diversity, Climatic Response, and Resilience in a Changing Climate. Forests **10**.

Tabor, C. R., C. J. Poulsen, and D. Pollard. 2014. Mending Milankovitch's theory: obliquity amplification by surface feedbacks. Clim. Past **10**:41-50.

Ter Braak, C. J. F. 1986. Canonical Correspondence Analysis: A new eigenvector technique for multivariate direct gradient analysis. Ecology **67**:1167-1179.

Ter Braak, C. J. F. 1987. The analysis of vegetation-environment relationships by canonical correspondence analysis. Vegetatio **69**:69-77.

Thonicke, K., S. Venevsky, S. Sitch, and W. Cramer. 2001. The role of fire disturbance for global vegetation dynamics: coupling fire into a Dynamic Global Vegetation Model. Global Ecology & Biogeography **10**:661-677.

Veblen, T. T., C. Donoso, T. Kitzberger, and A. J. Rebertus. 1996. Ecology of Southern Chilean and Argentinean Nothofagus Forests.*in* T. T. Veblen, R. S. Hill, and J. Read, editors. The Ecology and Biogeography of Nothofagus Forests. Yale University Press, New Haven, USA.

Veblen, T. T., T. Kitzberger, R. Villalba, and J. Donnegan. 1999. Fire History in Northern Patagonia: The Roles of Humans and Climatic Variation. Ecological Monographs **69**:47-67.

Vilanova, I., P. I. Moreno, C. G. Miranda, and R. P. Villa-Martínez. 2019. The last glacial termination in the Coyhaique sector of central Patagonia. Quaternary Science Reviews **224**.

Villalba, R., A. Lara, J. A. Boninsegna, M. Masiokas, S. Delgado, J. C. Aravena, F. A. Roig, A. Schmelter, A. Wolodarsky, and A. Ripalta. 2003. Large-Scale Temperature Changes across the Southern Andes: 20th-Century Variations in the Context of the Past 400 Years. Climatic Change **59**:177-232.

Villalba, R., and T. T. Veblen. 1997. Regional Patterns of Tree Population Age Structures in Northern Patagonia: Climatic andDisturbance Influences. Journal of Ecology **85**:113-124.

Wessel, P., H. F. S. Walters, R. Scharroo, J. Luis, and F. Wobbe. 2013. Generic Mapping Tools: Improved Version Released. Eos **94**:409-420.

Whitlock, C., M. M. Bianchi, P. J. Bartlein, V. Markgraf, J. Marlon, M. Walsh, and N. McCoy. 2006. Postglacial vegetation, climate, and fire history along the east side of the Andes (lat 41–42.5°S), Argentina. Quaternary Research **66**:187-201.

Whitlock, C., P. I. Moreno, and P. Bartlein. 2007. Climatic controls of Holocene fire patterns in southern South America. Quaternary Research **68**:28-36.

Zhang, Z., N. E. Zimmermann, A. Stenke, X. Li, E. L. Hodson, G. Zhu, C. Huang, and B. Poulter. 2017. Emerging role of wetland methane emissions in driving 21st century climate change. Proc Natl Acad Sci U S A **114**:9647-9652.

CHAPTER 4

CONCLUSIONS

In my dissertation, I examine the past and present-day climate-fire-vegetation dynamic of southern South America forest using the LPJ-GUESS DGVM. Northern Patagonia is well suited for this research due to the diversity of climate and environment on the biomass-rich vegetation, the longitudinal change in vegetation from the wet rainforest in the west to the xeric steppe in the east (Veblen et al. 1992, Kitzberger 2012).

In particular, the research undertaken in this dissertation aims to: (1) consider CO_2 and climate effects and their interaction on present-day vegetation and biomass in northern Patagonia, and the role of fire in modulating these effects by modeling scenarios without fire. By using an experimental set-up design, I was able to employ the paired *t*-test to illustrate substantial non-linearities by which, for example, climate modifies the effect of CO_2 concentration, and fire further modifies this effect; (2) to explore potential climate drivers of forest cover and treeline dynamics along the eastern Andes of northern Patagonia by relating simulated biomass to biotic parameters. So as to contribute to the discussion about the position of the upper and lower treeline from the late-glacial to postglacial periods.

Drivers of present-day forest cover change in southern South America

The simulated changes in northern Patagonia vegetation cover between 1930 and 2010 under historical climate (1901-2016) projected a significant increase in biomass with a moderate CO_2 fertilization effect. The highest carbon loss, approximately 23%, was under pre-industrial climate and low CO_2 (280 ppmv) with unlimited ignition. While the model

reproduced the observed increase in biomass under the current CO_2 concentration condition (400 ppmv), there are factors that constraint the potential expected level of biomass increase under elevated CO_2 (eCO_2). Plants nutrients such as phosphorus and nitrogen have been projected to mitigate the effect of rising CO_2 based on a global free-air CO_2 enrichment (FACE) and chamber experiments (Terrer et al. 2019). However, in northern Patagonia, there has been a steady shift from a pyrophytic to pyrophobic vegetation state, which has resulted in positive vegetation-fire feedback (Veblen and Lorenz 1988, Kitzberger et al. 2016). Due to the limited ignition ecosystem of northern Patagonia, the most significant sources of ignition are caused by anthropogenic activities and sometimes lightning strikes. The role of lightning in igniting massive fire has not been adequately accounted for due to the lack of multi-decadal records to quantify burned areas based on lightning strikes (Kitzberger et al. 2016). The results from the experimental setup suggested that CO_2 fertilization, climate variability, combined with a reduction in fire frequency, causes forest cover to increase.

The observed increased in forest cover, and a decrease in fire frequency is consistent with previous research in northern Patagonia that study changes in land cover (Veblen and Lorenz 1987, Veblen and Lorenz 1988, Kitzberger and Veblen 1999, Gowda et al. 2011). However, in this study using a DGVM we proposed that climate and CO_2 drives the increase in forest cover while empirical results from previous studies based on the analysis of century-old historical maps and remote sensing dataset attributed forest expansion to higher moisture, intentional fire suppression and more effective fire management, at the forest-steppe ecotone (Veblen and Lorenz 1988, Gowda et al. 2011). The increase in effective moisture at the forest-steppe ecotone increases the rate of seedling survival and establishment and, accompanied by a reduction in fire severity, creates a very suitable microenvironments for tree survival

(Kitzberger et al. 2005, Gowda et al. 2011). The role of year to year effective moisture largely controls the establishment at both ends of the moisture gradient (wet and dry), because regions with less direct solar radiation and higher precipitation favors tree growth and establishment, thereby facilitating forest growth (Gowda et al. 2011). For example, the cool-wet periods between 1963 and 1979 witnessed a massive regeneration of *Austrocedrus* at the xeric limit of its distribution, while the increase in warming (warm and dry) between 1980 and 1990 causes the near absent of regeneration (Villalba and Veblen 1997). Along the west to east precipitation gradient in northern Patagonia there is a differential effect of CO_2 concentration with the xeric (semi-arid) vegetation gradient benefiting more from the increase in CO_2 through reduced water stress by increasing water use efficiency (WUE) compared to the wet rainforest where the effect of eCO_2 is minimal. Based on the present condition with an increasing rise in global temperature and CO_2 concentration, the model predicts an increase in forest cover compared to the pre-industrial. Whereas the rapid rise in global temperature is suggested to result in the poleward and upward shift of potential vegetation and species distribution (Settele et al. 2014). However, the rapid rise in global atmospheric CO_2 concentration is suggested to cause wood thickening a process where trees replace grasslands in savannah region (Bragg et al. 2013).

Postglacial vegetation cover

The late-glacial (15 ka BP) vegetation reconstruction from pollen records reveal a landscape different from present-day, with the forest-steppe ecotone located west of its mean early-Holocene position and the vegetation were dominated by open *Nothofagu*s forest with woodland taxa (e.g., *Nothofagus antarctica*; Iglesias et al. 2011, Markgraf et al. 2013). LPJ-GUESS correctly reproduce the broad features of the postglacial vegetation driven by output from

GENMOM under different CO_2 concentration (Alder and Hostetler 2015). The agreement of the simulation result and pollen records especially at late-glacial, indicates that the model is capable of reconstructing long-term vegetation dynamics. Two conditions can be used to explain these changes in comparison to present-day vegetation: a colder and drier climate accompanied by a lower level of atmospheric CO_2 (220 ppmv). The modeling result supports the view that the physiological effect of a steep increase in late-glacial to postglacial CO_2 with an increase in temperature is the critical factor to explain postglacial vegetation changes (Harrison and Prentice 2003). The low level of atmospheric CO_2 has been suggested to affect plant-climate interactions due to its effect on the photosynthetic rate, stomatal conductance, and water-use efficiency (Prentice and Harrison 2009). Under the late-glacial CO_2 concentration level, the rate of stomatal conductance increases concomitantly with the number of stomata in order to increase the efficient use of the low CO_2. This process increases evapotranspiration and rate of water loss limiting the physiological range of distribution (Cowling and Sykes,1999). However, the sensitivity of simulated vegetation to low CO_2 depends on the background climate and vegetation type, with needleleaf trees being much more sensitive than broadleaf trees (Woillez et al. 2011).

During the early Holocene (9 ka BP), forest cover increased, which can be explained by the combination of increase in CO_2 concentration (from 220 to 260 ppmv), and an increase in the length of the growing season, controlled by an increase in winter temperature based on canonical correspondence analysis (CCA). The increase in simulated biomass from 15 to 9 ka BP obtained in this study generally corresponded to pollen records (Whitlock et al. 2007, Iglesias et al. 2011, de Porras et al. 2012, Iglesias et al. 2014, Jara and Moreno 2014, Nanavati et al. 2019). At this time Nothofagus abundance increased along with shrubs taxa into the

steppe (e.g., *Colletia*, *Berberis* and *Discaria*), conditions became more humid as infer from paleoenvironmental records, which was attributed to changes in atmospheric circulations patterns due to higher than present annual and winter insolation and weakening of the Southern Westerlies (Whitlock et al. 2006, Iglesias and Whitlock 2014, Iglesias et al. 2014, Nanavati et al. 2019). At 9 ka BP the position of the upper and lower treeline shifted eastward as conditions favor tree radial growth and seedling establishment.

The middle Holocene (6 ka BP) is characterized by a cooler and effectively wetter condition than the present-day. While pollen spectra documents the highest increase in pollen abundance, the most notably changes in forest cover was the sharp increase in Austrocedrus population size (Whitlock et al. 2007, Iglesias et al. 2011, de Porras et al. 2012, Markgraf et al. 2013, Iglesias et al. 2014, Jara and Moreno 2014, Nanavati et al. 2019). At 6ka BP the model simulated a slight reduction in forest cover compared to 9 ka BP which is not supported by pollen records. This discrepancy might be attributed to the sensitivity of our model to input climate drivers. The climate at 6 ka BP shows a colder condition than present. This is because in LPJ-GUESS modeled biomass changes can be ascribed to bioclimatic shift (i.e., temperature changes), while changes in plant productivity are related to precipitation (Brovkin et al. 2009).

The late Holocene (3 ka BP) witnessed an increase in effective moisture. The changes in growing season temperature accompanied by an increase in CO_2 concertation increase forest cover. The 3 ka BP period marks the development of ENSO related climate variability and also the equatorward displacement and strengthening of the Southern Westerlies (Vilanova et al. 2019). During this period, the treeline is located further east of its early Holocene position as a result of a change in the environmental conditions such as an increase in water availability. At 3 ka BP *Austrocedrus* population expanded significantly compared to 6 ka BP according to

pollen spectra, which was also supported by the model and marked the beginning of the modern-day vegetation.

Postglacial fire history

Fire controls biomass, especially at the forest-steppe ecotone, and it has been suggested to reduce average aboveground biomass by approximately 50 %, which if combined with climate change and landscape fragmentation (e.g., deforestation) will have a stronger impact on the vegetation dynamic (Dionizio et al. 2018). During the late-glacial low biomass contributed to the low fire activity, which was reproduced by the model with high simulated fire return interval. Charcoal records documents little forest fire as a consequence of sparse vegetation dominated by drought-tolerant shrubs (Whitlock et al. 2007, Iglesias et al. 2011, Iglesias et al. 2014, Jara and Moreno 2014). The influence of climate in controlling biomass burning was very evident because of the cold and dry conditions resulting in low fuel production. At early-Holocene, biomass burning increased, as evidenced by the lower simulated fire return interval. Charcoal records document the substantial increase in woody vegetation at the forest-steppe ecotone. Conditions were conducive to fuel accumulation and desiccation. Fire activity increased as evident from the high charcoal accumulation rate (Whitlock et al. 2007).

During the middle Holocene changes in vegetation, composition characterized this period and the climate becomes wetter and colder. Fire events increased as the conditions became more humid, which favors forest development. The general pattern found across northern Patagonia suggest the critical role of vegetation and climate in explaining fire dynamics during the postglacial. The highest increase in fire activity was observed at late

Holocene and is mainly related to forest expansion and the onset of ENSO climate variability, while the modern-day decline in biomass burning seems to be due to active fire suppression policies and increase landscape fragmentation (e.g., increase in agricultural activities, intensive land-use) at the forest-steppe ecotone (Kitzberger and Veblen 1999, Gowda et al. 2011)

Climate control of treeline dynamics

Globally, treelines are very sensitive to temperature changes, especially at high altitudes and latitudes, where low-temperature limits tree seedling establishment (Harsch et al. 2009). The thermal regime (e.g., changes in temperature) has been traditionally considered as the primary driver of global treeline dynamics (Jobbagy and Jackson 2000). For this reason, the treeline represents a region to study how the rise in global temperature will affect the spatiotemporal pattern of global vegetation (Holtmeier and Broll 2007). Apart from the constraints of thermal limits on the global altitudinal treeline, other factors influence treeline elevation and structure. For example, in mountainous forests, the influence of regional to local-scale factors (e.g., topography) overrides climate effect (e.g., temperature; Luckman and Kavanagh 1998). On aspects that receive significantly higher radiation or higher elevation with dry conditions, the influence of low soil moisture leads to more xeric conditions which masked the effect of temperature. Thereby complicating the role of temperature and local climate as drivers of vegetation growth at the treeline. In southern South America, the drivers of treeline dynamics varies depending on the prevailing climate in the area. In the Mediterranean-type climate of northern Patagonia, precipitation is the limiting factor due to its seasonal variability. Whereas, in Southern Patagonia where there is little seasonality in precipitation, temperature is the limiting factor controlling growth at treeline (Lara et al. 2005).

Future Work

Model-data comparison

The use of vegetation modeling and paleoecological methods can assist with a better understanding of how climate and the human effect on the landscape influence long-term vegetation changes. While the use of a DGVM might not be able to answer all the paleoecological questions related to past vegetation changes, it can, however, be used as a validation tool for observational data and therefore be of crucial importance to evaluate future vegetation dynamics in a changing earth system (Heiri et al. 2006). The accuracy between pollen reconstruction and vegetation modeling is paramount for it to be used as a reality check for models (Henne et al. 2012). The evaluation of the ability of Dynamic Global Vegetation Models (DGVMs) to simulate and reproduce biomass changes using paleoclimate data is a critical challenge in assessing model performance. While it is possible to evaluate present-day vegetation by comparing modeled results with observational data or remote sensing data, there is no direct way to evaluate paleovegetation simulations against pollen records. In order to evaluate model performance, we can compare with pollen reconstruction. These methods have been used, for example, Allen et al. (2010) to investigate the potential role of vegetation changes in megafaunal extinctions during the last glacial. Dallmeyer et al. (2011) used model-data comparison to investigate Holocene vegetation and biomass changes on the Tibetan Plateau using a transient numerical model DGVM. With this in mind, DGVM can, therefore, be forced with paleoclimate data generated from a coupled atmosphere-ocean climate model (AGCM) to further understand vegetation change and composition.

The northern Patagonia region represents a very interesting region to explore model and data comparison because of (1) the relative high number of pollen records (Markgraf 1983, 1984, Whitlock et al. 2006, Whitlock et al. 2007, de Porras et al. 2012, Markgraf et al. 2013, Iglesias and Whitlock 2014, Iglesias et al. 2014, Nanavati et al. 2019) (2) significant changes in past vegetation distribution are primarily controlled by changes in the seasonal cycle of insolation, which governs temperature and Pacific storm track position (Whitlock et al. 2006, Whitlock et al. 2007, Iglesias et al. 2011, Iglesias et al. 2012, Jara and Moreno 2014, Nanavati et al. 2019) (3) the limited human influence on the natural vegetation from the late-glacial to the postglacial (Markgraf 1983, Markgraf and Anderson 1994, Whitlock et al. 2006, Iglesias and Whitlock 2014, Nanavati et al. 2019).

The model-data comparison of Patagonia's vegetation builds off work by Iglesias et al. (2016). The study used modern pollen spectra from latitude 40.°5 - 44° S and analyzed the spatial patterns using pollen indicator, classification tree and modern analog techniques. The different methods were used to predict the postglacial vegetation at Laguna el Trebo (41.07° S; 71.5° W). Out of the three methods employed, the mean analog technique (MAT) performed the best. Pollen-inferred biomass trend based on mean analog technique (MAT; Bartlein and Whitlock 1993) in northern Patagonia since the late-glacial to postglacial periods were compared to simulated biomass conducted using the LPJ-GUESS DGVM forced with anomalies from GENMOM (Alder and Hostetler 2015). Although the spatial resolution of pollen and biomass differs, the model results agree with the MAT vegetation trend in northern Patagonia, permitting the discrimination of the different *Nothofagus-type* and *Cupressaceae* and improve on our current understanding of changes in postglacial vegetation (see supplementary results; S7a & b).

Final Remarks

This research further supports the hypothesis on the role of climate, CO_2, and fire in altering vegetation dynamics (Rogers et al. 2011, Loehman et al. 2014, Sheehan et al. 2019) and its influence on the northern Patagonia forest-steppe ecotone. The modeling results support previous works based on pollen and charcoal spectra reconstruction on the role of natural climate change is impacting the vegetation, such as the changes in insolation drives the observed temperature changes (Whitlock et al. 2006). The drivers of treeline are complicated, and questions relating to drivers of treeline dynamic cannot be answered from single studies. Global emphasis has been placed on coarse-scale climate drivers such as temperature while ignoring microenvironmental factors that differentiate different treeline regions. We conclude that it is important to use process-based models in the analysis of the effect of past, present and future role of different environmental drivers which are likely to change in complex ways.

References

Alder, J. R., and S. W. Hostetler. 2015. Global climate simulations at 3000-year intervals for the last 21 000 years with the GENMOM coupled atmosphere–ocean model. Climate of the Past **11**:449-471.

Allen, J. R. M., T. Hickler, J. S. Singarayer, M. T. Sykes, P. J. Valdes, and B. Huntley. 2010. Last glacial vegetation of northern Eurasia. Quaternary Science Reviews **29**:2604-2618.

Bartlein, P. J., and C. Whitlock. 1993. Paleoclimatic interpretation of the Elk Lake pollen record. Pages 275-293 *in* J. P. Bradbury and W. E. Dean, editors. Evidence for Rapid Climate Change in the North-Central, United States: The Elk Lake Record. Geological Society of America, Boulder, CO.

Bragg, F. J., I. C. Prentice, S. P. Harrison, G. Eglinton, P. N. Foster, F. Rommerskirchen, and J. Rullkötter. 2013. Stable isotope and modelling evidence for CO₂ as a driver of glacial–interglacial vegetation shifts in southern Africa. Biogeosciences **10**:2001-2010.

Brovkin, V., T. Raddatz, C. H. Reick, M. Claussen, and V. Gayler. 2009. Global biogeophysical interactions between forest and climate. Geophysical Research Letters **36**:n/a-n/a.

Dallmeyer, A., M. Claussen, U. Herzschuh, and N. Fischer. 2011. Holocene vegetation and biomass changes on the Tibetan Plateau – a model-pollen data comparison. Climate of the Past **7**:881-901.

de Porras, M. E., A. Maldonado, A. M. Abarzúa, M. L. Cárdenas, J. P. Francois, A. Martel-Cea, C. R. Stern, C. Méndez, and O. Reyes. 2012. Postglacial vegetation, fire and climate dynamics at Central Chilean Patagonia (Lake Shaman, 44°S). Quaternary Science Reviews **50**:71-85.

Dionizio, E. A., M. Heil Costa, A. D. d. A. Castanho, G. Ferreira Pires, B. Schwantes Marimon, B. Hur Marimon-Junior, E. Lenza, F. Martins Pimenta, X. Yang, and A. K. Jain. 2018. Influence of climate variability, fire and phosphorus limitation on vegetation structure and dynamics of the Amazon–Cerrado border. Biogeosciences **15**:919-936.

Gowda, J. H., T. Kitzberger, and A. C. Premoli. 2011. Landscape responses to a century of land use along the northern Patagonian forest-steppe transition. Plant Ecology **213**:259-272.

Harrison, S. P., and C. I. Prentice. 2003. Climate and CO2 controls on global vegetation distribution at the last glacial maximum: analysis based on palaeovegetation data, biome modelling and palaeoclimate simulations. Global change Biology **9**:983-1004.

Harsch, M. A., P. E. Hulme, M. S. McGlone, and R. P. Duncan. 2009. Are treelines advancing? A global meta-analysis of treeline response to climate warming. Ecol Lett **12**:1040-1049.

Heiri, C., H. Bugmann, W. Tinner, O. Heiri, and H. Lischke. 2006. A model-based reconstruction of Holocene treeline dynamics in the Central Swiss Alps. Journal of Ecology **94**:206-216.

Henne, P. D., C. Elkin, D. Colombaroli, S. Samartin, H. Bugmann, O. Heiri, and W. Tinner. 2012. Impacts of changing climate and land use on vegetation dynamics in a Mediterranean ecosystem: insights from paleoecology and dynamic modeling. Landscape Ecology **28**:819-833.

Holtmeier, F. K., and G. E. Broll. 2007. Treeline advance - driving processes and adverse factors. Landscape Online **1**:1-33.

Iglesias, V., F. Quintana, W. Nanavati, and C. Whitlock. 2016. Interpreting modern and fossil pollen data along a steep environmental gradient in northern Patagonia. The Holocene **27**:1008-1018.

Iglesias, V., and C. Whitlock. 2014. Fire responses to postglacial climate change and human impact in northern Patagonia (41-43 degrees S). Proc Natl Acad Sci U S A **111**:E5545-5554.

Iglesias, V., C. Whitlock, M. M. Bianchi, G. Villarosa, and V. Outes. 2011. Holocene climate variability and environmental history at the Patagonian forest/steppe ecotone: Lago Mosquito (42°29'37.89"S, 71°24'14.57"W) and Laguna del Cóndor (42°20'47.22"S, 71°17'07.62"W). The Holocene **22**:1297-1307.

Iglesias, V., C. Whitlock, M. M. Bianchi, G. Villarosa, and V. Outes. 2012. Climate and local controls of long-term vegetation dynamics in northern Patagonia (Lat 41°S). Quaternary Research **78**:502-512.

Iglesias, V., C. Whitlock, V. Markgraf, and M. M. Bianchi. 2014. Postglacial history of the Patagonian forest/steppe ecotone (41–43°S). Quaternary Science Reviews **94**:120-135.

Jara, I. A., and P. I. Moreno. 2014. Climatic and disturbance influences on the temperate rainforests of northwestern Patagonia (40 °S) since ~14,500 cal yr BP. Quaternary Science Reviews **90**:217-228.

Jobbagy, E. G., and R. B. Jackson. 2000. Global controls of forest line elevation in the northern and southern hemispheres. Global Ecology and Biogeography **9**:253-268.

Kitzberger, T. 2012. Ecotones as Complex Arenas of Disturbance, Climate, and Human Impacts: The Trans-Andean Forest-Steppe Ecotone of Northern Patagonia. Pages 59-88 *in* R. Myster, editor. Ecotones Between Forest and Grassland. Springer, New York.

Kitzberger, T., G. L. W. Perry, J. Paritsis, J. H. Gowda, A. J. Tepley, A. Holz, and T. T. Veblen. 2016. Fire–vegetation feedbacks and alternative states: common mechanisms of temperate forest vulnerability to fire in southern South America and New Zealand. New Zealand Journal of Botany **54**:247-272.

Kitzberger, T., E. Raffaele, K. Heinemann, and M. J. Mazzarino. 2005. Effects of fire severity in a north Patagonian subalpine forest. Journal of Vegetation Science **16**:5-12.

Kitzberger, T., and T. T. Veblen. 1999. Fire-induced changes in northern Patagonian landscapes. Landscape Ecology **14**:1-15.

Lara, A., R. Villalba, A. Wolodarsky-Franke, J. C. Aravena, B. H. Luckman, and E. Cuq. 2005. Spatial and Temporal Variation in Nothofagus pumillo Growth at Tree Line along ItsLatitudinal Range (35°40'-55° S) in the Chilean Andes. Journal of Biogeography **32**:879-893.

Loehman, R. A., E. Reinhardt, and K. L. Riley. 2014. Wildland fire emissions, carbon, and climate: Seeing the forest and the trees – A cross-scale assessment of wildfire and carbon dynamics in fire-prone, forested ecosystems. Forest Ecology and Management **317**:9-19.

Luckman, B. H., and T. A. Kavanagh. 1998. Documenting the effects of recent climate change at treeline in the canadian rockies. Pages 121-144 *in* M. Beniston and J. L. Innes, editors. The Impacts of Climate Variability on Forests. Springer Berlin Heidelberg, Berlin, Heidelberg.

Markgraf, V. 1983. Late and Postglacial Vegetational and Paleoclimatic Changes in Subantarctic, Temperate, and Arid Environments in Argentina. Palynology **7**:43-70.

Markgraf, V. 1984. Pleistocene and Holocene vegetation history of temperate Argentina: Lago Morenito, Bariloche. Dissertation Botanique **72**:235-254.

Markgraf, V., and L. Anderson. 1994. Fire history of Patagonia: Climate versus human caus. Revista do Justituto Geologia Sao Paulo **15**:35-47.

Markgraf, V., V. Iglesias, and C. Whitlock. 2013. Late and postglacial vegetation and fire history from Cord?n Serrucho Norte, northern Patagonia. Palaeogeography, Palaeoclimatology, Palaeoecology **371**:109-118.

Nanavati, W. P., C. Whitlock, V. Iglesias, and M. E. de Porras. 2019. Postglacial vegetation, fire, and climate history along the eastern Andes, Argentina and Chile (lat. 41-55 degrees S). Quaternary Science Reviews **207**:145-160.

Prentice, I. C., and S. P. Harrison. 2009. Ecosystem effects of CO2 concentration: evidence from past climates. Climate of the Past **5**:297-307.

Rogers, B. M., R. P. Neilson, R. Drapek, J. M. Lenihan, J. R. Wells, D. Bachelet, and B. E. Law. 2011. Impacts of climate change on fire regimes and carbon stocks of the U.S. Pacific Northwest. Journal of Geophysical Research **116**.

Settele, J., R. Scholes, R. A. Betts, S. Bunn, P. Leadley, D. Nepstad, J. Overpeck, M. A. Taboada, A. Fischlin, J. M. Moreno, T. Root, M. Musche, and M. Winter. 2014. Terrestrial and Inland Water Systems. Pages 271-360 *in* I. P. o. C. Change, editor. Climate Change 2014 Impacts, Adaptation and Vulnerability: Part A: Global and Sectoral Aspects. Cambridge University Press.

Sheehan, T., D. Bachelet, and K. Ferschweiler. 2019. Fire, CO2, and climate effects on modeled vegetation and carbon dynamics in western Oregon and Washington. PLoS One **14**:e0210989.

Terrer, C., R. B. Jackson, I. C. Prentice, T. F. Keenan, C. Kaiser, S. Vicca, J. B. Fisher, P. B. Reich, B. D. Stocker, B. A. Hungate, J. Peñuelas, I. McCallum, N. A. Soudzilovskaia, L. A. Cernusak, A. F. Talhelm, K. Van Sundert, S. Piao, P. C. D. Newton, M. J. Hovenden, D. M. Blumenthal, Y. Y. Liu, C. Müller, K. Winter, C. B. Field, W. Viechtbauer, C. J. Van Lissa, M. R. Hoosbeek, M. Watanabe, T. Koike, V. O. Leshyk, H. W. Polley, and O. Franklin. 2019. Nitrogen and phosphorus constrain the CO2 fertilization of global plant biomass. Nature Climate Change **9**:684-689.

Veblen, T. T., T. Kitzberger, and A. Lara. 1992. Disturbance and Forest Dynamics Along a Transect from Andean Rain-Forest to Patagonian Shrubland. Journal of Vegetation Science **3**:507-520.

Veblen, T. T., and D. C. Lorenz. 1987. Post-Fire Stand Development of Austrocedrus-Nothofagus Forests in Northern Patagonia. Vegetatio **71**:113-126.

Veblen, T. T., and D. C. Lorenz. 1988. Recent Vegetation Changes along the Forest/Steppe Ecotone of Northern Patagonia. Annals of the Association of American Geographers **78**:93-111.

Vilanova, I., P. I. Moreno, C. G. Miranda, and R. P. Villa-Martínez. 2019. The last glacial termination in the Coyhaique sector of central Patagonia. Quaternary Science Reviews **224**.

Villalba, R., and T. T. Veblen. 1997. Regional Patterns of Tree Population Age Structures in Northern Patagonia: Climatic andDisturbance Influences. Journal of Ecology **85**:113-124.

Whitlock, C., M. M. Bianchi, P. J. Bartlein, V. Markgraf, J. Marlon, M. Walsh, and N. McCoy. 2006. Postglacial vegetation, climate, and fire history along the east side of the Andes (lat 41–42.5°S), Argentina. Quaternary Research **66**:187-201.

Whitlock, C., P. I. Moreno, and P. Bartlein. 2007. Climatic controls of Holocene fire patterns in southern South America. Quaternary Research **68**:28-36.

Woillez, M. N., M. Kageyama, G. Krinner, N. de Noblet-Ducoudré, N. Viovy, and M. Mancip. 2011. Impact of CO₂ and climate on the Last Glacial Maximum vegetation: results from the ORCHIDEE/IPSL models. Climate of the Past **7**:557-577.

REFERENCES CITED

Alder, J. R., and S. W. Hostetler. 2015. Global climate simulations at 3000-year intervals for the last 21 000 years with the GENMOM coupled atmosphere–ocean model. Climate of the Past **11**:449-471.

Allen, J. R. M., T. Hickler, J. S. Singarayer, M. T. Sykes, P. J. Valdes, and B. Huntley. 2010. Last glacial vegetation of northern Eurasia. Quaternary Science Reviews **29**:2604-2618.

Arroyo, M. T. K., M. Riveros, A. Peñaloza, L. Cavieres, and A. M. Faggi. 1996. Phytogeographic Relationships and Regional Richness Patterns of the Cool Temperate Rainforest Flora of Southern South America. Pages 134-172 *in* R. G. Lawford, E. Fuentes, and P. B. Alaback, editors. High-Latitude Rainforests and Associated Ecosystems of the West Coast of the Americas. Springer New York.

Avaria, C. E. 2013. Simulating current regional pattern and composition of Chilean native forests using a dynamic ecosystem model. Lund University, Sweden.

Avitabile, V., M. Herold, G. B. Heuvelink, S. L. Lewis, O. L. Phillips, G. P. Asner, J. Armston, P. S. Ashton, L. Banin, N. Bayol, N. J. Berry, P. Boeckx, B. H. de Jong, B. DeVries, C. A. Girardin, E. Kearsley, J. A. Lindsell, G. Lopez-Gonzalez, R. Lucas, Y. Malhi, A. Morel, E. T. Mitchard, L. Nagy, L. Qie, M. J. Quinones, C. M. Ryan, S. J. Ferry, T. Sunderland, G. V. Laurin, R. C. Gatti, R. Valentini, H. Verbeeck, A. Wijaya, and S. Willcock. 2016. An integrated pan-tropical biomass map using multiple reference datasets. Glob Chang Biol **22**:1406-1420.

Bartholomé, E., and A. S. Belward. 2007. GLC2000: a new approach to global land cover mapping from Earth observation data. International Journal of Remote Sensing **26**:1959-1977.

Bartholomeus, R. P., J.-P. M. Witte, P. M. van Bodegom, J. C. van Dam, and R. Aerts. 2008. Critical soil conditions for oxygen stress to plant roots: Substituting the Feddes-function by a process-based model. Journal of Hydrology **360**:147-165.

Bartlein, P. J., and C. Whitlock. 1993. Paleoclimatic interpretation of the Elk Lake pollen record. Pages 275-293 *in* J. P. Bradbury and W. E. Dean, editors. Evidence for Rapid Climate Change in the North-Central, United States: The Elk Lake Record. Geological Society of America, Boulder, CO.

Batjes, N. H. 2015. World soil property estimates for broad-scale modellling (WISE30sec,ver.1.0). Report 2015/01, ISRIC - World Soil Information, Wageningen.

Bekker, M. F. 2005. Positive Feedback Between Tree Establishment and Patterns of Subalpine Forest Advancement, Glacier National Park, Montana, U.S.A. Arctic, Antarctic, and Alpine Research **37**:97-107.

Bianchi, E., R. Villalba, M. Viale, F. Couvreux, and R. Marticorena. 2016. New precipitation and temperature grids for northern Patagonia: Advances in relation to global climate grids. Journal of Meteorological Research **30**:38-52.

Blanke, J. H., M. Lindeskog, J. Lindström, and V. Lehsten. 2016. Effect of climate data on simulated carbon and nitrogen balances for Europe. Journal of Geophysical Research: Biogeosciences **121**:1352-1371.

Blois, J. L., J. W. Williams, M. C. Fitzpatrick, S. T. Jackson, and S. Ferrier. 2013. Space can substitute for time in predicting climate-change effects on biodiversity. Proc Natl Acad Sci U S A **110**:9374-9379.

Bond, W. J. 2008. What Limits Trees in C4 Grasslands and Savannas? Annual Review of Ecology, Evolution, and Systematics **39**:641-659.

Bond, W. J., and J. E. Keeley. 2005. Fire as a global 'herbivore': the ecology and evolution of flammable ecosystems. Trends Ecol Evol **20**:387-394.

Bragg, F. J., I. C. Prentice, S. P. Harrison, G. Eglinton, P. N. Foster, F. Rommerskirchen, and J. Rullkötter. 2013. Stable isotope and modelling evidence for CO₂ as a driver of glacial–interglacial vegetation shifts in southern Africa. Biogeosciences **10**:2001-2010.

Breiman, L. 2001. Machine Learning **45**:5-32.

Brovkin, V., T. Raddatz, C. H. Reick, M. Claussen, and V. Gayler. 2009. Global biogeophysical interactions between forest and climate. Geophysical Research Letters **36**:n/a-n/a.

Bugmann, H. 2001. A Review of Forest Gap Models. Climatic Change **51**:259-305.

Ciais, P., M. J. Schelhaas, S. Zaehle, S. L. Piao, A. Cescatti, J. Liski, S. Luyssaert, G. Le-Maire, E. D. Schulze, O. Bouriaud, A. Freibauer, R. Valentini, and G. J. Nabuurs. 2008. Carbon accumulation in European forests. Nature Geoscience **1**:425-429.

Cullen, L. E., G. H. Stewart, R. P. Duncan, and J. G. Palmer. 2001. Disturbance and Climate Warming Influences on New Zealand Nothofagus Tree-LinePopulation Dynamics. Journal of Ecology **89**:1061-1071.

Dale, V. H., L. A. Joyce, S. McNulty, R. P. Neilson, M. P. Ayres, M. D. Flannigan, P. J. Hanson, L. C. Irland, A. E. Lugo, C. J. Peterson, D. Simberloff, F. J. Swanson, B. J. Stocks, and B. M. Wotton. 2001. Climate Change and Forest Disturbances: Climate change can affect forests by altering the frequency, intensity, duration, and timing of fire, drought, introduced species, insect and pathogen outbreaks, hurricanes, windstorms, ice storms, or landslides. BioScience **51**:723-734.

Dallmeyer, A., M. Claussen, U. Herzschuh, and N. Fischer. 2011. Holocene vegetation and biomass changes on the Tibetan Plateau – a model-pollen data comparison. Climate of the Past **7**:881-901.

Danby, R. K., and D. S. Hik. 2007. Responses of white spruce (Picea glauca) to experimental warming at a subarctic alpine treeline. Global change Biology **13**:437-451.

Daniels, L. D., and T. T. Veblen. 2004. Spatiotemporal influences of climate on altitudinal treeline in northern Patagonia. Ecology **85**:1284-1296.

De Kauwe, M. G., B. E. Medlyn, S. Zaehle, A. P. Walker, M. C. Dietze, Y. P. Wang, Y. Luo, A. K. Jain, B. El-Masri, T. Hickler, D. Warlind, E. Weng, W. J. Parton, P. E. Thornton, S. Wang, I. C. Prentice, S. Asao, B. Smith, H. R. McCarthy, C. M. Iversen, P. J. Hanson, J. M. Warren, R. Oren, and R. J. Norby. 2014. Where does the carbon go? A model-data intercomparison of vegetation carbon allocation and turnover processes at two temperate forest free-air CO2 enrichment sites. New Phytol **203**:883-899.

de Porras, M. E., A. Maldonado, A. M. Abarzúa, M. L. Cárdenas, J. P. Francois, A. Martel-Cea, C. R. Stern, C. Méndez, and O. Reyes. 2012. Postglacial vegetation, fire and climate dynamics at Central Chilean Patagonia (Lake Shaman, 44°S). Quaternary Science Reviews **50**:71-85.

Dionizio, E. A., M. Heil Costa, A. D. d. A. Castanho, G. Ferreira Pires, B. Schwantes Marimon, B. Hur Marimon-Junior, E. Lenza, F. Martins Pimenta, X. Yang, and A. K. Jain. 2018. Influence of climate variability, fire and phosphorus limitation on vegetation structure and dynamics of the Amazon–Cerrado border. Biogeosciences **15**:919-936.

Donoso, C. 2006. Especies arbóreas de los bosques templados de Chile y Argentina: autoecología. Marisa Cuneo Eds, Santiago de Chile:.

Erdős, L., D. Ambarlı, O. A. Anenkhonov, Z. Bátori, D. Cserhalmi, M. Kiss, G. Kröel-Dulay, H. Liu, M. Magnes, Z. Molnár, A. Naqinezhad, Y. A. Semenishchenkov, C. Tölgyesi, P. Török, and B. Jiménez-Alfaro. 2018. The edge of two worlds: A new review and synthesis on Eurasian forest-steppes. Applied Vegetation Science **21**:345-362.

Erdős, L., C. Tölgyesi, M. Horzse, D. Tolnay, Á. Hurton, N. Schulcz, L. Körmöczi, A. Lengyel, and Z. Bátori. 2014. Habitat complexity of the Pannonian forest-steppe zone and its nature conservation implications. Ecological Complexity **17**:107-118.

Flato, G., J. Marotzke, B. Abiodun, P. Braconnot, S. C. Chou, W. Collins, P. Cox, F. Driouech, S. Emori, V. Eyring, C. Forest, P. Gleckler, E. Guilyardi, C. Jakob, V. Kattsov, C. Reason, M. Rummukainen, T. F. Stocker, D. Qin, G.-K. Plattner, M. Tignor, S. K. Allen, J. Doschung, A. Nauels, Y. Xia, V. Bex, and P. M. Midgley. 2013. Evaluation of Climate Models. Pages 741-866 Climate Change 2013: The Physical Science Basis. Contribution of Working Group I to the Fifth Assessment Report of the Intergovernmental Panel on Climate Change.

Forkel, M., N. Carvalhais, J. Verbesselt, M. Mahecha, C. Neigh, and M. Reichstein. 2013. Trend Change Detection in NDVI Time Series: Effects of Inter-Annual Variability and Methodology. Remote Sensing **5**:2113-2144.

Friedlingstein, P., and I. C. Prentice. 2010. Carbon–climate feedbacks: a review of model and observation based estimates. Current Opinion in Environmental Sustainability **2**:251-257.

Garreaud, R. D., M. Vuille, R. Compagnucci, and J. Marengo. 2009. Present-day South American climate. Palaeogeography, Palaeoclimatology, Palaeoecology **281**:180-195.

Gerhart, L. M., and J. K. Ward. 2010. Plant responses to low [CO2] of the past. New Phytol **188**:674-695.

Giglio, L., L. Boschetti, D. P. Roy, M. L. Humber, and C. O. Justice. 2018. The Collection 6 MODIS burned area mapping algorithm and product. Remote Sens Environ **217**:72-85.

Gowda, J. H., T. Kitzberger, and A. C. Premoli. 2011. Landscape responses to a century of land use along the northern Patagonian forest-steppe transition. Plant Ecology **213**:259-272.

Green, R. H., R. H. G. Jongman, C. J. F. Braak, and O. F. R. V. Tongeren. 1990. Data Analysis in Community and Landscape Ecology. Biometrics **46**.

Harris, I., P. D. Jones, T. J. Osborn, and D. H. Lister. 2014. Updated high-resolution grids of monthly climatic observations - the CRU TS3.10 Dataset. International Journal of Climatology **34**:623-642.

Harrison, S. P., and C. I. Prentice. 2003. Climate and CO2 controls on global vegetation distribution at the last glacial maximum: analysis based on palaeovegetation data, biome modelling and palaeoclimate simulations. Global change Biology **9**:983-1004.

Harsch, M. A., P. E. Hulme, M. S. McGlone, and R. P. Duncan. 2009. Are treelines advancing? A global meta-analysis of treeline response to climate warming. Ecol Lett **12**:1040-1049.

Haxeltine, A., and I. C. Prentice. 1996. BIOME3: An equilibrium terrestrial biosphere model based on ecophysiological constraints, resource availability, and competition among plant functional types. Global Biogeochemical Cycles **10**:693-709.

Heiri, C., H. Bugmann, W. Tinner, O. Heiri, and H. Lischke. 2006. A model-based reconstruction of Holocene treeline dynamics in the Central Swiss Alps. Journal of Ecology **94**:206-216.

Henne, P. D., C. Elkin, D. Colombaroli, S. Samartin, H. Bugmann, O. Heiri, and W. Tinner. 2012. Impacts of changing climate and land use on vegetation dynamics in a Mediterranean ecosystem: insights from paleoecology and dynamic modeling. Landscape Ecology **28**:819-833.

Heusser, C. J. 1966. Late-Pleistocene pollen digrams from the Province of Llanquihue, southern Chile. Proceedings of the American Philosophical Society **110**:269-305.

Heusser, C. J. 1974. Vegetation and climate of the southern Chilean Lake District during and since the last interglaciation. Quaternary Research **4**:290-315.

Hickler, T., A. Rammig, and C. Werner. 2015. Modelling CO2 Impacts on Forest Productivity. Current Forestry Reports **1**:69-80.

Hickler, T., B. Smith, I. C. Prentice, K. MjÖFors, P. Miller, A. Arneth, and M. T. Sykes. 2008. CO2fertilization in temperate FACE experiments not representative of boreal and tropical forests. Global change Biology **14**:1531-1542.

Hickler, T., B. Smith, M. T. Sykes, M. B. Davis, S. Sugita, and K. Walker. 2004. Using a generalized vegetation model to simulate vegetation dynamics in northeastern USA. Ecology **85**:519-530.

Hickler, T., K. Vohland, J. Feehan, P. A. Miller, B. Smith, L. Costa, T. Giesecke, S. Fronzek, T. R. Carter, W. Cramer, I. Kühn, and M. T. Sykes. 2012. Projecting the future distribution of European potential natural vegetation zones with a generalized, tree species-based dynamic vegetation model. Global Ecology and Biogeography **21**:50-63.

Hijmans, R. J., S. E. Cameron, J. L. Parra, P. G. Jones, and A. Jarvis. 2005. Very high resolution interpolated climate surfaces for global land areas. International Journal of Climatology **25**:1965-1978.

Hirota, M., M. Holmgren, E. H. Van Nes, and M. Scheffer. 2011. Global Resilience of Tropical Forest and Savanna to Critical Transitions. Science **334**:232.

Holtmeier, F. K., and G. E. Broll. 2007. Treeline advance - driving processes and adverse factors. Landscape Online **1**:1-33.

Holz, A., T. Kitzberger, J. Paritsis, and T. T. Veblen. 2012. Ecological and climatic controls of modern wildfire activity patterns across southwestern South America. Ecosphere **3**.

Holz, A., J. Paritsis, I. A. Mundo, T. T. Veblen, T. Kitzberger, G. J. Williamson, E. Araoz, C. Bustos-Schindler, M. E. Gonzalez, H. R. Grau, and J. M. Quezada. 2017. Southern Annular Mode drives multicentury wildfire activity in southern South America. Proc Natl Acad Sci U S A **114**:9552-9557.

Holz, A., and T. T. Veblen. 2012. Wildfire activity in rainforests in western Patagonia linked to the Southern Annular Mode. International Journal of Wildland Fire **21**:114.

Hostetler, S., N. Pisias, and A. Mix. 2006. Sensitivity of Last Glacial Maximum climate to uncertainties in tropical and subtropical ocean temperatures. Quaternary Science Reviews **25**:1168-1185.

Iglesias, V., S. G. Haberle, A. Holz, and C. Whitlock. 2018. Holocene Dynamics of Temperate Rainforests in West-Central Patagonia. Frontiers in Ecology and Evolution **5**.

Iglesias, V., F. Quintana, W. Nanavati, and C. Whitlock. 2016. Interpreting modern and fossil pollen data along a steep environmental gradient in northern Patagonia. The Holocene **27**:1008-1018.

Iglesias, V., and C. Whitlock. 2014. Fire responses to postglacial climate change and human impact in northern Patagonia (41-43 degrees S). Proc Natl Acad Sci U S A **111**:E5545-5554.

Iglesias, V., C. Whitlock, M. M. Bianchi, G. Villarosa, and V. Outes. 2011. Holocene climate variability and environmental history at the Patagonian forest/steppe ecotone: Lago Mosquito (42°29'37.89"S, 71°24'14.57"W) and Laguna del Cóndor (42°20'47.22"S, 71°17'07.62"W). The Holocene **22**:1297-1307.

Iglesias, V., C. Whitlock, M. M. Bianchi, G. Villarosa, and V. Outes. 2012. Climate and local controls of long-term vegetation dynamics in northern Patagonia (Lat 41°S). Quaternary Research **78**:502-512.

Iglesias, V., C. Whitlock, V. Markgraf, and M. M. Bianchi. 2014. Postglacial history of the Patagonian forest/steppe ecotone (41–43°S). Quaternary Science Reviews **94**:120-135.

Iglesias, V., G. I. Yospin, and C. Whitlock. 2015. Reconstruction of fire regimes through integrated paleoecological proxy data and ecological modeling. Front Plant Sci **5**:785.

IPCC. 2013. Climate Change 2013: The Physical Science Basis. Contribution of Working Group I to the Fifth Assessment Report of the Intergovernmental Panel on Climate Change. Cambridge University Press, Cambridge, United Kingdom and New York, NY, USA.

IPCC. 2018. Summary for Policymakers. In: Global warming of 1.5°C. An IPCC Special Report on the impacts of global warming of 1.5°C above pre-industrial levels and related global greenhouse gas emission pathways, in the context of strengthening the global response to the threat of climate change, sustainable development, and efforts to eradicate poverty. World Meteorological Organization,, Geneva, Switzerland.

Jara, I. A., and P. I. Moreno. 2014. Climatic and disturbance influences on the temperate rainforests of northwestern Patagonia (40 °S) since ~14,500 cal yr BP. Quaternary Science Reviews **90**:217-228.

Jobbagy, E. G., and R. B. Jackson. 2000. Global controls of forest line elevation in the northern and southern hemispheres. Global Ecology and Biogeography **9**:253-268.

Jung, M., G. Le Maire, S. Zaehle, S. Luyssaert, M. Vetter, G. Churkina, P. Ciais, N. Viovy, and M. Reichstein. 2007. Assessing the ability of three land ecosystem models to simulate gross carbon uptake of forests from boreal to Mediterranean climate in Europe. Biogeosciences Discussions **4**:1353-1375.

Kaplan, J. O. 2003. Climate change and Arctic ecosystems: 2. Modeling, paleodata-model comparisons, and future projections. Journal of Geophysical Research **108**.

Kaplan, J. O., I. C. Prentice, W. Knorr, and P. J. Valdes. 2002. Modeling the dynamics of terrestrial carbon storage since the Last Glacial Maximum. Geophysical Research Letters **29**:31-31-31-34.

Kirschbaum, M. U. F., M. S. Watt, A. Tait, and A.-G. E. Ausseil. 2012. Future wood productivity of Pinus radiata in New Zealand under expected climatic changes. Global change Biology **18**:1342-1356.

Kitzberger, T. 2012. Ecotones as Complex Arenas of Disturbance, Climate, and Human Impacts: The Trans-Andean Forest-Steppe Ecotone of Northern Patagonia. Pages 59-88 *in* R. Myster, editor. Ecotones Between Forest and Grassland. Springer, New York.

Kitzberger, T., G. L. W. Perry, J. Paritsis, J. H. Gowda, A. J. Tepley, A. Holz, and T. T. Veblen. 2016. Fire–vegetation feedbacks and alternative states: common mechanisms of temperate forest vulnerability to fire in southern South America and New Zealand. New Zealand Journal of Botany **54**:247-272.

Kitzberger, T., E. Raffaele, K. Heinemann, and M. J. Mazzarino. 2005. Effects of fire severity in a north Patagonian subalpine forest. Journal of Vegetation Science **16**:5-12.

Kitzberger, T., and T. T. Veblen. 1999. Fire-induced changes in northern Patagonian landscapes. Landscape Ecology **14**:1-15.

Kitzberger, T., and T. T. Veblen. 2003. Influence of climate on fire in northern Patagonia, Argentina. Pages 296-321 *in* T. T. Veblen, W. L. Baker, G. Montenegro, and T. W. Swetnam, editors. Fire regimes and climatic chnage in temperate ecosystem of the western Americas. Springer-Verlag, New York, USA.

Kitzberger, T., T. T. Veblen, and R. Villalba. 1997. Climatic influences on fire regimes along a rain forest to xeric woodland gradient in northern Patagonia, Argentina. Journal of Biogeography **24**:35-47.

Lara, A., R. Villalba, A. Wolodarsky-Franke, J. C. Aravena, B. H. Luckman, and E. Cuq. 2005. Spatial and Temporal Variation in Nothofagus pumillo Growth at Tree Line along

ItsLatitudinal Range (35°40'-55° S) in the Chilean Andes. Journal of Biogeography **32**:879-893.

Leach, M. K., and T. J. Givnish. 1999. Gradients in the composition, structure, and diversity of remnant oak savannas in southern Wisconsin. Ecological Monographs **69**:353-374.

LeCain, D. R., J. A. Morgan, M. A. R., and J. A. Nelson. 2003. Soil and Plant Water Relations Determine Photosynthetic Responses of C_3 and C_4 Grasses ina Semi-arid Ecosystem under Elevated CO_2. Annals of Botany **92**:41-52.

Liaw, A., and M. Wiener. 2002. Classification and Regression by randomForest. R News **2**:18-22.

Lindeskog, M., A. Arneth, A. Bondeau, K. Waha, J. Seaquist, S. Olin, and B. Smith. 2013. Implications of accounting for land use in simulations of ecosystem services and carbon cycling in Africa. Earth System Dynamics Discussions **4**:235-278.

Loehman, R. A., E. Reinhardt, and K. L. Riley. 2014. Wildland fire emissions, carbon, and climate: Seeing the forest and the trees – A cross-scale assessment of wildfire and carbon dynamics in fire-prone, forested ecosystems. Forest Ecology and Management **317**:9-19.

Luckman, B. H., and T. A. Kavanagh. 1998. Documenting the effects of recent climate change at treeline in the canadian rockies. Pages 121-144 *in* M. Beniston and J. L. Innes, editors. The Impacts of Climate Variability on Forests. Springer Berlin Heidelberg, Berlin, Heidelberg.

Markgraf, V. 1983. Late and Postglacial Vegetational and Paleoclimatic Changes in Subantarctic, Temperate, and Arid Environments in Argentina. Palynology **7**:43-70.

Markgraf, V. 1984. Pleistocene and Holocene vegetation history of temperate Argentina: Lago Morenito, Bariloche. Dissertation Botanique **72**:235-254.

Markgraf, V., and L. Anderson. 1994. Fire history of Patagonia: Climate versus human caus. Revista do Justituto Geologia Sao Paulo **15**:35-47.

Markgraf, V., V. Iglesias, and C. Whitlock. 2013. Late and postglacial vegetation and fire history from Cord?n Serrucho Norte, northern Patagonia. Palaeogeography, Palaeoclimatology, Palaeoecology **371**:109-118.

Markgraf, V., E. Romero, and C. Villagran. 1996. History and paleoecology of South American Nothofagus forests. Pages 354-386 *in* T. T. Veblen, R. S. Hill, and J. Read, editors. Ecology and Biogeography of Nothofagus Forests. Yale University Press, New Heaven.

Markgraf, V., C. Whitlock, and S. Haberle. 2007. Vegetation and fire history during the last 18,000 cal yr B.P. in Southern Patagonia: Mallín Pollux, Coyhaique, Province Aisén (45°41'30" S, 71°50'30" W, 640 m elevation). Palaeogeography, Palaeoclimatology, Palaeoecology **254**:492-507.

Martin Calvo, M., and I. C. Prentice. 2015. Effects of fire and CO2 on biogeography and primary production in glacial and modern climates. New Phytol **208**:987-994.

Martin Calvo, M., I. C. Prentice, and S. P. Harrison. 2014. Climate versus carbon dioxide controls on biomass burning: a model analysis of the glacial–interglacial contrast. Biogeosciences **11**:6017-6027.

Mátyás, C., and G. Sun. 2014. Forests in a water limited world under climate change. Environmental Research Letters **9**.

Mermoz, M., T. Kitzberger, and T. T. Veblen. 2005. Landscape Influences on Occurrence and Spread of Wildfires in Patagonian Forests and Shrublands. Ecology **86**:2705-2715.

Miller, P. A., T. Giesecke, T. Hickler, R. H. W. Bradshaw, B. Smith, H. Seppä, P. J. Valdes, and M. T. Sykes. 2008. Exploring climatic and biotic controls on Holocene vegetation change in Fennoscandia. Journal of Ecology **96**:247-259.

Mundo, I. A., R. Villalba, T. T. Veblen, T. Kitzberger, A. Holz, J. Paritsis, and A. Ripalta. 2017. Fire history in southern Patagonia: human and climate influences on fire activity in Nothofagus pumilio forests. Ecosphere **8**.

Nanavati, W. P., C. Whitlock, V. Iglesias, and M. E. de Porras. 2019. Postglacial vegetation, fire, and climate history along the eastern Andes, Argentina and Chile (lat. 41-55 degrees S). Quaternary Science Reviews **207**:145-160.

Oksanen, J., F. G. Blanchet, M. Friendly, R. Kindt, P. Legendre, D. McGlinn, P. R. Minchin, R. B. O'Hara, G. L. Simpson, P. Solymos, M. H. H. Steven, E. Szoecs, and H. Wagner. 2019. Vegan: community ecology package. R package version 2.5-6.

Olson, D. M., E. Dinerstein, E. D. Wikramanayake, N. D. Burgess, G. V. N. Powell, E. C. Underwood, J. A. D'Amico, I. Itoua, H. E. Strand, J. C. Morrison, C. J. Loucks, T. F. Allnutt, T. H. Ricketts, Y. Kura, J. F. Lamoreux, W. W. Wettengel, P. Hedao, and K. R. Kassem. 2001. Terrestrial Ecoregions of the World: A New Map of Life on Earth. BioScience **51**:933-938.

Pacanowski, R. C. 1996. MOM 2 Version 2.0 (Beta) Documentation: User's Guide and Reference Manual, Technical Report 3.2, NOAA GFDL Ocean Group, GFDL. Princeton, New Jersey.

Pan, Y., J. M. Melillo, A. D. McGuire, D. W. Kicklighter, L. F. Pitelka, K. Hibbard, L. L. Pierce, S. W. Running, D. S. Ojima, W. J. Parton, D. S. Schimel, and V. m. Other.

1998. Modeled responses of terrestrial ecosystems to elevated atmospheric CO2: a comparison of simulations by the biogeochemistry models of the Vegetation/Ecosystem Modeling and Analysis Project (VEMAP). Oecologia **114**:389-404.

Paritsis, J., J. Landesmann, T. Kitzberger, F. Tiribelli, Y. Sasal, C. Quintero, R. Dimarco, M. Barrios-García, A. Iglesias, J. Diez, M. Sarasola, and M. Nuñez. 2018. Pine Plantations and Invasion Alter Fuel Structure and Potential Fire Behavior in a Patagonian Forest-Steppe Ecotone. Forests **9**.

Paruelo, J. M., A. B. Beltran, E. G. Jobbagy, O. E. Sala, and R. A. Golluscio. 1998. The climate of Patagonia: general patterns and controls on biotic processes. Ecologia Austral **8**:85-101.

Piao, S., S. Sitch, P. Ciais, P. Friedlingstein, P. Peylin, X. Wang, A. Ahlstrom, A. Anav, J. G. Canadell, N. Cong, C. Huntingford, M. Jung, S. Levis, P. E. Levy, J. Li, X. Lin, M. R. Lomas, M. Lu, Y. Luo, Y. Ma, R. B. Myneni, B. Poulter, Z. Sun, T. Wang, N. Viovy, S. Zaehle, and N. Zeng. 2013. Evaluation of terrestrial carbon cycle models for their response to climate variability and to CO2 trends. Glob Chang Biol **19**:2117-2132.

Pollard, D., and S. L. Thompson. 1997. Climate and ice-sheet mass balance at the last glacial maximum from the genesis version 2 global climate model,. Quaternary Science Reviews **16**:841-863.

Pollmann, W., and T. T. Veblen. 2004. Nothofagus Regeneration Dynamics in South-Central Chile: A Test of a General Model. Ecological Monographs **74**:615-634.

Prentice, I. C. 1983. Pollen Mapping of Regional Vegetation Patterns in South and Central Sweden. Journal of Biogeography **10**:441-454.

Prentice, I. C., and S. P. Harrison. 2009. Ecosystem effects of CO2 concentration: evidence from past climates. Climate of the Past **5**:297-307.

Rogers, B. M., R. P. Neilson, R. Drapek, J. M. Lenihan, J. R. Wells, D. Bachelet, and B. E. Law. 2011. Impacts of climate change on fire regimes and carbon stocks of the U.S. Pacific Northwest. Journal of Geophysical Research **116**.

Schultz, J. 2005. The Ecozones of the World. Springer Berlin, Germany.

Settele, J., R. Scholes, R. A. Betts, S. Bunn, P. Leadley, D. Nepstad, J. Overpeck, M. A. Taboada, A. Fischlin, J. M. Moreno, T. Root, M. Musche, and M. Winter. 2014. Terrestrial and Inland Water Systems. Pages 271-360 *in* I. P. o. C. Change, editor. Climate Change 2014 Impacts, Adaptation and Vulnerability: Part A: Global and Sectoral Aspects. Cambridge University Press.

Sheehan, T., D. Bachelet, and K. Ferschweiler. 2019. Fire, CO2, and climate effects on modeled vegetation and carbon dynamics in western Oregon and Washington. PLoS One **14**:e0210989.

Sitch, S., P. Friedlingstein, N. Gruber, S. D. Jones, G. Murray-Tortarolo, A. Ahlström, S. C. Doney, H. Graven, C. Heinze, C. Huntingford, S. Levis, P. E. Levy, M. Lomas, B. Poulter, N. Viovy, S. Zaehle, N. Zeng, A. Arneth, G. Bonan, L. Bopp, J. G. Canadell, F. Chevallier, P. Ciais, R. Ellis, M. Gloor, P. Peylin, S. L. Piao, C. Le Quéré, B. Smith, Z. Zhu, and R. Myneni. 2015. Recent trends and drivers of regional sources and sinks of carbon dioxide. Biogeosciences **12**:653-679.

Sitch, S., B. Smith, I. C. Prentice, A. Arneth, A. Bondeau, W. Cramer, J. O. Kaplans, S. Levis, W. Lucht, M. T. Sykes, and K. Thonicke. 2003. Evaluation of ecosystem dynamics,plant geography and terrestial carbon cycling in the LPJ dynamic global vegetation model. Global change Biology **9**:25.

Smith, B., I. C. Prentice, and M. T. Sykes. 2001. Representation of vegetation dynamics in the modelling of terrestrial ecosystems: comparing two contrasting approaches within European climate space. Global Ecology and Biogeography **10**:621-637.

Stan, K., and A. Sanchez-Azofeifa. 2019. Tropical Dry Forest Diversity, Climatic Response, and Resilience in a Changing Climate. Forests **10**.

Steffen, W., A. Persson, L. Deutsch, J. Zalasiewicz, M. Williams, K. Richardson, C. Crumley, P. Crutzen, C. Folke, L. Gordon, M. Molina, V. Ramanathan, J. Rockstrom, M. Scheffer, H. J. Schellnhuber, and U. Svedin. 2011. The anthropocene: from global change to planetary stewardship. Ambio **40**:739-761.

Sykes, M. T., I. C. Prentice, and W. Cramer. 1996. A bioclimatic model for the potential distributions of north European tree species under present and future climates. Journal of Biogeography **23**:203-233.

Tabor, C. R., C. J. Poulsen, and D. Pollard. 2014. Mending Milankovitch's theory: obliquity amplification by surface feedbacks. Clim. Past **10**:41-50.

Tang, G., and B. Beckage. 2010. Projecting the distribution of forests in New England in response to climate change. Diversity and Distributions **16**:144-158.

Ter Braak, C. J. F. 1986. Canonical Correspondence Analysis: A new eigenvector technique for multivariate direct gradient analysis. Ecology **67**:1167-1179.

Ter Braak, C. J. F. 1987. The analysis of vegetation-environment relationships by canonical correspondence analysis. Vegetatio **69**:69-77.

Terrer, C., R. B. Jackson, I. C. Prentice, T. F. Keenan, C. Kaiser, S. Vicca, J. B. Fisher, P. B. Reich, B. D. Stocker, B. A. Hungate, J. Peñuelas, I. McCallum, N. A. Soudzilovskaia,

L. A. Cernusak, A. F. Talhelm, K. Van Sundert, S. Piao, P. C. D. Newton, M. J. Hovenden, D. M. Blumenthal, Y. Y. Liu, C. Müller, K. Winter, C. B. Field, W. Viechtbauer, C. J. Van Lissa, M. R. Hoosbeek, M. Watanabe, T. Koike, V. O. Leshyk, H. W. Polley, and O. Franklin. 2019. Nitrogen and phosphorus constrain the CO2 fertilization of global plant biomass. Nature Climate Change **9**:684-689.

Thonicke, K., S. Venevsky, S. Sitch, and W. Cramer. 2001a. The role of fire disturbance for global vegetation dynamics: coupling fire into a Dynamic Global Vegetation Model. Global Ecology and Biogeography **10**:661-677.

Thonicke, K., S. Venevsky, S. Sitch, and W. Cramer. 2001b. The role of fire disturbance for global vegetation dynamics: coupling fire into a Dynamic Global Vegetation Model. Global Ecology & Biogeography **10**:661-677.

Tucker, C. J., J. E. Pinzon, M. E. Brown, D. A. Slayback, E. W. Pak, R. Mahoney, E. F. Vermote, and N. El Saleous. 2010. An extended AVHRR 8-km NDVI dataset compatible with MODIS and SPOT vegetation NDVI data. International Journal of Remote Sensing **26**:4485-4498.

van der Werf, G. R., J. T. Randerson, L. Giglio, G. J. Collatz, M. Mu, P. S. Kasibhatla, D. C. Morton, R. S. DeFries, Y. Jin, and T. T. van Leeuwen. 2010. Global fire emissions and the contribution of deforestation, savanna, forest, agricultural, and peat fires (1997–2009). Atmospheric Chemistry and Physics **10**:11707-11735.

Veblen, T. T., C. Donoso, T. Kitzberger, and A. J. Rebertus. 1996. Ecology of Southern Chilean and Argentinean Nothofagus Forests.*in* T. T. Veblen, R. S. Hill, and J. Read, editors. The Ecology and Biogeography of Nothofagus Forests. Yale University Press, New Haven, USA.

Veblen, T. T., A. Holz, J. Paritsis, E. Raffaele, T. Kitzberger, and M. Blackhall. 2011. Adapting to global environmental change in Patagonia: What role for disturbance ecology? Austral Ecology **36**:891-903.

Veblen, T. T., T. Kitzberger, and A. Lara. 1992. Disturbance and Forest Dynamics Along a Transect from Andean Rain-Forest to Patagonian Shrubland. Journal of Vegetation Science **3**:507-520.

Veblen, T. T., T. Kitzberger, R. Villalba, and J. Donnegan. 1999a. Fire History in Northern Patagonia: The Roles of Humans and Climate Variation. Ecological Monography **69**:47-67.

Veblen, T. T., T. Kitzberger, R. Villalba, and J. Donnegan. 1999b. Fire History in Northern Patagonia: The Roles of Humans and Climatic Variation. Ecological Monographs **69**:47-67.

Veblen, T. T., and D. C. Lorenz. 1987. Post-Fire Stand Development of Austrocedrus-Nothofagus Forests in Northern Patagonia. Vegetatio **71**:113-126.

Veblen, T. T., and D. C. Lorenz. 1988. Recent Vegetation Changes along the Forest/Steppe Ecotone of Northern Patagonia. Annals of the Association of American Geographers **78**:93-111.

Venevsky, S., K. Thonicke, S. Sitch, and W. Cramer. 2002. Simulating fire regimes in human-dominated ecosystems: Iberian penisula case study. Global change Biology **8**:984-998.

Vilanova, I., P. I. Moreno, C. G. Miranda, and R. P. Villa-Martínez. 2019. The last glacial termination in the Coyhaique sector of central Patagonia. Quaternary Science Reviews **224**.

Villalba, R., A. Lara, J. A. Boninsegna, M. Masiokas, S. Delgado, J. C. Aravena, F. A. Roig, A. Schmelter, A. Wolodarsky, and A. Ripalta. 2003. Large-Scale Temperature Changes across the Southern Andes: 20th-Century Variations in the Context of the Past 400 Years. Climatic Change **59**:177-232.

Villalba, R., and T. T. Veblen. 1997. Regional Patterns of Tree Population Age Structures in Northern Patagonia: Climatic andDisturbance Influences. Journal of Ecology **85**:113-124.

Villalba, R., and T. T. Veblen. 1998. Influences of large-scale climatic variability on episodic tree mortality in northern Patagonia. Ecology **79**:2624-2640.

Wessel, P., H. F. S. Walters, R. Scharroo, J. Luis, and F. Wobbe. 2013. Generic Mapping Tools: Improved Version Released. Eos **94**:409-420.

Whitlock, C., M. M. Bianchi, P. J. Bartlein, V. Markgraf, J. Marlon, M. Walsh, and N. McCoy. 2006. Postglacial vegetation, climate, and fire history along the east side of the Andes (lat 41–42.5°S), Argentina. Quaternary Research **66**:187-201.

Whitlock, C., P. I. Moreno, and P. Bartlein. 2007. Climatic controls of Holocene fire patterns in southern South America. Quaternary Research **68**:28-36.

Woillez, M. N., M. Kageyama, G. Krinner, N. de Noblet-Ducoudré, N. Viovy, and M. Mancip. 2011. Impact of CO2 and climate on the Last Glacial Maximum vegetation: results from the ORCHIDEE/IPSL models. Climate of the Past **7**:557-577.

Wramneby, A., B. Smith, S. Zaehle, and M. T. Sykes. 2008. Parameter uncertainties in the modelling of vegetation dynamics—Effects on tree community structure and ecosystem functioning in European forest biomes. Ecological Modelling **216**:277-290.

Wu, C., S. Venevsky, S. Sitch, Y. Yang, M. Wang, L. Wang, and Y. Gao. 2017. Present-day and future contribution of climate and fires to vegetation composition in the boreal forest of China. Ecosphere **8**.

Zhang, Z., N. E. Zimmermann, A. Stenke, X. Li, E. L. Hodson, G. Zhu, C. Huang, and B. Poulter. 2017. Emerging role of wetland methane emissions in driving 21st century climate change. Proc Natl Acad Sci U S A **114**:9647-9652.

Zhu, Z., S. Piao, R. B. Myneni, M. Huang, Z. Zeng, J. G. Canadell, P. Ciais, S. Sitch, P. Friedlingstein, A. Arneth, C. Cao, L. Cheng, E. Kato, C. Koven, Y. Li, X. Lian, Y. Liu, R. Liu, J. Mao, Y. Pan, S. Peng, J. Peñuelas, B. Poulter, T. A. M. Pugh, B. D. Stocker, N. Viovy, X. Wang, Y. Wang, Z. Xiao, H. Yang, S. Zaehle, and N. Zeng. 2016. Greening of the Earth and its drivers. Nature Climate Change **6**:791-795.

APPENDICES

APPENDIX A

SUPLEMENTARY RESULTS FOR CHAPTER TWO

Climate data	Resolution	Time Period	Variables	Region
CRU	0.5º	1901-2014	Precipitation &Temperature	Latitude (35º to 44ºS)
WORLDCLIM (WC)	1.0º	1950-2000	Precipitation &Temperature	Latitude (39º to 46ºS)
NPCG	2.0º	1997-2010	Precipitation &Temperature	Latitude (34º to 45ºS)
CRU-WC	1.0º	1901-2016	Precipitation &Temperature	Latitude (35º to 44ºS)

The table above described the climate data used for this analysis**.** The NPCG data (Northern Patagonia Climate Group data) was given to us by Bianchi et al. (2016). The new CRU-WC climate data was downscaled to 1 km using the WC climatology climate data as the reference data based on the method described by Zhang et al. (2017)

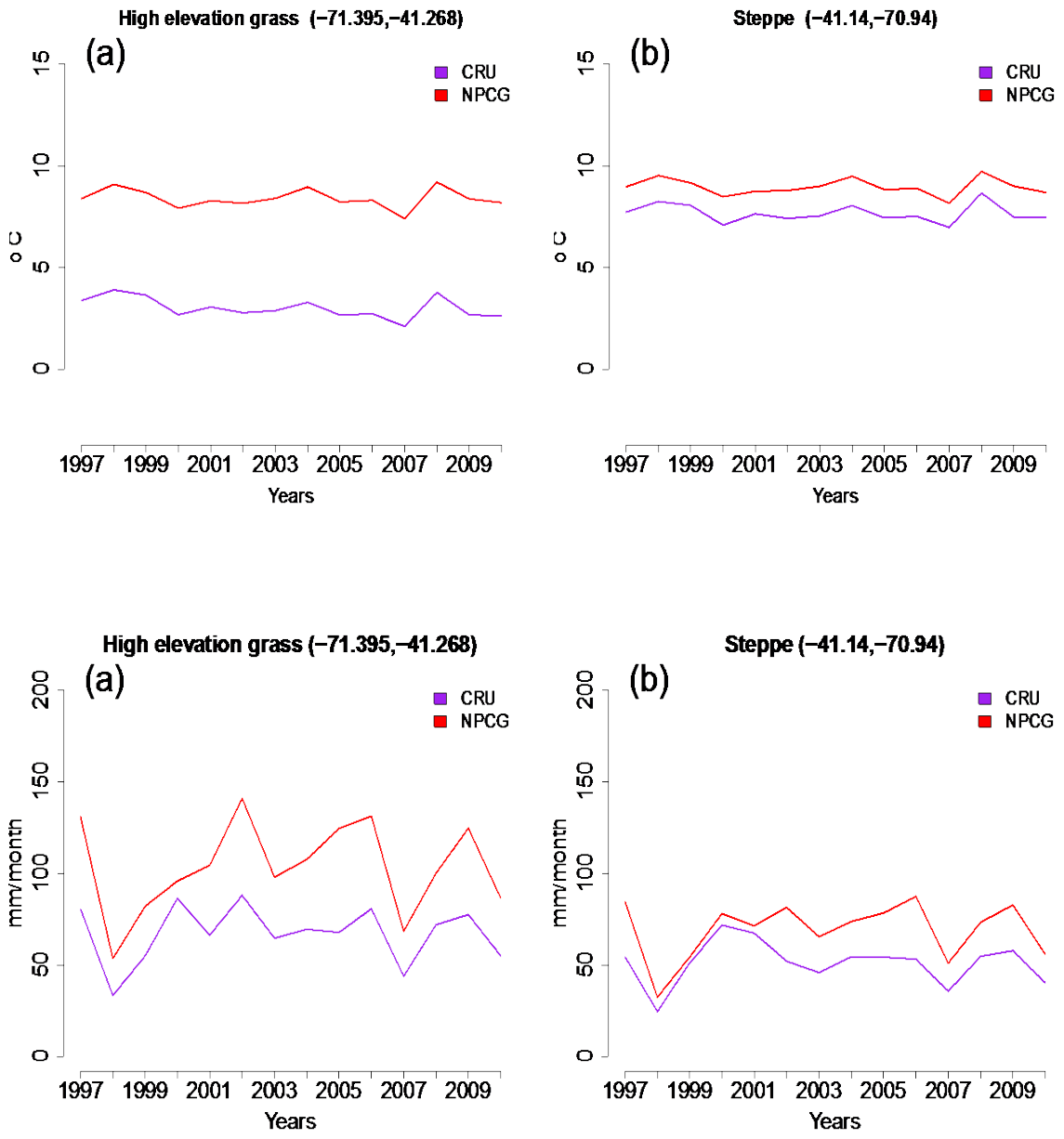

Figure S1: Time series plot comparing downscaled CRU 1 km spatial resolution (Climate Research Unit) and Northern Patagonia Climate Grid 20 km spatial resolution (NPCG). The data for the grid cells containing the study site were thus taken as representative for the site's temperature and precipitation.

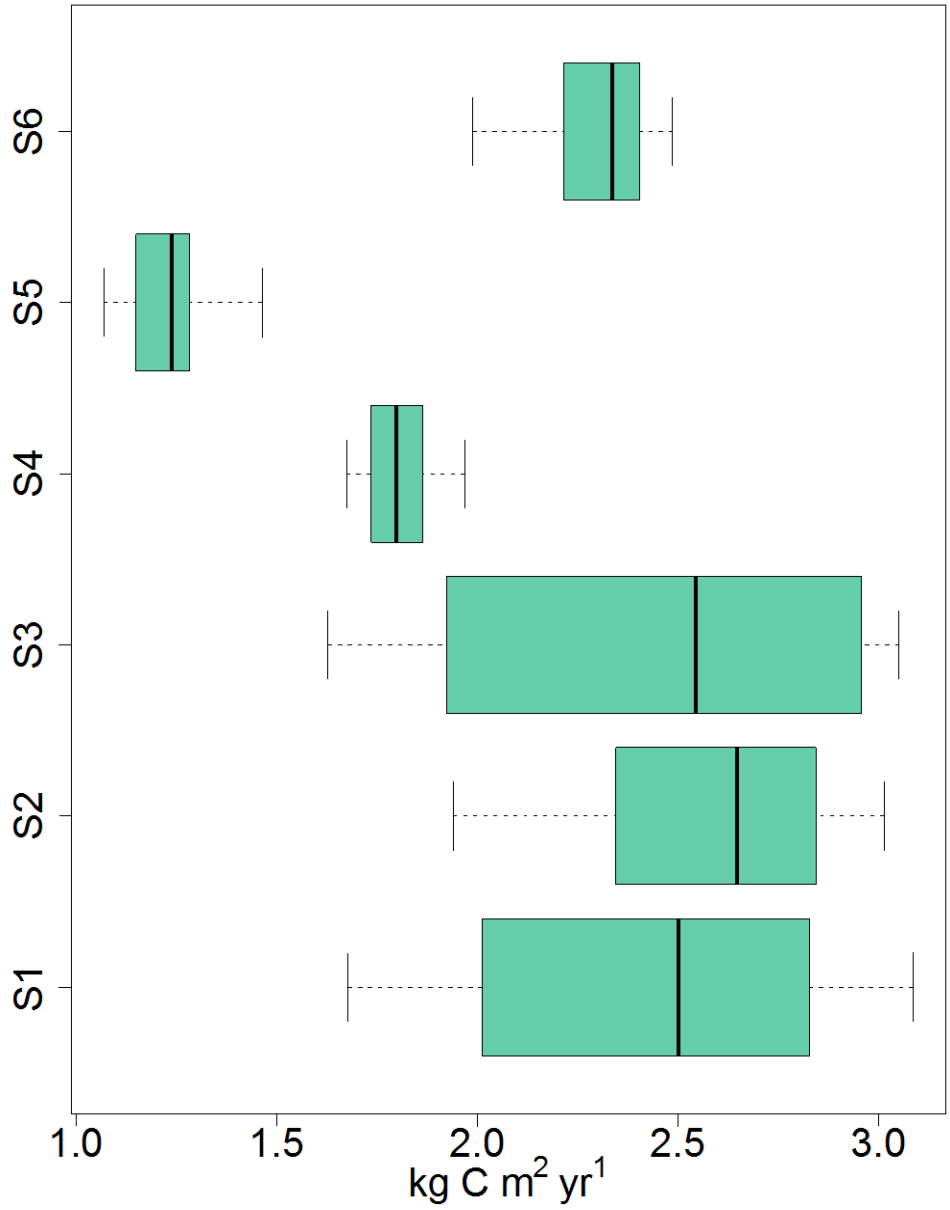

Fig S2: Boxplot of average biomass sample at the forest-steppe (-71.07, -40.45) from 1981-2010.

Table S1: Statistical output from AAT NDVI Analysis

--- Trend ----------

Calculate trends and trend changes on time series

Time series start: 1981 1

Time series end: 2016 1

Time series length: 36

Trend method: AAT

Test for structural change

OLS-based MOSUM test for structural change

statistic: 0.407839

p-value: 0.6725938

Breakpoints: Breakpoints were not detected.

Trends in segments of the time series

segment	slope	%	p-value	MK tau	MK p-value
1	-0.00257	-0.584	0.121	-0.175	0.138

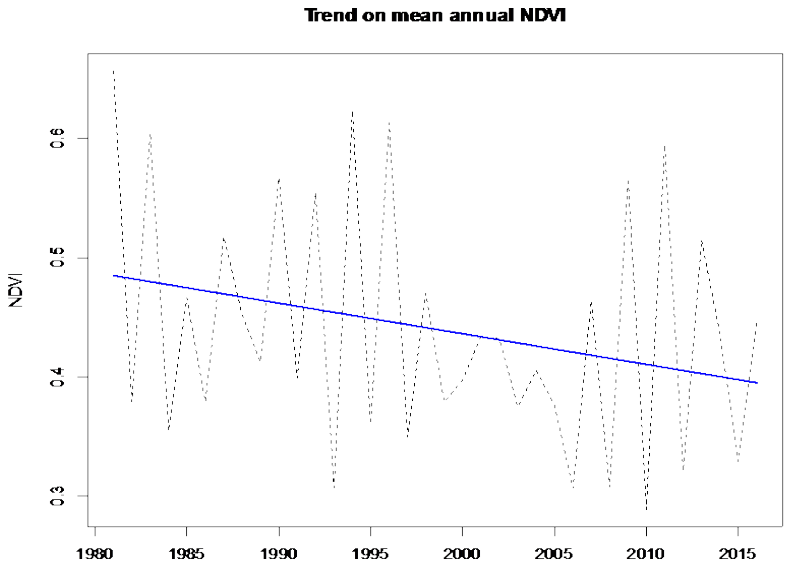

Fig S3: Mean annual GIMMS NDVI from 1981 to2016. The linear regression line shows a decreasing trend in mean annual NDVI.

High elevation grass

Low elevation grass

Mixed evergreen shrub

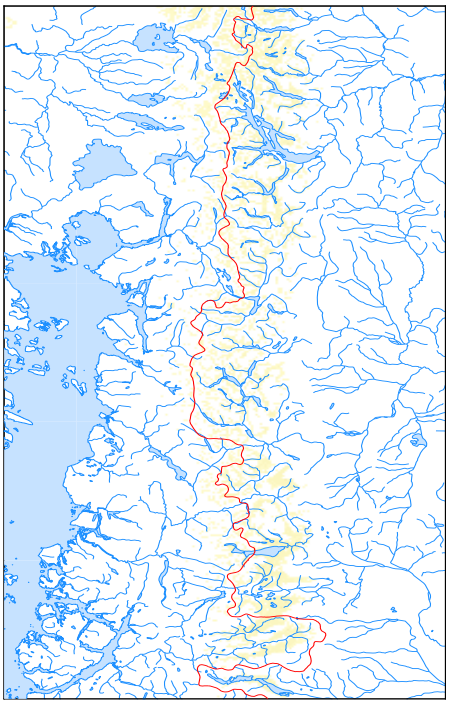

BLEWT

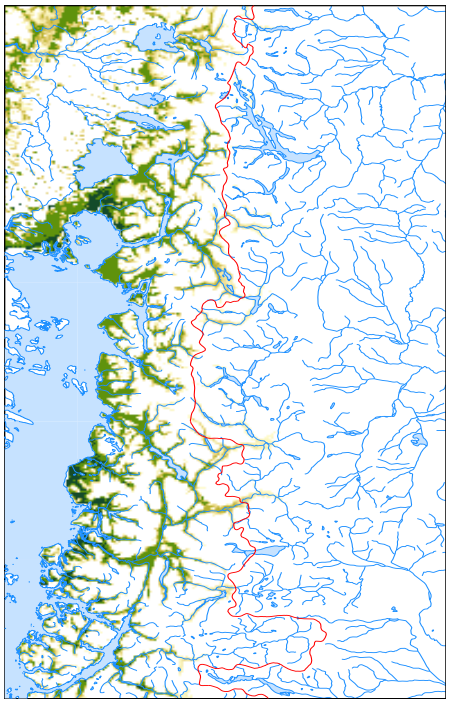

Austocedrus chilensis

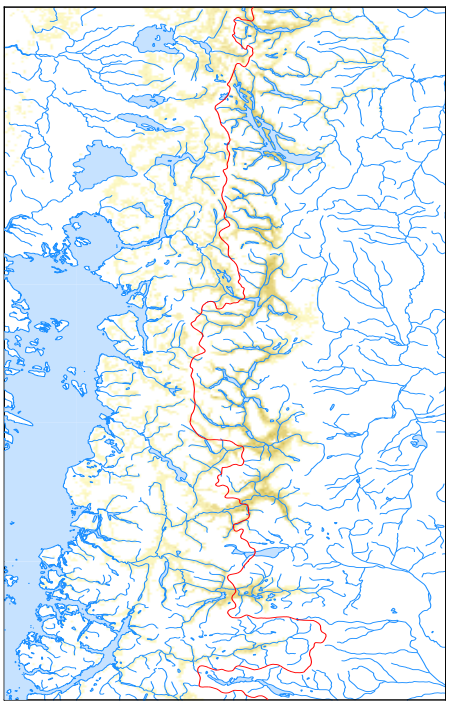

Fitzroya cupressoides

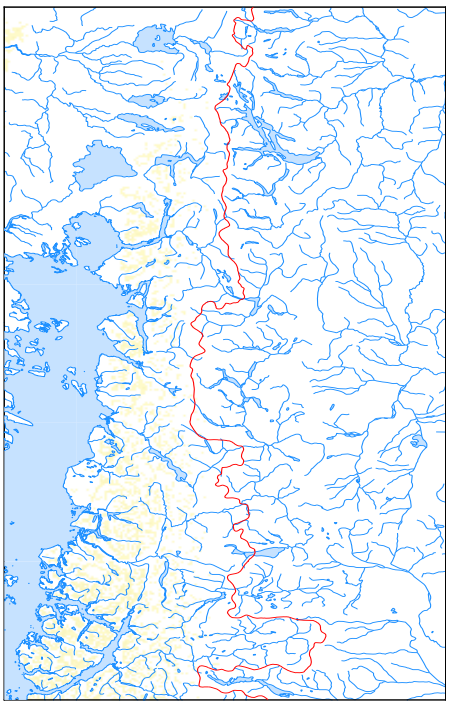

Chusque culeou

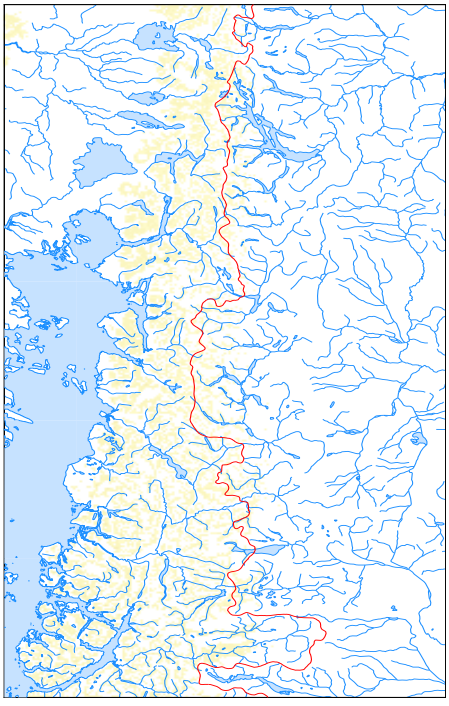

Nothofagus dombeyii

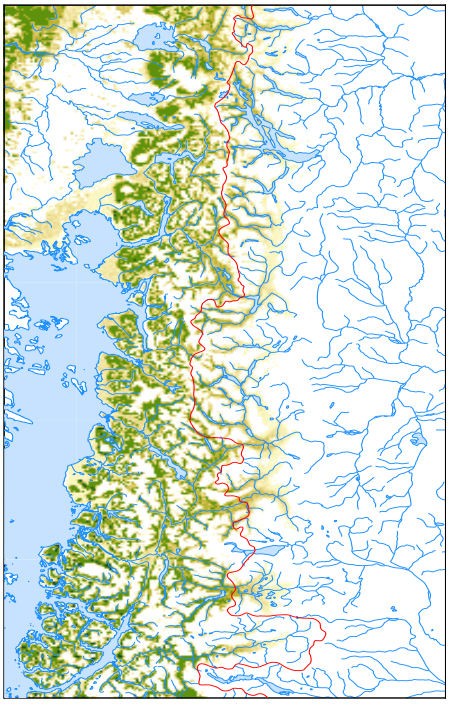

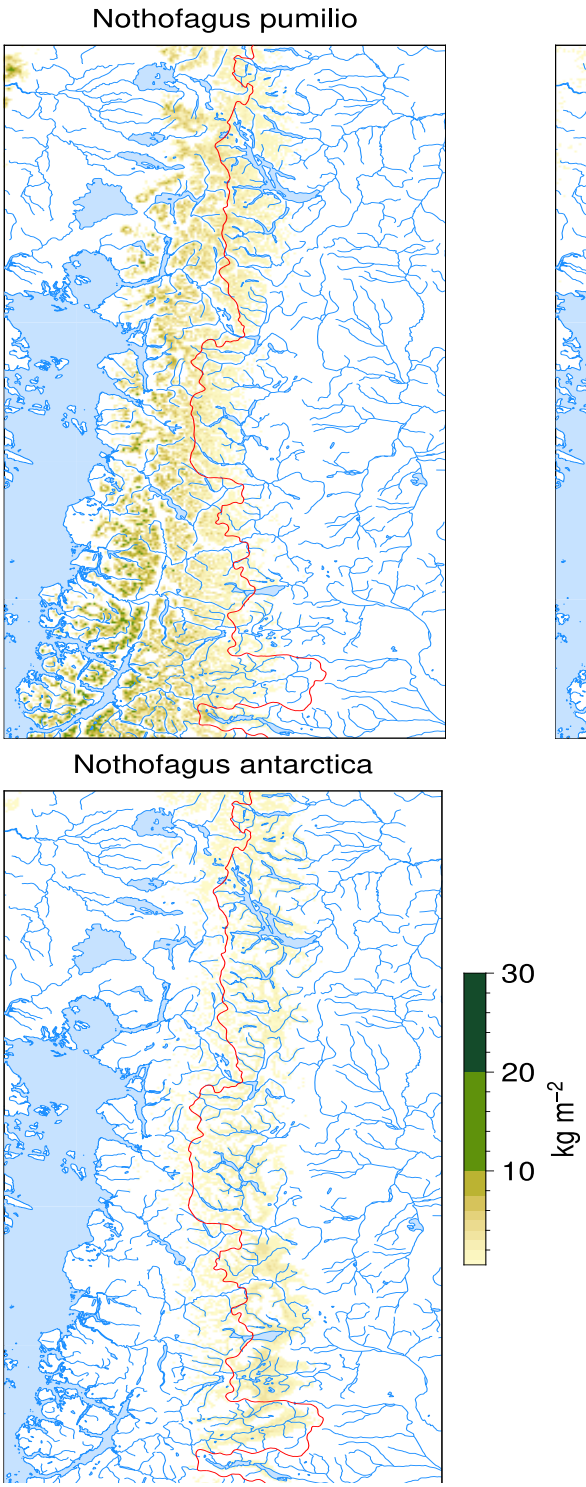

Fig. S4: Spatial map of LPJ-GUESS simulated biomass for the two PFTs and seven local tree species using S2 (historical climate, historical CO2, masking on). The red line shows the border between Chile and Argentina.

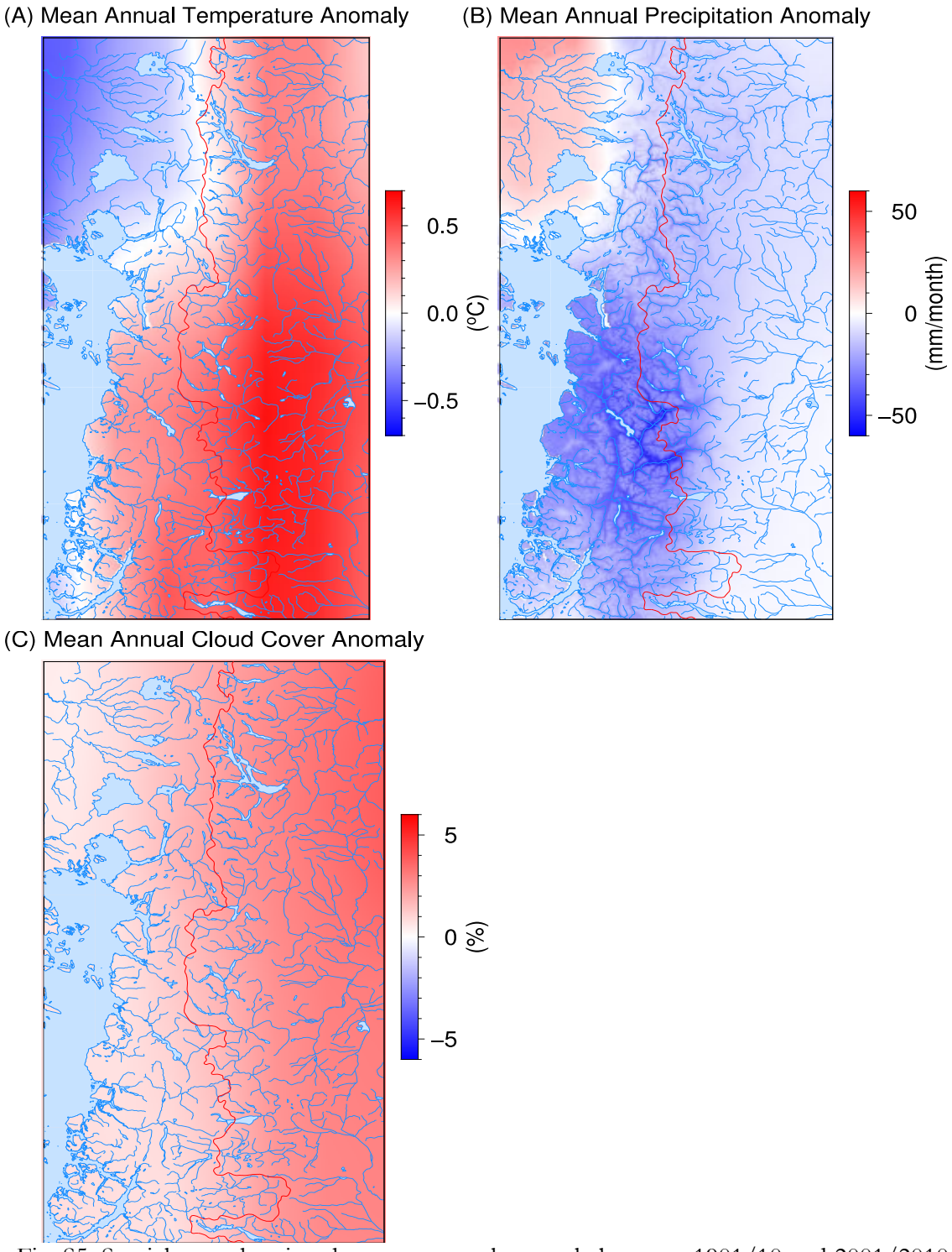

Fig. S5: Spatial map showing the mean annual anomaly between 1901/10 and 2001/2010 for (a) Temperature, (b) Precipitation, (c) Cloud cover. Positive value indicates a warmer temperature for present-period (2001/2010) relative to historical (1901/1910), while negative value indicates a colder present-period relative to historical period. Fig. S5b: same as Fig. S5a but for precipitation. Fig. S5c: same as Fig. S5a but for cloud cover.

APPENDIX B

SUPPLEMENTARY RESULTS FOR CHAPTER THREE

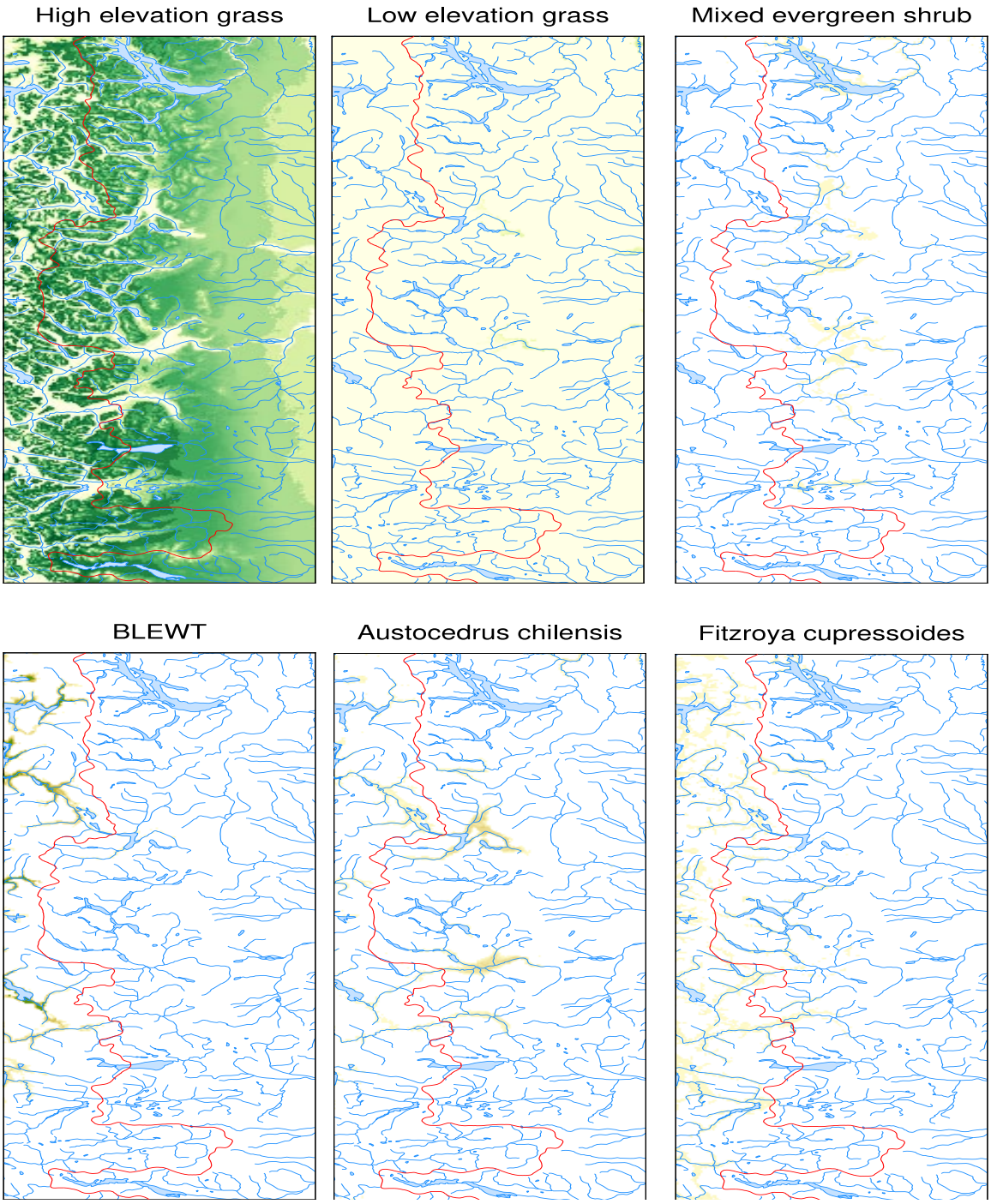
High elevation grass
Low elevation grass
Mixed evergreen shrub
BLEWT
Austocedrus chilensis
Fitzroya cupressoides

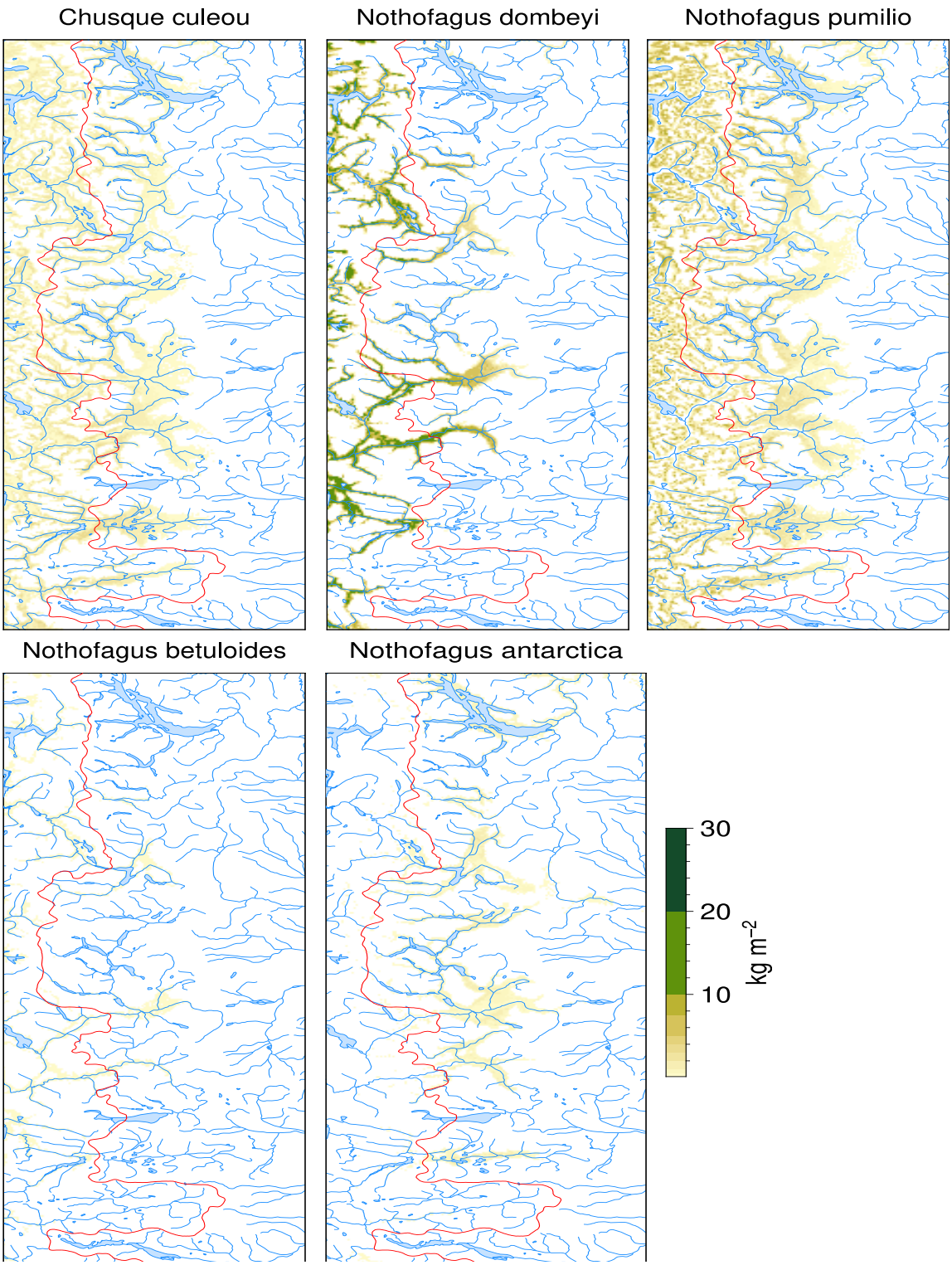

Fig. S1: Spatial map of LPJ-GUESS simulated biomass for the two PFTs and seven local tree species at 15 ka BP. The red line shows the border between Chile and Argentina.

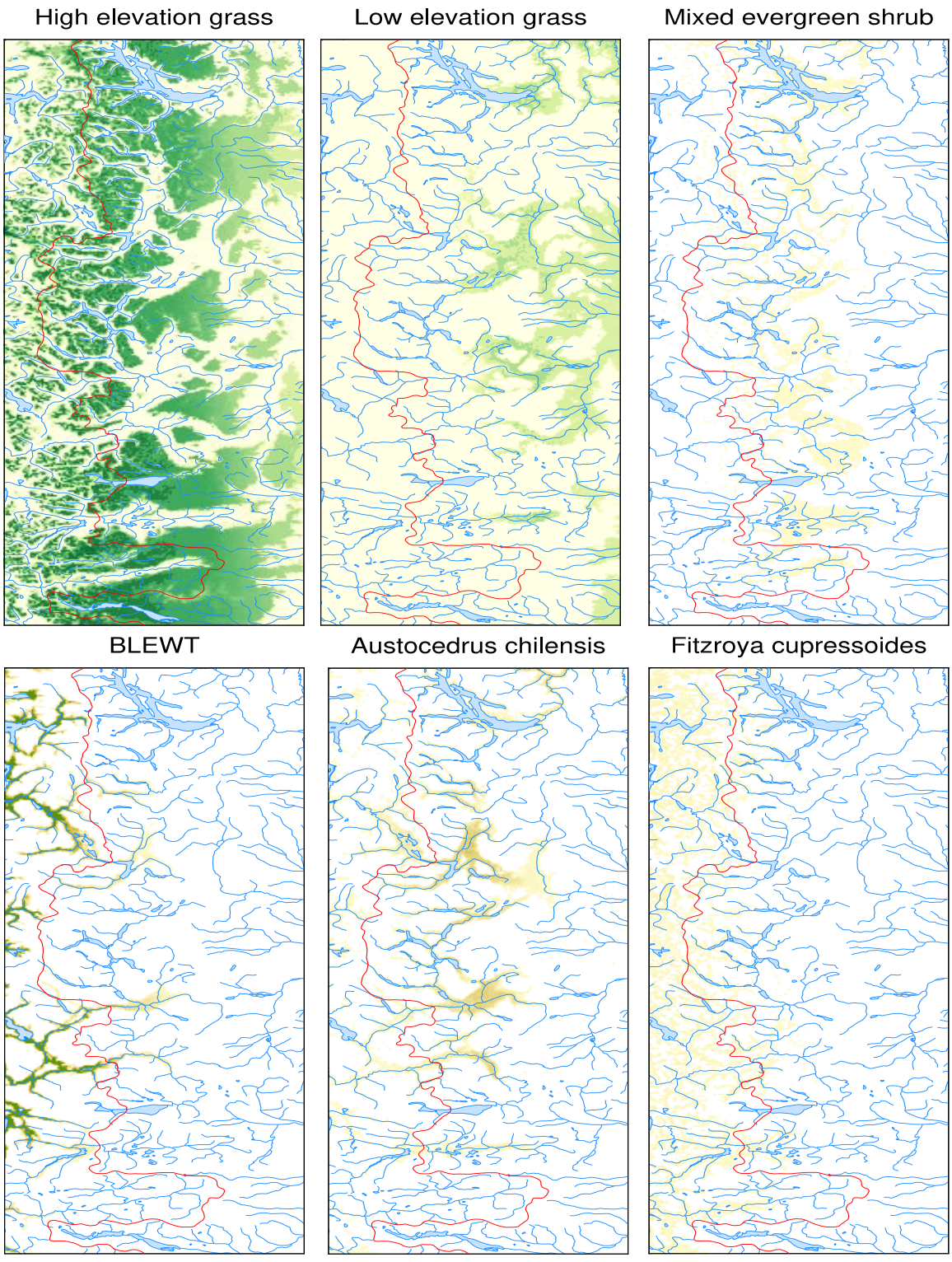
High elevation grass
Low elevation grass
Mixed evergreen shrub
BLEWT
Austocedrus chilensis
Fitzroya cupressoides

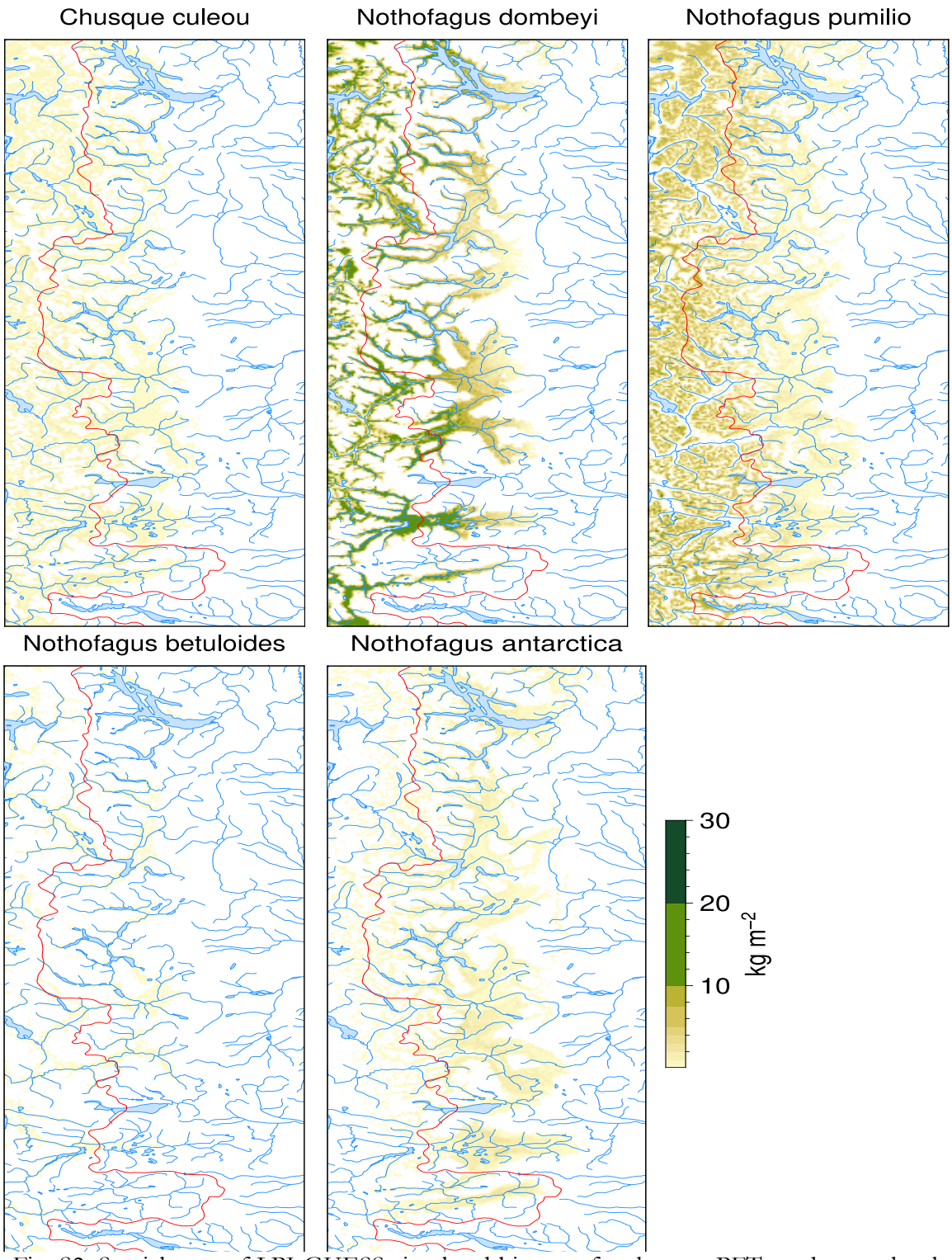

Fig. S2: Spatial map of LPJ-GUESS simulated biomass for the two PFTs and seven local tree species at 6 ka BP. The red line shows the border between Chile and Argentina.

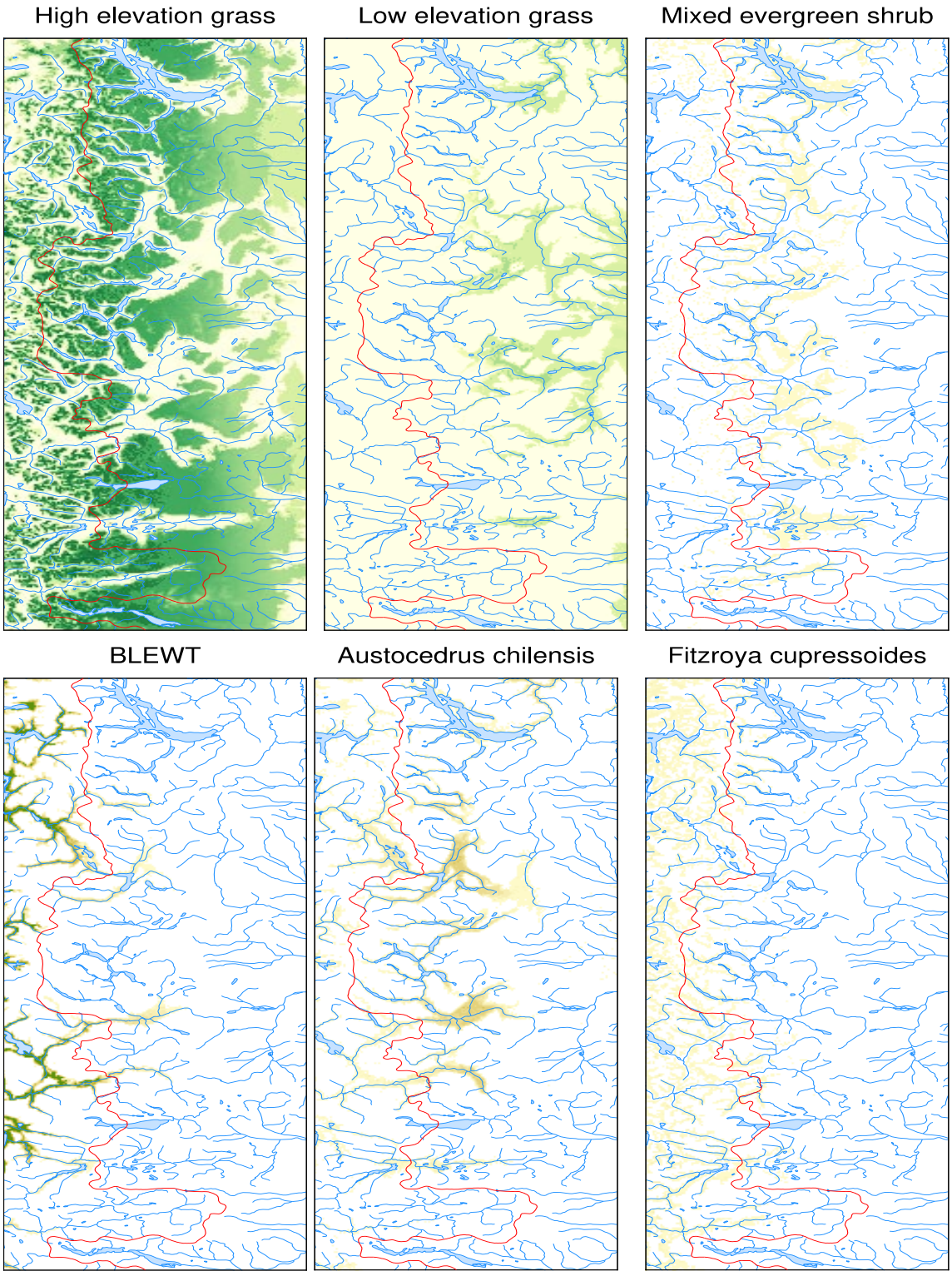
High elevation grass
Low elevation grass
Mixed evergreen shrub
BLEWT
Austocedrus chilensis
Fitzroya cupressoides

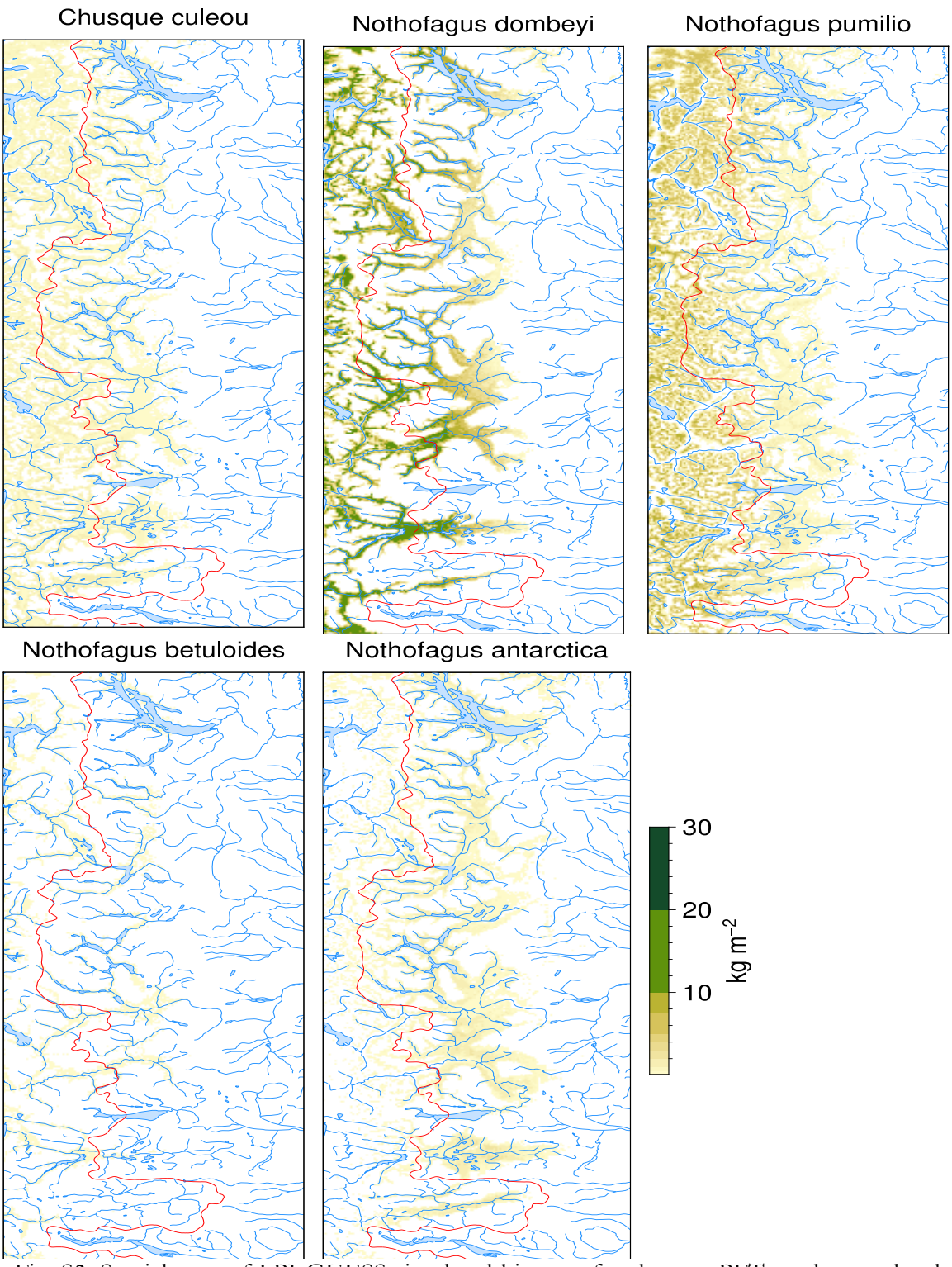

Fig. S3: Spatial map of LPJ-GUESS simulated biomass for the two PFTs and seven local tree species at 6 ka BP. The red line shows the border between Chile and Argentina.

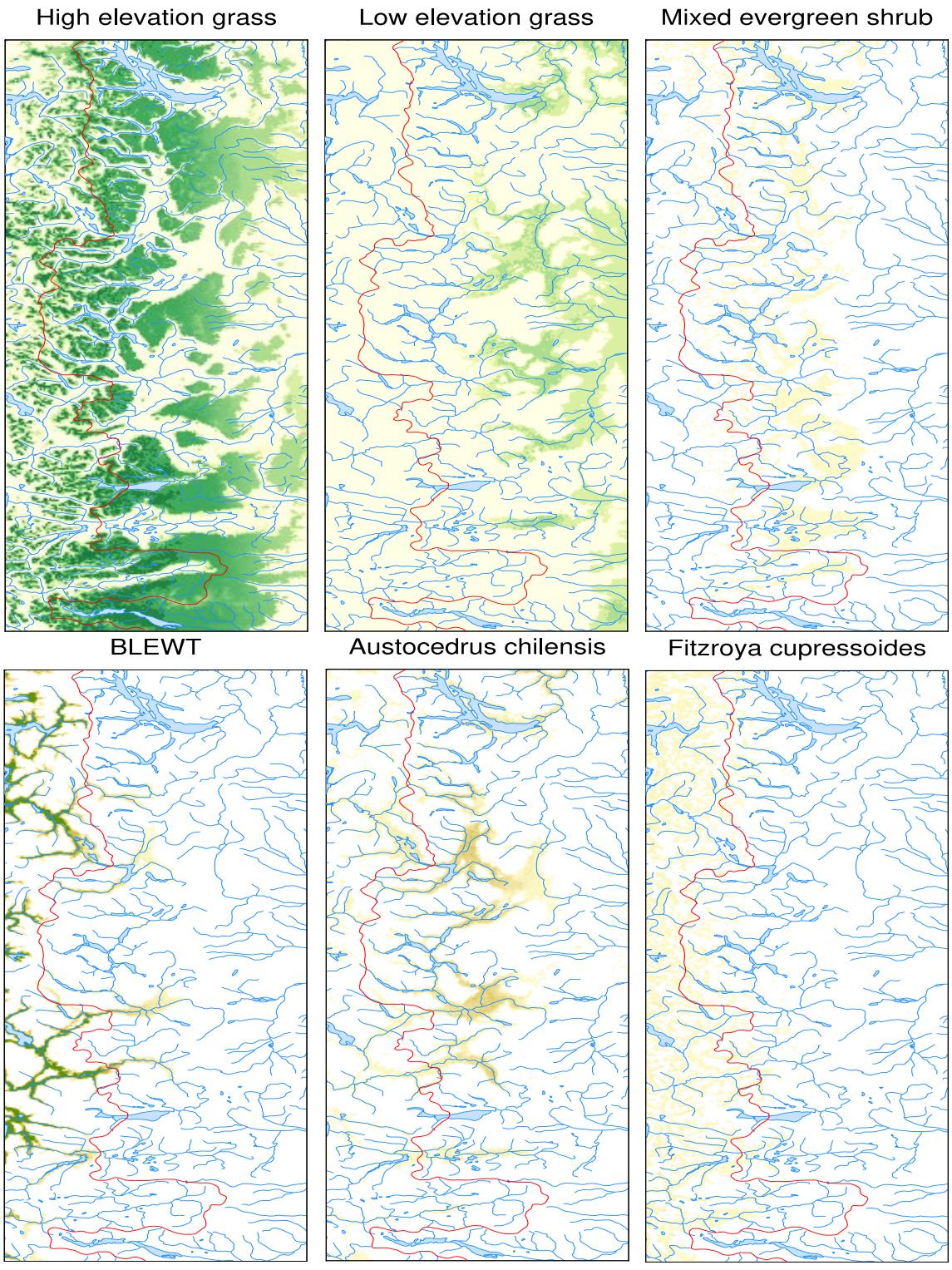
High elevation grass
Low elevation grass
Mixed evergreen shrub
BLEWT
Austocedrus chilensis
Fitzroya cupressoides

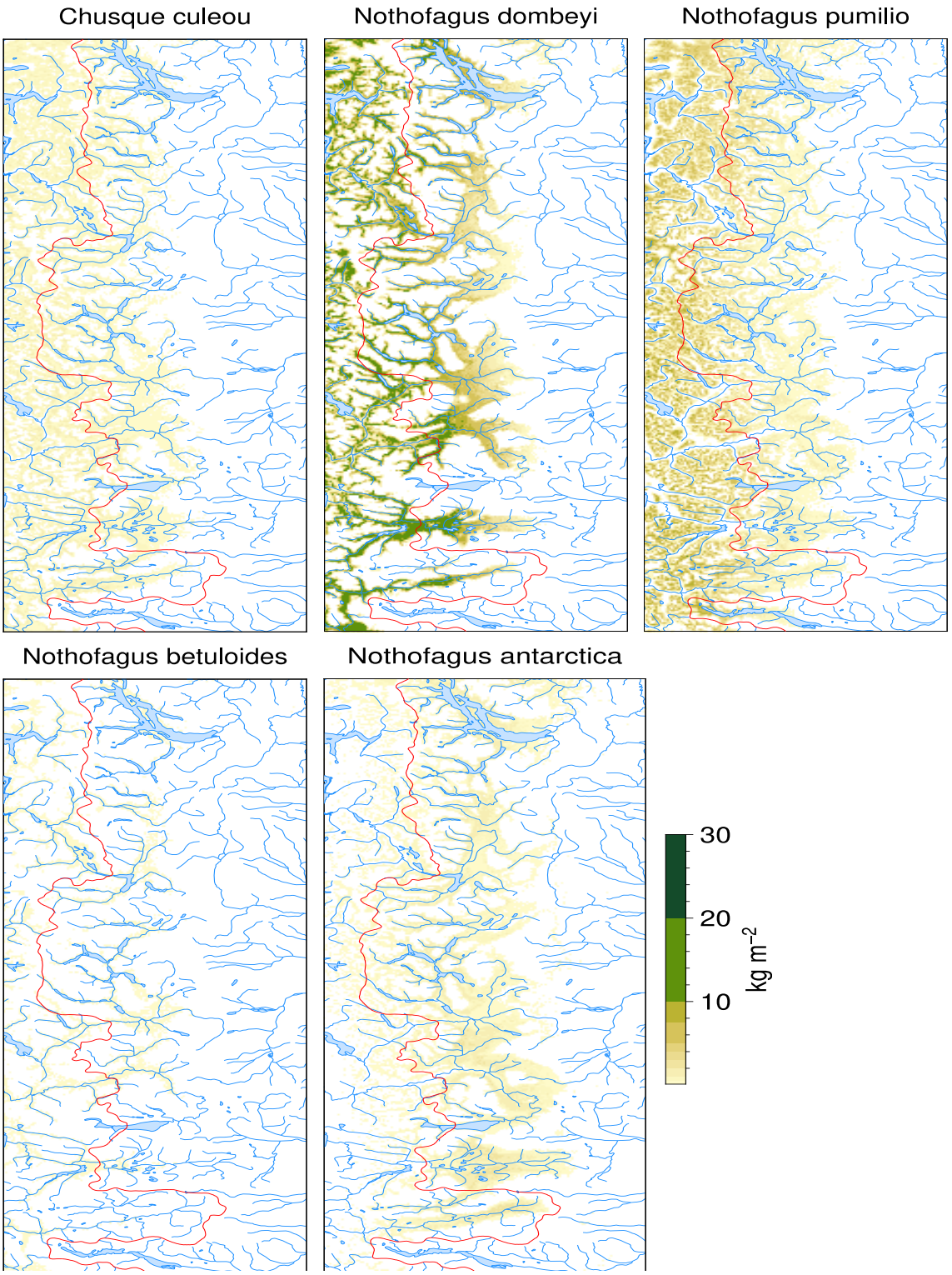

Fig. S4: Spatial map of LPJ-GUESS simulated biomass for the two PFTs and seven local tree species at 6 ka BP. The red line shows the border between Chile and Argentina.

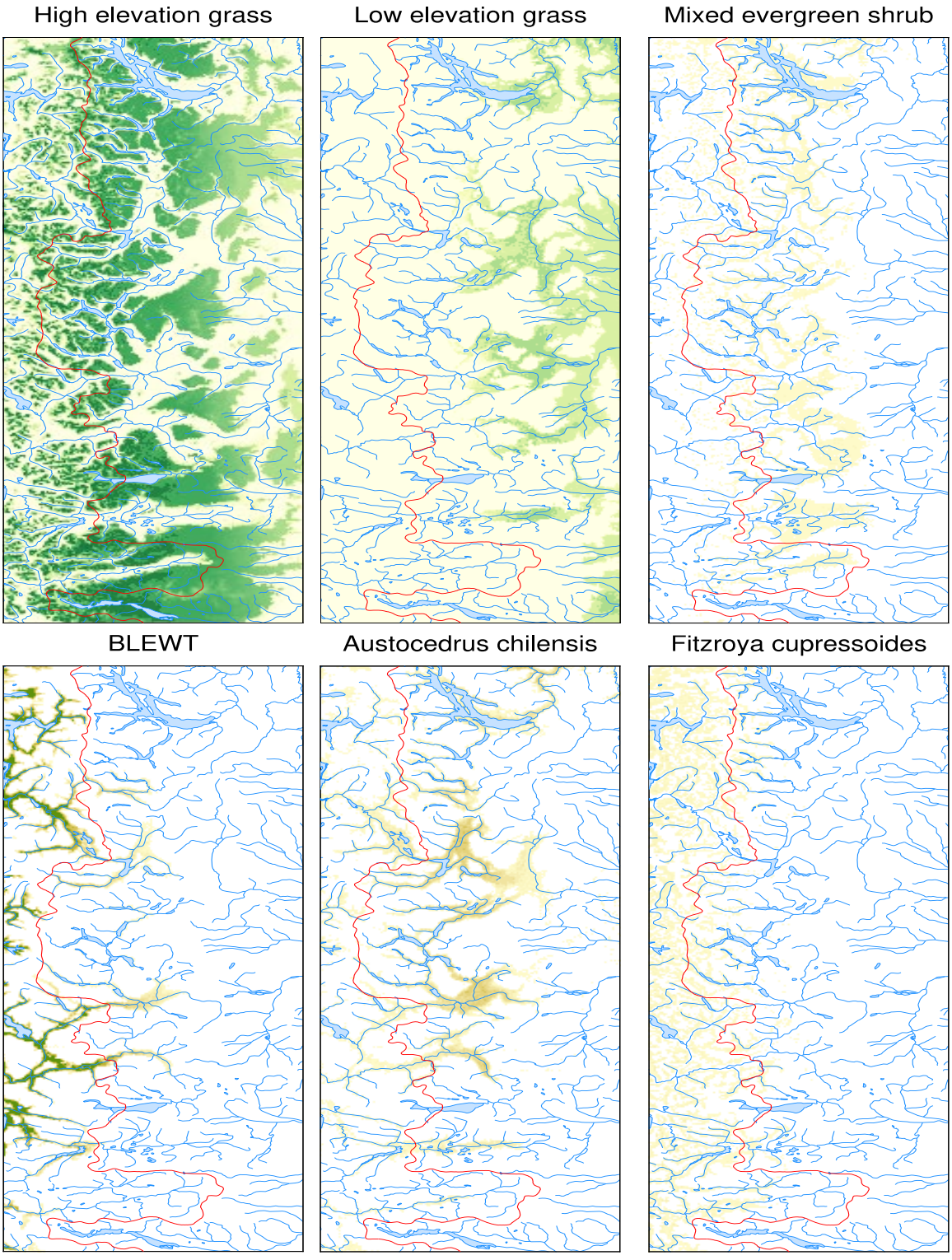
High elevation grass
Low elevation grass
Mixed evergreen shrub
BLEWT
Austocedrus chilensis
Fitzroya cupressoides

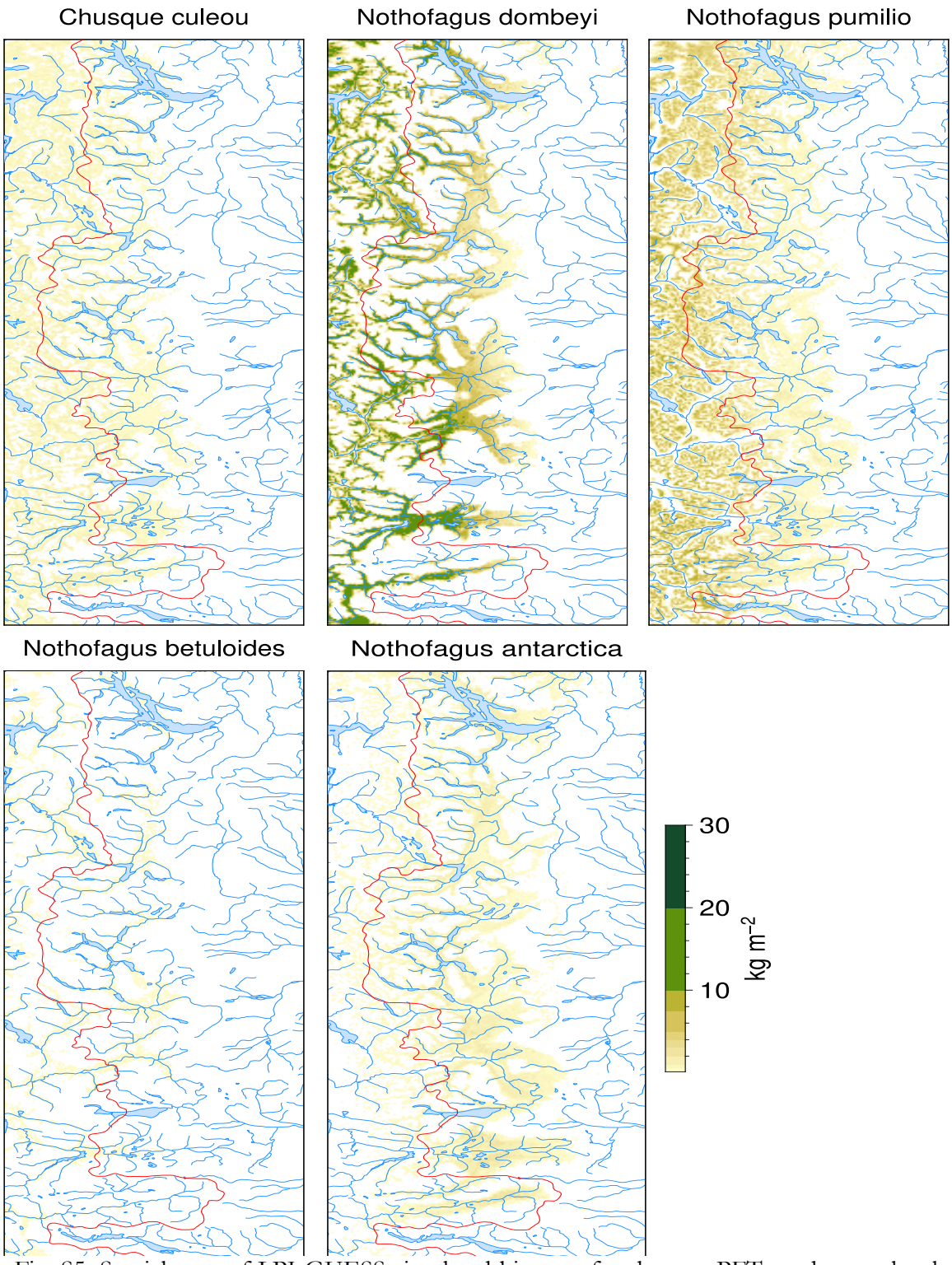

Fig. S5: Spatial map of LPJ-GUESS simulated biomass for the two PFTs and seven local tree species at 3 ka BP. The red line shows the border between Chile and Argentina.

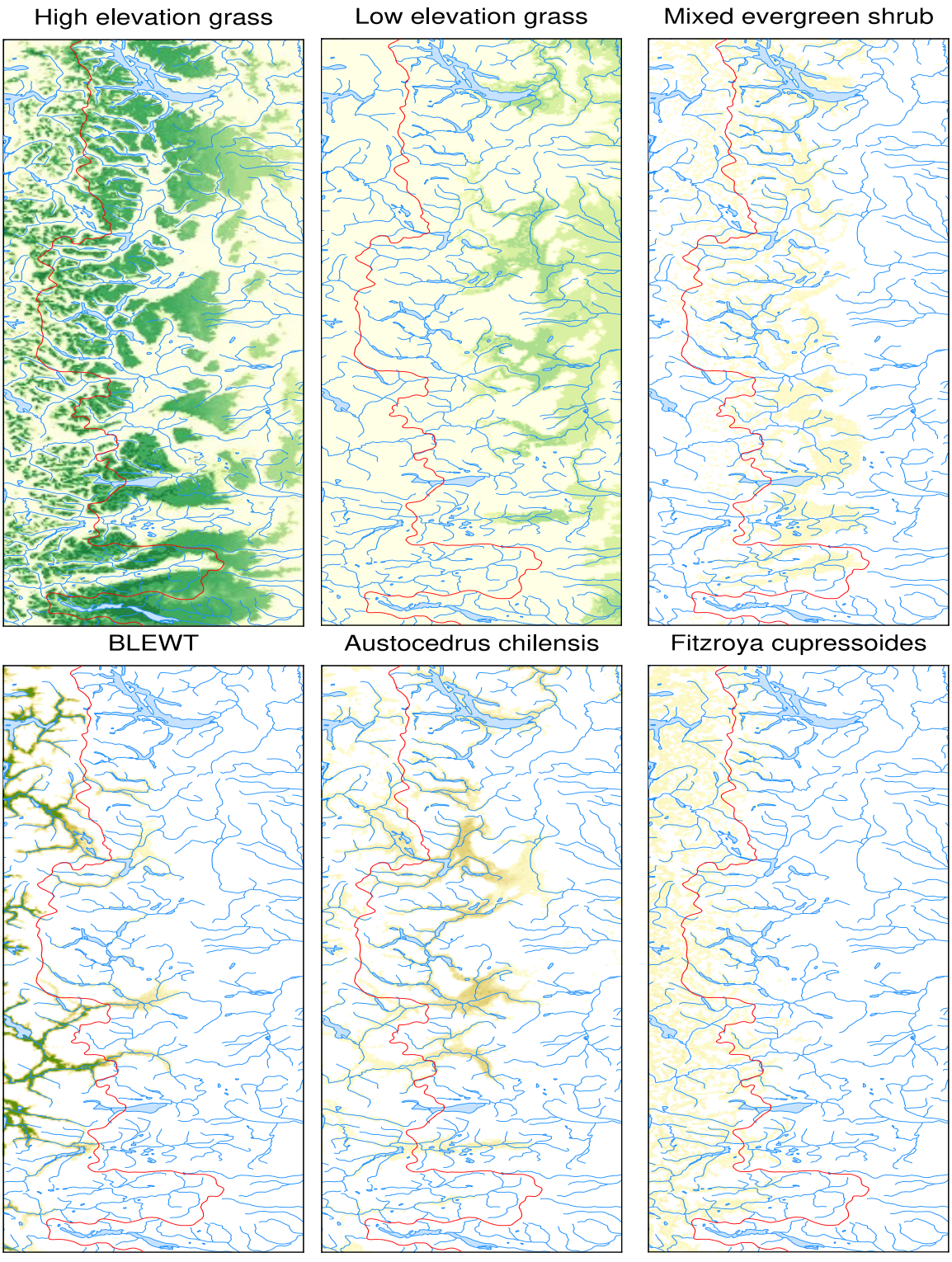
High elevation grass
Low elevation grass
Mixed evergreen shrub
BLEWT
Austocedrus chilensis
Fitzroya cupressoides

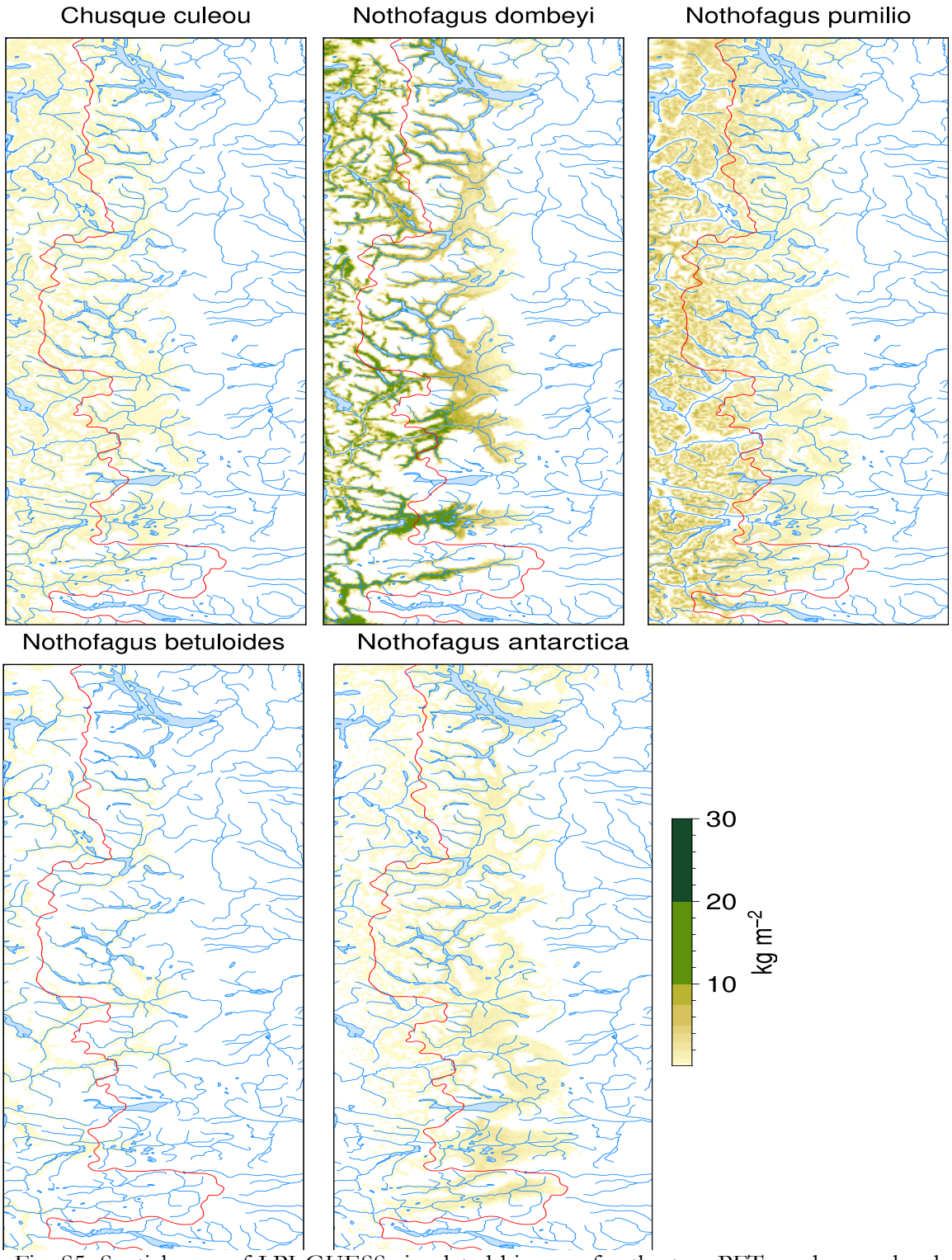

Fig. S5: Spatial map of LPJ-GUESS simulated biomass for the two PFTs and seven local tree species at 3 ka BP. The red line shows the border between Chile and Argentina.

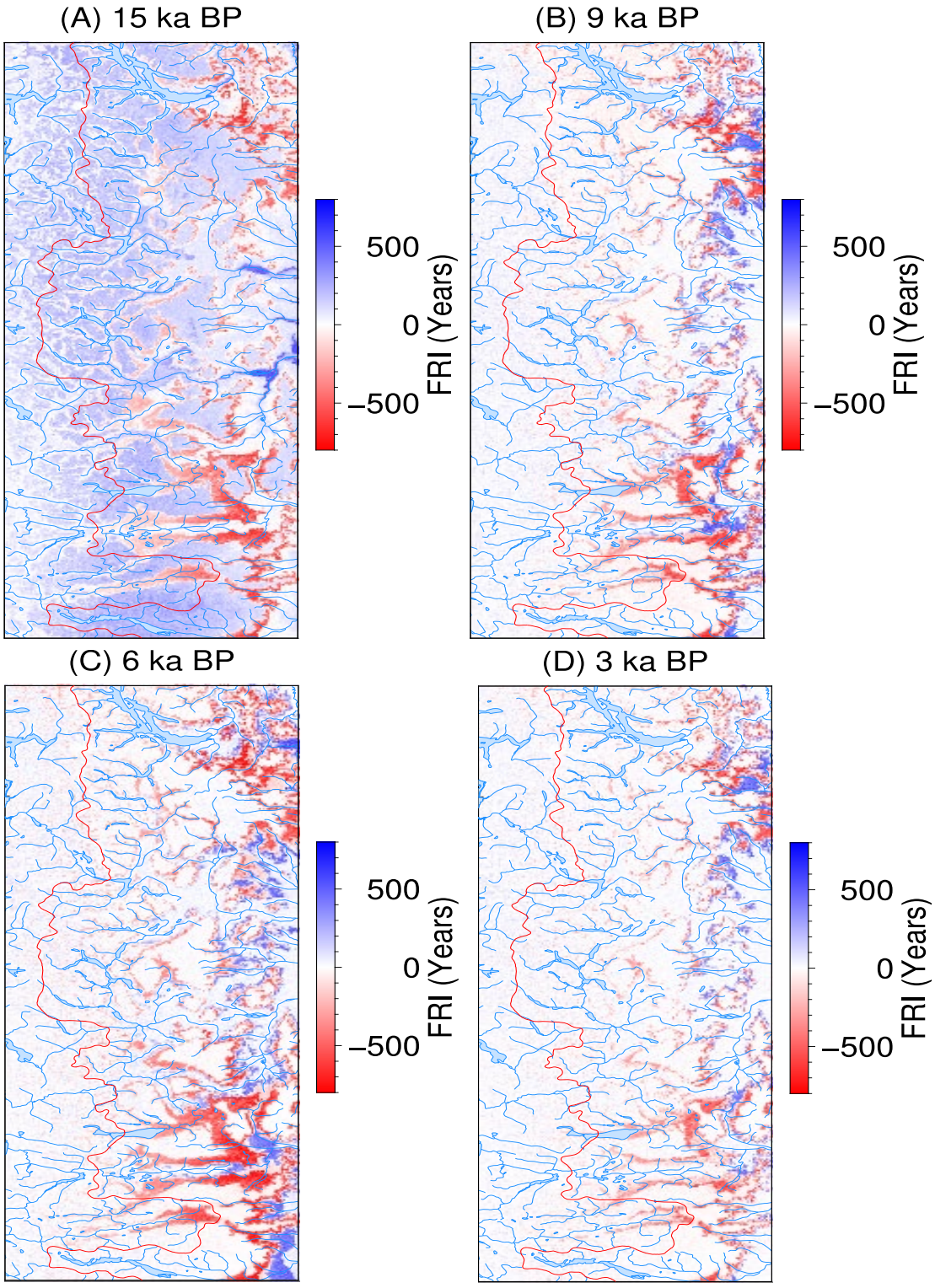

Fig. S6: Spatial map of the change in simulated fire return interval (FRI) using LPJ-GUESS (a) 15, (b) 9, (c) 6, and (d) 3 ka BP. The change in fire is the difference between each time slice and the control (0 ka BP).

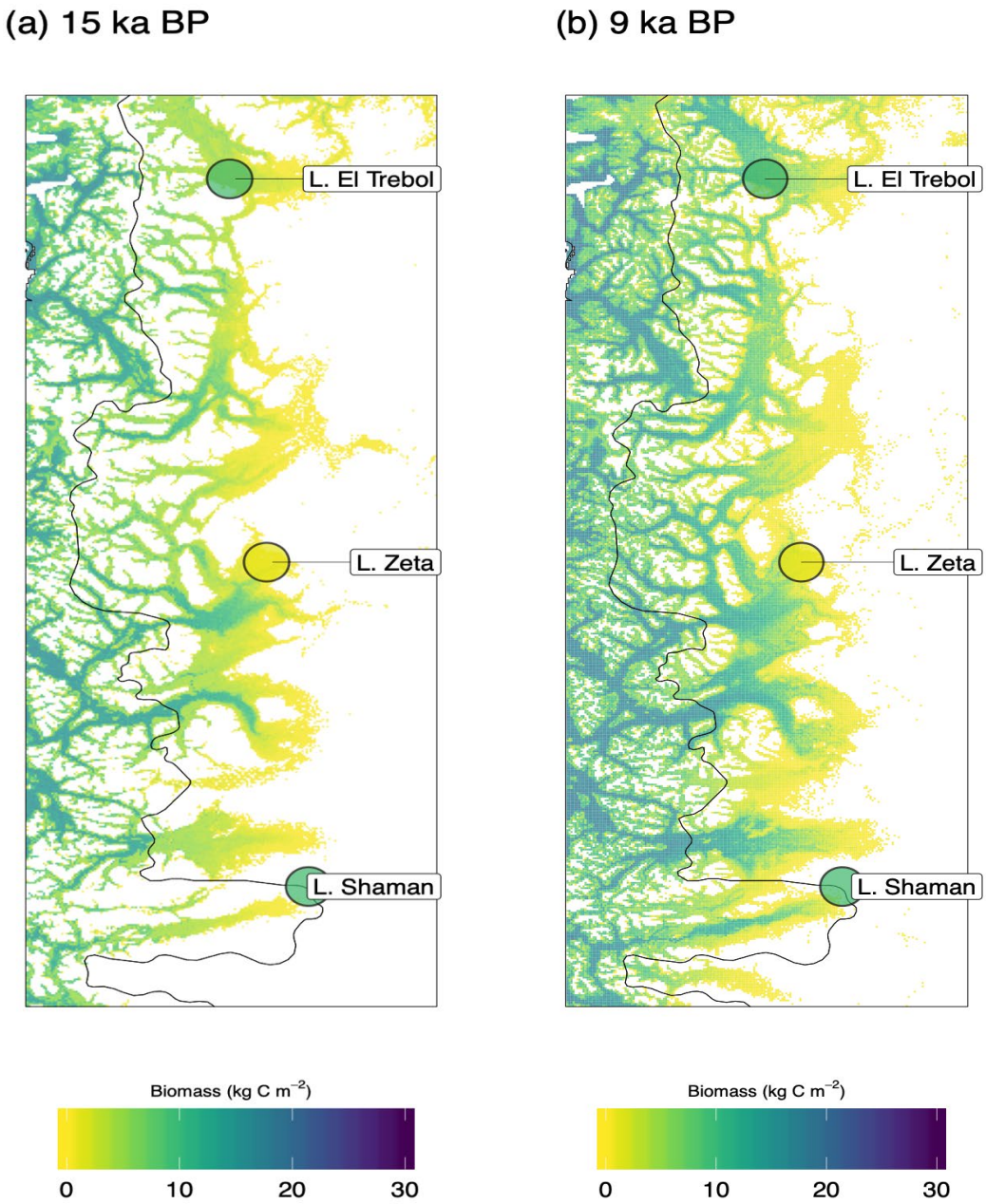

Fig. S7a: Spatial Map showing LPJ-GUESS simulated biomass for 15 & 9 ka BP, the points on the maps correspond to biomass value based on mean analog technique (MAT) for three selected sites. The biomass value used for the MAT was sampled from the mean aggregated trees and shrubs from control simulation (0ka BP). The MAT predicts the amount of biomass that is likely to be present at the sites during the time periods.

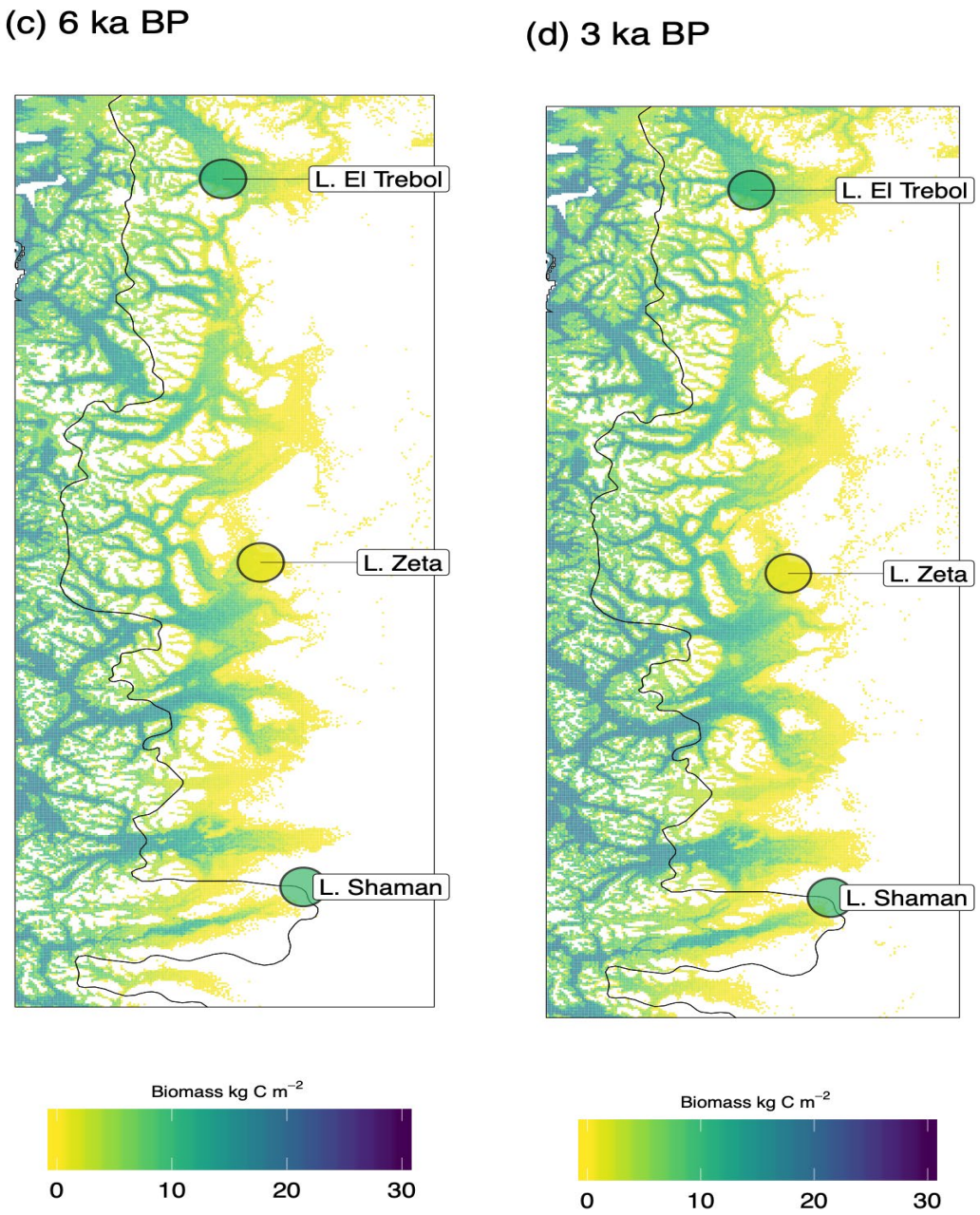

Fig. S7b: Spatial Map showing LPJ-GUESS simulated biomass for 6 & 3 ka BP, the points on the maps correspond to biomass value based on mean analog technique (MAT). The biomass value used for the MAT was sampled from the mean aggregated trees and shrubs from control simulation (0ka BP). The MAT predicts the amount of biomass that is likely to be present at the sites during the time periods.